Implementation of a Low Impact Development Test Bed at The University of Texas at San Antonio Main Campus

prepared by

Dr. Marcio H. Giacomoni Dr. Abtin Shahrokh Hamedani Dr. Heather Shipley

THE UNIVERSITY OF TEXAS AT SAN ANTONIO
Klesse College of Engineering and Integrated Design
School of Civil & Environmental Engineering, and Construction Management

December 2022

for

City of San Antonio's (COSA) Proposition 1 Edwards Aquifer Protection Venue Project

San Antonio River Authority (SARA)

TABLE OF CONTENTS

TABLE	OF CONTENTSii
LIST OF	TABLESv
LIST OF	FIGURESvii
ACRON	YMS AND ABBREVIATIONSxi
EXECU	TIVE SUMMARY1
CHAPTI	ER ONE: INTRODUCTION
1.1.	Background5
1.2. l	Knowledge Gaps7
1.3.	Research Goals and Objectives
1.3.1	Pilot-scale Study – Column Experiments
1.3.2	2. Field-scale Study – LID Testbed
1.3.3	3. Stormwater Modeling and Analysis
CHAPTE	ER TWO: PILOT TEST - COLUMN EXPERIMENTS 10
2.1.	Introduction
2.2.	Column and Media Specification
2.2.1	I. Column Experiments-Phase I
2.2.2	2. Column Experiments-Phase II
2.2.3	3. Column Experiments-Phase III
2.3.	Synthetic Stormwater
2.4.	Experimental Procedure
2.5.	Water Quality Analysis
2.6.	Statistical Analysis
2.7.	Results and Discussion
2.7.1	1. Media Physical and Chemical Properties
2.7.2	2. Water Quality Analysis

Column Experiments – Phase I	22
Column Experiments – Phase II	26
Column Experiments – Phase III	31
2.8. Conclusions	35
CHAPTER THREE: FIELD TEST – LOW IMPACT DEVELOPMENT TESTBED	37
3.1. Introduction	37
3.2. Low Impact Development (LID) Testbed	40
3.3. Field Monitoring	43
3.3.1. Hydrologic Performance	43
3.3.2. Treatment Performance	
3.3.3. Statistical Analysis	
Regression Analysis	50
Correlation Analysis	51
3.4. Soil Core Sampling	52
3.5. Results and Discussion	54
3.5.1. Pre-implementation Monitoring	54
3.5.2. Phase I: without Internal Water Storage (IWS)	57
Hydrologic Performance	58
Treatment Performance	61
3.5.3. Phase II: with Internal Water Storage (IWS)	70
Hydrologic Performance	70
Treatment Performance	74
3.5.4 Correlation Analysis	82

Impact of Storm Regime on Water Quality	82
Relationship between various pollutants and potential co-contaminants	86
3.5.5. Soil Core Sampling	87
3.6. Conclusion	90
CHAPTER FOUR: STORMWATER MODELING – SWMM MODEL	94
4.1. Introduction	94
4.2. SWMM Model Development	95
4.3. Calibration and Validation	98
4.4. Hydrologic Performance Under Continuous Simulation	99
4.5. Results and Discussion	100
4.5.1. Calibration and Validation	100
4.5.2. Hydrologic Performance	103
4.6. Conclusion	108
CHAPTER FIVE: COST-BENEFIT ANALYSIS	111
CHAPTER SIX: MAINTENANCE	113
SUMMARY, CONCLUSION AND RECOMMENDATIONS	116
Recommendations	119
Future Research	120
APPENDIX A	122
REFERENCES	131

LIST OF TABLES

Table 2- 1. Targeted concentration (mg/L) of pollutants, required volume of stock solution for 5
gallons DI water and chemicals used in manufacturing the stock solution
Table 2- 2. Water quality parameters, units, methods, instrumentation, and detection limits 20
Table 2- 3. Physical and Chemical properties of the tested filtration media
Table 2- 4. Mean influent and effluent concentration and standard deviation of measured water
quality parameters - Phase I
Table 2- 5. Removal efficiencies (%) of water quality parameters – Phase I and Phase II 30
Table 2- 6. Removal efficiencies (%) of water quality parameters before & after plant addition-
Phase III
Table 3- 1. Physical and chemical Properties of the LID testbed media
Table 3- 2. Water quality parameters, units, methods, instrumentation, and detection limits 47
Table 3- 3. list of pre-implementations monitored storm events January 2018-May 2019 55
Table 3- 4. Median pollutants' EMC and loading, pre-implementation monitoring
Table 3- 5. Mean pollutant concentration of first flush samples vs total collected samples 57
Table 3- 6. List of monitored storm events June 2019 – April 2021
Table 3- 7. Mean hydrologic performance indicators, Phase I – no IWS
Table 3- 8. Median EMC efficiency for the various pollutants – Phase I
Table 3- 9. Median percent load removal for various pollutants – Phase I
Table 3- 10. List of monitored storm events April 2021 - October 2022
Table 3- 11. Mean hydrologic performance indicators, Phase II – IWS
Table 3- 12. Median EMC efficiency for the various pollutants – Phase II with IWS
Table 3- 13. Median percent load removal for various pollutants – Phase II with IWS

Table 3-14. Median pollutant content (mg/Kg) in collected samples and initial soil media pollutar
content8
Table 4- 1. Characteristics of the subcatchments in the LID testbed drainage basin
Table 4- 2. Calibration parameters range and final value
Table 4- 3. Validation of the model under continuous 5-min simulation
Table 4- 4. Watershed response under continuous simulation for phase I and II
Table 4- 5. Hydrologic performance of the LID testbed, 3.5-year continuous simulation 10-
Table 4- 6. Long-term hydrologic performance of the LID testbed under 15- year period 10
Table 5- 1. Total capital, maintenance and operating cost for the whole monitoring period 11
Table 5- 2. Unit volume reduction and pollutant removal cost
Table A1. Effluent flow weighted mean concentration (FWMC) values for each media 12.
Table A 2. Details of captured storm events at the LID testbed, phase I and II
Table A 3. Median EMC for six qualified storm events, phase I
Table A 4. Median EMC for five qualified storm events, phase II
Table A 5. Total (sum) pollutant loading for six qualified storm events, phase I
Table A 6. Total (sum) pollutant loading for five qualified storm events, phase II
Table A 7. Particle size distribution of tested media

LIST OF FIGURES

Figure 2- 1. Profile of columns composition and injection apparatus including feed tank, agitator,
peristaltic pump and distributing gutter; and rain gauges to record outflow
Figure 2- 2. Paired boxplots of influent and effluent concentration for TP and TN (mg/L) 22
Figure 2- 3. Paired boxplots of influent and effluent concentration for dissolved and total heavy
metals including (a,b) Copper ($\mu g/L$), (c,d) Zinc ($\mu g/L$) and (e,f) Lead ($\mu g/L$) – Phase I 25
Figure 2- 4. Paired boxplots of influent and effluent concentration for (a) TP and (b) TN (mg/L)
comparing sand to the standard and customized bioretention soil mixtures (phase I and II) 27
Figure 2- 5. Paired boxplots of influent and effluent concentration for dissolved metals ($\mu g/L$) (a)
Copper, (b) Zinc, and (c) Lead, comparing sand to the bioretention soil mixtures
Figure 2- 6. Paired boxplots of influent and effluent concentration (mg/L) for (a) TP, (b) N, and
(c) TN, comparing phase II and phase III.
Figure 3- 1. LID testbed drainage area, white star is the pre-implementation monitoring location
41
Figure 3- 2. Aerial view of the LID testbed, water movement and monitoring locations
Figure 3- 3. Cross-section profile view of the LID testbed cells, blue arrows show water infiltration
to the sublayer through unlined cells. Cell 1 and 2 contain Limestone-Mix media, Cells 3 and 4
Bioretention-Mix, and Cells 5 and 6 Limestone Sand
Figure 3- 4. Field monitoring equipment and sensors at the LID testbed
Figure 3- 5. Sample collection and laboratory analysis, TSS samples and digested samples for
Total Metals (TM) showing the first flush effect and reduced solids for consecutive samples 48
Figure 3- 6. Soil sampling locations at the LID testbed

Figure 3- 7. Soil sample collection and analysis
Figure 3- 8. Hydrograph and Pollutographs for selected storm – 12/07/2018 57
Figure 3- 9. Influent volume/peak flow versus the effluent volume/peak flow - Phase I 58
Figure 3- 10. Pump system installed in November 2020 to expand the contributing drainage area
Figure 3-11. EMC Boxplots, Inlet vs. outlets - Phase I. h-value of 1 indicates significant difference
between the median EMCs (p<0.05)
Figure 3- 12. [a, c] Total coliform and [b, d] E. coli bacteria EMC Boxplots, Inlet vs. outlets -
Phase I. h-value of 1 indicates significant difference between the median EMCs (p<0.05) 66
Figure 3- 13. Bioretentions outlet vs. inlet EMC scatter plots (observed), regression lines
(predicted), and 95% confidence and prediction intervals
Figure 3- 14. Sand filters outlet vs. inlet EMC scatter plots (observed), regression lines (predicted),
95% confidence and prediction intervals
Figure 3- 15. Influent volume/peak flow versus the effluent volume/peak flow - Phase II 71
Figure 3- 16. Difference of hydrologic performance, cumulative volume and flow duration curve
showing the outflow variations over phase I [a, c] and phase II [b, d]
Figure 3- 17. EMC Boxplots, Inlet vs. outlets - Phase II. h-value of 1 indicates significant
difference between the median EMCs (p<0.05)
Figure 3- 18. [a, c] Total coliform and [b, d] E. coli bacteria EMC Boxplots, Inlet vs. outlets -
Phase II. h-value of 1 indicates significant difference between the median EMCs (p<0.05) 77
Figure 3- 19. EMC variations over the 3.5-year monitoring period
Figure 3- 20. Difference of plant growth in two bioretention designs – 4/29/2020

Figure 3- 21. Average among all six cells percent total load removal (%) for Phase I (No IWS) and
Phase II (With IWS)
Figure 3- 22. The cumulative volume percent (%) and particle size distribution (μm) of influent
and effluent samples - 2 selected storms on 05/28/2021 and 07/05/2021 is shown
Figure 3- 22. Spearman's rank correlation coefficient matrix – Impact of storm characteristics on
[a] influent pollutant EMC, [b] influent pollutant load, and [c] total percent load reduction
considering all 11 captured storm events (phase I and II).
Figure 3- 23. Spearman's rank correlation coefficient matrix for [a] influent and [b] effluents
EMCs
Figure 3- 24. [a] Total copper, [b] Total lead and [c] Total zinc content in surface soil samples
(mg/Kg)
Figure 3- 25. [a] Total phosphorus and [b] Total nitrogen content in surface soil samples (mg/Kg)
90
Figure 4- 1. Modeling process by SWMM (Rossman & Huber, 2015)
Figure 4- 2. SWMM model – The LID testbed and the drainage area
Figure 4- 3. Calibration and validation shown for 2 selected storms comparing the predicted and
observed inlet and outlet hydrographs, and the values for goodness of fit indictors 102
Figure 4- 4. Difference of hydrologic performance, Modeled cumulative volume - phase I [a],
phase II [b]
Figure 4- 5. Frequency plot, 15-year total outflow with [a] no IWS, [b] IWS
Figure 6- 1. Monthly and annual maintenance to remove debris, weeds and dead plants 113
Figure 6- 2. Before [a] November 2020, and after maintenance [b] December 2020, and [c]
February 2021

Figure A1. Heavy metals EMC Boxplots, Inlet vs. outlets - Phase I. h-value of 1 indicates
significant difference between the median EMCs (p<0.05)
Figure A2. Inlet versus outlet EMC scatter plots (observed), regression lines (predicted), 95%
confidence and prediction intervals for [a-g] Bioretentions, and [h-n] Sand filter basins 124
Figure A3. Heavy metals EMC Boxplots, Inlet vs. outlets - Phase II. h-value of 1 indicates
significant difference between the median EMCs (p<0.05)
Figure A 4. Rating curves assigned to the LID testbed cells' outlets [a] Phase I with no IWS, [b]
Phase II with IWS

ACRONYMS AND ABBREVIATIONS

ADP Antecedent Dry Period

BMP Best management practice

CFU Colony forming units
CFS Cubic feet per second

COOP Cooperative Observer Program

COSA City of San Antonio

DO Dissolved Oxygen

DCu Dissolved copper

DPb Dissolved lead

DZn Dissoved zinc

EPA U.S. Environmental Protection Agency

EMC Event mean concentration

FWMC Flow weighed mean concentration

IWS Internal water storage

LID Low impact development

MDL Method detection limit

mg/L milligrams per liter

N Nitrogen

ND Non-detect

NLCD National Landcover Database

NOx Nitrate + nitrite and nitrate

NPS Non-point source

NSE Nash-Sutcliffe efficiency

P Phosphorus as Orthophosphate

PBIAS Percent bias

QR Peak flow reduction

RR Removal Rate

r2 Coefficient of determination

R_{peak} Peak flow reduction ratio

SARA San Antonio River Authority

SCS CN Soil conversation service curve number

STIR-UP South Texas Interdisciplinary Research For Undergraduate Programs

SPLP Synthetic Precipitation Leaching Procedure

STATSGO State Soil Geographic Data Base

SWMM Stormwater Management Model

TCEQ Texas Commission of Environmental Quality

TCu Total copper

TKN Total Kjeldhal Nitrogen

TM Total metals

TN Total nitrogen

TP Total phosphorus

TPb Total lead

TSS Total suspended solids

TVS Total volatile solids

TZn Total zinc

UH Unit hydrograph

UTSA University of Texas at San Antonio

USGS U.S. Geological Survey

VR Total volume reduction

μg/L Micrograms per liter

EXECUTIVE SUMMARY

This project is a part of the proposition 1, the Edwards Aquifer Protection Venue Project by City of San Antonio (COSA) and administered by San Antonio River Authority (SARA), to provide information about benefits and risks of Low Impact Development. The study investigated three main questions. The first question relates to requirement of the Texas Commission of Environmental Quality (TCEQ) that LID features contain an impermeable liner that impedes water to infiltrate into the soil. Therefore, the question the study addressed was whether impermeable liner provides enhanced water quality treatment in comparison to unlined systems. Another question evaluated by the investigation was how much additional recharge could be achieved by unlined systems. The third question is about the differences between sand filters and bioretention systems. Sand filter basins are common stormwater treatments utilized in the region of South Central Texas and on top of the Edwards Aquifer Recharge Zone. The study analyzed whether bioretention systems provided better overall water quality treatment in comparison to sand filter basins. The study also evaluated different filter media. Specifically, the project tested different media types with the goal of identifying filter media locally sourced that could enhance stormwater treatment. Lastly, the study examined the impact of internal water storage (IWS) on the performance of sand filters and bioretention systems. All the questions were evaluated through a multi-phase study: (1) pilot test using column experiments, (2) field tests using a full scale LID testbed, and (3) using stormwater modeling software.

In the first phase of the study, a pilot-scale study was conducted to evaluate pollutant removal efficiencies of various filtration media using synthetic stormwater and bioretention columns in controlled setting. A total of nine filtration media were tested, including conventional commonly

used media in LID systems as well as custom media. The results established that the pollutant removal processes are strongly impacted by the media physical and chemical characteristics, such as gradation, and phosphorus and organic matter content. We found significant improvement in pollutant removal efficiencies with use of limestone sand alone and in the bioretention soil mixture, particularly for the dissolved pollutants due to its high adsorption capacity. Accordingly, three top performing media – including two bioretention soil mixtures of bioretention-mix (standard silicabased sandy loam) and limestone-mix (custom limestone sandy loam) and limestone sand - were selected to be implemented in the field-scale LID testbeds for the next phase of the study.

The LID testbed is composed of six parallel cells containing the three media in duplicates, with and without impermeable liner. Hence, continuous monitoring of the LID testbed provides extensive dataset and allowed the investigators to perform a performance assessment of (1) sand filter basins vs. bioretention basins, (2) different bioretention media and impact of limestone sand usage in the bioretention soil mixture, and (3) lined vs. unlined systems and the potential impact of impermeable liner on the effluent water quality. This extensive dataset also provided the data and model development needs for further assessments of these systems.

The field monitoring composed of pre- and post- implementation monitoring. One year of preimplementation monitoring provided a baseline of the watershed hydrologic response and the
stormwater quality matrix in the study area. Three and a half years of monitoring data on the
hydrologic and treatment performance of the LID testbed was used for comparative evaluation of
the three LID designs under two monitoring phases of with and without internal water storage
(IWS) layer. Overall, we found no significant difference between the effluent water quality of
bioretention systems versus sand filter basins, as well as lined versus unlined cells. The tested
water quality parameters included: TSS, VSS, nutrients (nitrogen and phosphorus), metals (zinc,

lead and copper), and bacteria. The results suggested significant enhanced pollutant removal efficiencies with use of limestone sand in the sand filter basin as well as the bioretention basin. Whereas the regular bioretention-mix leached most pollutants due to its high nutrient and organic matter content. Although the hydrologic performance was not significantly different between the three-filtration media, unlined cells provided greater runoff volume and peak flow control as a consequent of seepage and direct infiltration.

The operation of the systems with IWS reduced outflow volume and peak flow in all cells, and increased recharge substantially in unlined cells. Moreover, IWS presence enhanced removal of particulate pollutants including TSS, bacteria and heavy metals, while nutrient removal was adversely impacted. Bioretention-mix, predominantly, showed even greater leaching of nutrients that is likely due to desorption and washoff of nitrogenous solids from the dead plant tissues as well as incomplete denitrification processes. Maintenance was found to be an important factor in achieving reliable pollutant removal, since substantially higher effluent pollutant load was observed during plants' die-off season that was significantly reduced subsequent to the annual maintenance. Cost-benefit analysis suggested bioretention-mix as the least beneficial media considering its high maintenance cost and pollutant export, while unlined cells were found to be more cost-effective providing greater volume and pollutant load reduction at lower unit cost.

An EPA-SWMM model was developed using the field monitoring data to further investigate the hydraulics of the LID testbed, and to better quantify the mass balance considering the climatic components (e.g., evaporation) of the system over continuous simulation. The model estimated 10-20% more volume reduction in unlined cells representing recharge through subsurface infiltration. The model was used to examine the long-term performance of the LID testbed, with

and without IWS layer. The results of the 15-year continuous simulation suggested 20% and 40-45% recharge increase for unlined sand filter and bioretention cells in presence of IWS layer.

This project had a strong educational impact for many students. The project provided K-12 students/school tours in collaboration with UTSA engineering summer school, and undergraduate research partnership with STIR-UP student cohort and internships. Over the 4-year period, the project hosted total of 339 middle/high school students for the UTSA engineering summer camps and 6 undergraduate students for the STIR-UP student cohort program. Educational materials were also prepared, including videos of the LID testbed and filtration lab experiment for the 2020 virtual engineering summer camp. A total of nine undergraduate students and three graduate students have been involved in the LID testbed project. The students presented their research at national and local conferences, including the UTSA annual undergraduate research showcase. Additionally, LID educational modules were prepared and included in the curriculum of undergraduate classes for civil engineering students at UTSA.

The findings of this project suggested filtration media composition as the major key indicator of LID systems' effectiveness, regardless of the LID design type. Use of bioretention soil mixtures with low initial nutrient, metals and organic matter content ensures effective pollutant removal, and can also increase maintenance efficiency. Timely and proper maintenance was also found crucial for reliable treatment performance; thus, we recommend quarterly to biannual full maintenance, including harvesting and pruning of plants. Additionally, we recommend the use of limestone sand as an extra filtration layer or within the bioretention soil mixture to further capture the leachates. Moreover, combination of unlined cells with IWS layer is recommended for enhanced hydrologic as well as treatment performance.

CHAPTER ONE: INTRODUCTION

1.1. Background

Throughout the recent decades, rapid population growth has caused large rural to urban migration resulting in over half of the world's population (54%) living in urban areas. The continuing trend is projected to add 2.5 billion people to the urban population by 2050, indicating an overall increase of 66% in the urban population worldwide (United Nations 2014). Urbanization results in changes in land cover and land use from forests, pasture, agricultural and other pervious land to industrial, residential and urban areas (Shang et al. 2018) leading to increased imperviousness, causing significant increase in the generation of surface runoff (USGPR 2017), and reduction of infiltration and groundwater recharge (Hejazi and Markus 2009). Additionally, water quality is degraded due to non-point source pollutants (NPS) that are transported as runoff flows off impervious surfaces during storm events (Tong et al. 2009).

San Antonio follows the global trend and has a rapid population growth and urban development. US census bureau reports San Antonio as one of the fast-growing cities in United States, with 13% population growth from 1.3 million in 2010 to 1.5 million in 2017 (US Census Bureau 2017). San Antonio is located on top of the Edwards Aquifer, which can be adversely impacted. Karst Aquifers, such as the Edwards, are extremely vulnerable to reduced/rapid recharge and chemical contamination due to their geological formation (Ford and Williams 2007). Karst aquifers are composed of highly soluble rocks, such as limestone that is the major constituent of the Edwards aquifer. Overtime, as groundwater has moved through the aquifer, dissolution of rocks has led to increased porous zones (Ford and Williams 2007) providing habitat to 14 threatened and endangered species (Musgrove et al. 2016). Moreover, the increased permeability of Edward's

aquifer contributes to very fast water movement in the upper zone of the aquifer. This rapid recharge and the cavernous nature of the aquifer creates a dynamic flow system with reduced contact time, which mitigates the auto-purification processes and results in rapid contaminant transport to the downstream (Ford and Williams 2007; USGS Groundwater 2012), hence endangering its ecological habitat (Belson 1999) and threatening major water supplies of large population centers. The Edwards Aquifer is the main freshwater supply for South-Central Texas and extends over 180 miles along the southern and eastern edge of the Edwards Plateau (Roos and Peace 2015). The rapid population growth and subsequent increased water demand, and also the prolonged periods of droughts in previous years has put Edwards aquifer under extreme pressure, making it one of the top ten endangered karst ecosystems globally (Belson 1999). Edwards' formation is not unique and nearly 15% of the contiguous Unites States has carbonate rock formation (Peck et al. 1988) and karst aquifers supply fresh water for approximately 25% of the global population (Musgrove et al. 2016). Given the circumstance, protection of karst aquifers against negative impacts of urbanization is a global issue and effective mitigation strategies are essential for the sustainability water systems and ecosystems.

Low impact development (LID) practices or green infrastructure (GI) are strategies used to mitigate adverse impacts of urbanization on the hydrologic regime and the environment by restoring the natural hydrologic flow regime (US EPA 2007). LID practices manage stormwater by mimicking the natural flow through preserving the natural landscape and restoring the infiltration, and remove pollutants through physical, chemical and biological treatment processes (Prince George's County 1999; US EPA 2007). LID performance is highly variable and dependent on the design components (such as filtration media composition), location and sizing, and the climate.

1.2. Knowledge Gaps

Numerous studies have evaluated stormwater control capacity of different LID systems in terms of quantity and quality, in order to identify advantages and disadvantages, limitations, and performance variations of each system under different characteristics and settings. Scientists have employed different approaches from pilot-scale and field-scale monitoring to use of modeling tools to explore and better understand the performance of LIDs aiming to improve their effectiveness and resilience. The substantial literature review of the previous studies (explicitly discussed in subsequent chapters) provides a good assessment of hydrological and treatment performance of various LID systems considering the soil composition, climate conditions and storm characteristics. Moreover, various techniques are examined to enhance their performance such as soil amendments, internal water storage and combined layered systems. Although LID systems and various techniques (such as soil amendments, internal water storage and combined layered systems) to improve their performance have been the subject of many studies, these studies have been conducted under distinct settings with varying environmental and design parameters, making it difficult to compare these systems in the same context. Hence, a comparative evaluation of these systems under identical setting is still lacking.

Moreover, the difference of performance between lined and unlined LID systems in stormwater quality and quantity control is not fully investigated. Lined LIDs are regulated in most jurisdictions to prevent groundwater contamination, however limited studies have determined the risk of stormwater contamination to the aquifers, as well as the recharge that can be achieved through direct infiltration in unlined systems, and the potential tradeoffs between these two mechanisms. Thus, due to the current knowledge gap on the liner's application, further research is needed to

evaluate the treatment and hydrologic performance of lined versus unlined systems and to determine if lined systems are essential to protect the groundwater quality.

Additionally, lack of continuous field data leads to challenges in assessing the performance of LID systems under various conditions and impact of environmental factors on their performance such as the storm regime, seasonality and aging. Moreover, limited data hinders developing accurate models that can be used for future predictions and strategic planning on the long-term performance of LIDs.

1.3. Research Goals and Objectives

The overall goal is to analyze and compare treatment and hydrological performance of various LID designs under same conditions aiming to identify the enhanced properties sand filter and bioretention systems. To achieve this overall goal, the study was divided into four major thrusts with specific research objectives of:

1.3.1. Pilot-scale Study – Column Experiments

The first research objective is to identify an enhanced bioretention media design using bioretention columns experiments.

The results of the pilot-scale study answer the following questions:

- What are the differences and limitations of sand and standard bioretention media?
- What are the alternative native and abundant media that could provide cost-effective and enhanced filtration media?
- Could the use of manufactured sand from limestone and recycled glass improve the treatment performance of bioretention systems?
- How the use of vegetation improves pollutant removal and to what extent?

1.3.2. Field-scale Study – LID Testbed

The second research objective is to evaluate performance of three parallel different LID designs under same conditions in a single full-scale LID testbed.

The results of the field-scale study answer the following questions:

- How performance of different LID designs compares under same climatic, hydrologic and hydraulic, and pollution load conditions?
- What are the water quality differences between treating stormwater with sand filter and bioretention basins? And different bioretention media?
- What are the water quality differences between treating stormwater with and without liners?
 And how much recharge can be generated in an unlined system?
- How water quality treatment is affected by the use of internal water storage (IWS) and how it impacts recharge and outflows?

1.3.3. Stormwater Modeling and Analysis

The third research objective is to assess effectiveness of LID under changing conditions and different scenarios, and also to assess capability of different stormwater quality models in generating accurate predictions.

The results of the stormwater modeling and analysis answer the following questions:

- How the hydrologic performance of different LID designs compares and what's the mass balance in each individual cell?
- How the performance of different LID design compares under long-term continuous simulation?
- How much recharge can be achieved in unlined cells over long-term continuous simulation?

CHAPTER TWO: PILOT TEST - COLUMN EXPERIMENTS

This chapter describes the first phase of the study, where we conducted series of column experiments to examine treatment performance of different conventional filtration media, and custom innovative blends. The objective was to identify best performing filtration media and identify custom enhanced filtration media by using native and cost-effective alternatives in the filtration media's composition.

2.1. Introduction

Low impact development (LID) practices or green infrastructure (GI) are strategies used to mitigate the adverse impacts of urbanization on the hydrologic regime and the environment by restoring the natural hydrologic flow (US EPA 2007). LID practices control stormwater quantity by mimicking the natural flow, and enhance stormwater quality through natural physical, chemical, and biological treatment processes (Prince George's County 1999; US EPA 2007). The treatment performance of LID practices is dependent on the design components such as media composition and local conditions such as climate, leading to variable performances. The literature indicates that some LID practices fail to remove some pollutants: for instance, several studies show leaching of nutrients such as phosphorus and nitrogen species (Ahiablame et al. 2012; Barrett 2003; Eckart et al. 2018; TCEQ 2005; Wang et al. 2019).

Two of the most commonly used LID stormwater control measures—especially in arid and semi-arid regions—are bioretention and sand filter basins. Studies have shown that sand filter basins perform well in reducing the peak flow and runoff volume as well as removing particulate pollutant. However, they are not effective in the removal of dissolved pollutants (Barrett 2003; Shahrokh Hamedani et al. 2019; Zarezadeh et al. 2018). On the other hand, bioretention systems

have the potential to improve the removal of dissolved pollutants because of the chemical and biological processes that occur within the soil media and plants, including adsorption, biotransformation, bioaccumulation, and bio-uptake (Davis et al. 2010; Hsieh and Davis 2005b; US EPA 2007). One limitation of bioretention systems is the high nutrient content of the bioretention soil mixtures that can lead to high effluent nutrient concentration, and subsequently eutrophication (TCEQ 2005). Furthermore, bioretention systems might retain the antibiotic-resistant bacterial communities in the stormwater, leading to contaminated soil and plants that can later be transmitted to humans (Scaccia et al. 2020).

Numerous studies have investigated impacts of soil media, soil amendments, and vegetation on the performance of bioretention systems. Hsieh and Davis (2005a) examined the impact of media characteristics on removal efficiencies by conducting field and pilot tests. The authors observed consistent removal rates for oil/grease and heavy metals, while nutrient removal rates were inconsistent both in the bioretention columns and on-site facilities. Nutrient removal was impacted by the runoff flow path through the media and the contact time, whereas the removal of heavy metals was directly linked to the adsorption capacity of the soil media (Blecken et al. 2009; Davis et al. 2010; Hsieh and Davis 2005a). More than 90% of the heavy metals were captured by the bioretention media, while the role of plants was found to be less significant (Sun and Davis 2007). Barrett et al. (2013) observed greater pollutant removal efficiencies for bioretention soil mixtures compared to the sand filter medium. The results of this laboratory column study showed nutrient export of as much as twice the influent concentration for the bioretention soil mixtures alone, while a significant nutrient removal enhancement was achieved after the addition of plants. Therefore, vegetation was identified as the key component of the bioretention systems for the effective removal of nutrients (Barrett et al. 2013; DelVecchio et al. 2017; Limouzin et al. 2011). Studies

have also reported enhanced and consistent pollutant removal by the use of engineered soil mixtures with added soil amendments such as biochar and spent lime in the bioretention systems (Guo and Urbonas 2009; Shrestha et al. 2019; Tian et al. 2019; Ulrich et al. 2017; Wan et al. 2017; Yang et al. 2020).

Although bioretention systems and sand filters have shown improved stormwater quality, they are still not widely applied, mainly due to the perceived high capital and operation costs. Therefore, the use of abundant or recycled materials can be very beneficial. One of the alternative and inexpensive materials that has been used in wastewater treatment filtration systems is crushed recycled glass (CWC 1995; Elliot 2001; Horan and Lowe 2007; Rutledge and Gagnon 2002). Horan and Lowe (2007) found that use of recycled glass as a tertiary filter medium reduces media usage by 10% and treats 10% more flow with up to 70% TSS removal. Elliot (2001) recommended recycled glass as a substitute for sand because of its satisfactory filtration performance, lower cost, and durability that makes it more economical. Barrett et al. (2013) and Limouzin et al. (2011) have suggested the use of limestone gravel in the sub-merged zone of the bioretention systems for the further removal of phosphorus. Limestone is a natural mineral composed of calcites—principally calcium and magnesium carbonates (CaCO3, MgCO3) resulting in high adsorption capacity. Previous studies have found limestone effective in the removal of phosphorus through the adsorption and formation of hydroxyapatite (Ca₅(PO₄)₃OH) (Mateus et al. 2012; Oates 2007), and heavy metals through adsorption and precipitation processes (Aziz et al. 2001, 2008; Oates 1998). At low concentrations, metals adsorb to the calcite surface via exchange, while at high concentrations, the precipitation of metal oxides and metal carbonates is the dominant removal process (Aziz et al. 2008). Limestone is also widely available and is

relatively inexpensive worldwide, since about 10% of the earth's land surface is covered with limestone deposits (Oates 1998).

The objective of this study was to analyze and compare the treatment performance of different sand and bioretention soil mixtures enriched with alternative materials. In particular, this investigation aimed to answer whether the use of manufactured sand from limestone and recycled glass could improve the treatment performance of bioretention systems. To answer this question, pilot-scale column experiments were designed to test the treatment performances of nine different soil media. The column experiments were carried out in three main phases. The objectives of the first phase were to compare sand to the commonly used standard bioretention soil mixture and also to introduce potential native and abundant media that could reduce the cost and enhance the pollutant removal efficiencies. Initial results suggested im-proved removal efficiencies for the limestone sand, as the native and abundant media. In the second phase, a new bioretention soil mixture was manufactured by substituting regular sand with limestone sand in the media composition. After identification of the two best performing media, the impact of vegetation on pollutant removal rate was investigated in the third phase by studying the performance of three drought-tolerant plants.

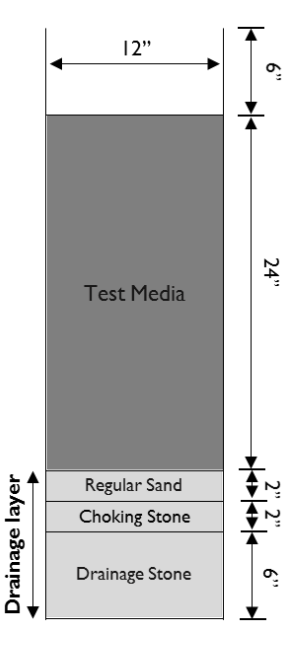
2.2. Column and Media Specification

A series of column experiments were carried out under three main phases. The objectives of the first phase were to compare the sand to the commonly used standard bioretention soil mixture, and also to introduce potential native media that could reduce the cost and improve the treatment performance. Initial results suggested improved removal efficiencies for the limestone sand, as native media, compared to other tested media. Thus, the second phase of tests was developed with objective of producing an innovative bioretention design using limestone sand instead of silica-

based sand in the standard bioretention soil mixture, and to compare their removal efficiencies.

After identification of two best performing media, the column experiment proceeded to the third phase to study impact of vegetation on treatment performances for synthetics stormwater.

In order to maintain consistency and to reduce the impacts of environmental variables, the column experiments were conducted in a controlled greenhouse environment. A total of twelve columns 101.6 cm (40 in) in height with 30.5cm (12 in) internal diameter were built using PVC pipes (Figure 2- 1). The columns had three main layers following the typical design of bioretention systems prescribed by the San Antonio River Authority (SARA) LID Technical Design Guidance (Dorman et al. 2013). The drainage layer consists of 15.2 cm (6 in) of drainage stone (ASTM#57) on the bottom, 5.1 cm (2 in) of choking stone (ASTM#8), and 5.1 cm (2 in) of regular sand (ASTM#9). The 61 cm (24 in) of filtration layer contains the test media and the transparent bowl (15.2 cm-6 in) is placed on top of the columns to hold the vegetation in the last phase of the experiment.



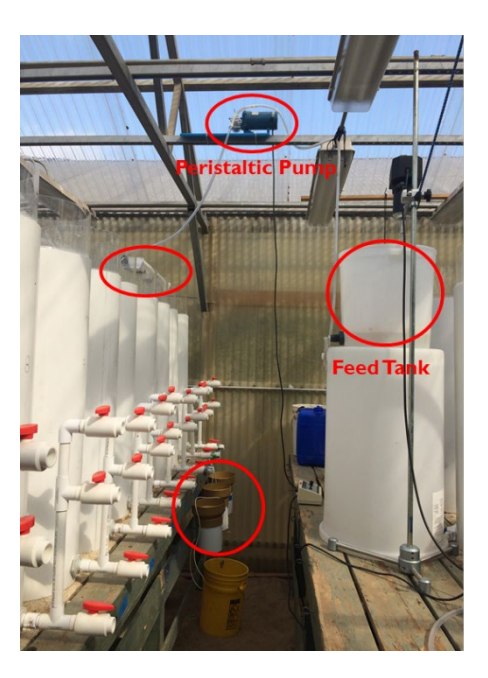


Figure 2- 1. Profile of columns composition and injection apparatus including feed tank, agitator, peristaltic pump and distributing gutter; and rain gauges to record outflow.

A total of nine different soil media were tested in phase one and two of the column experiments, including:

- Regular **Sand**: silica-based sand that is typically used in sand filter basins.
- Limestone Sand (Man. Sand): manufactured sand from crushed limestone.
- **Biofilter532**: sandy loam commonly used in bioretention areas manufactured with regular sand, fines, and biosolids as organic matter.
- Recycled Glass+Biofilter532 (**R.G.+Biofilter**): blend composed of half recycled glass and half Biofilter532.
- Lime-Mix: mixture of limestone sand and clay-loam (25% crushed limestone sand, 70% clay-loam and 5% of hardwood mulch).
- **Blend#1**: blend of limestone sand, fines and organic matter following the standard bioretention soil mixture specifications.
- **Blend#2**: the iron-amended version of Blend#1.
- **Biofilter433**: the improved version of Biofilter532. This media has green waste as organic matter instead of biosolids to reduce the phosphorus content.
- **Biofilter433MS**: has a similar composition of the Biofilter433 with use of limestone sand instead of regular sand.

Prior to running the column tests, sieve analysis and hydraulic conductivity tests were performed on the media. Sieve analysis was conducted following the ASTM standard method C33/C33M and C136/C136M, which provides characterization of the size distribution of each media. The hydraulic conductivity and porosity tests were performed according to the ASTM standard methods F1815 and C20, respectively. The Synthetic Precipitation Leaching Procedure

(SPLP) test (SW-846 Test Method 1312) was also performed to determine the pollutant content of the soil media prior to the column tests.

2.2.1. Column Experiments-Phase I

The first four media were tested in the first phase of the study. Sand and Biofilter532 were tested to compare the performance of sand filters versus bioretention areas. Additionally, two alternative media including crushed recycled glass and limestone sand were selected with the purpose of (1) water quality performance enhancement and (2) cost reduction. Recycled glass was chosen because of its low cost and abundance, and also due to its filtration capacity (CWC 1995; Elliot 2001; Horan and Lowe 2007; Rutledge and Gagnon 2002). A half and half blend of recycled glass and Biofilter532 was manufactured. Limestone sand was selected considering its lower cost as native and abundant material and its high adsorption capacity due to its chemical composition (Barrett et al. 2013). Limestone is widely available and is relatively inexpensive throughout the United States. According to Oates (2007), over 70% of the total quarries in the country for construction and building use is limestone.

2.2.2. Column Experiments-Phase II

A limestone-based bioretention soil mixture (Lime-Mix) was manufactured in the UTSA concrete laboratory following the standard bioretention soil mixture specifications by San Antonio River Basin LID Technical Guidance Manual (Dorman et al. 2013). Because the Lime-Mix was not reproducible in large volumes due to the limitations of laboratory equipment, local material supplier companies were contacted to produce customized mixtures using limestone sand. Accordingly, the second phase of the column test was performed by testing media 5 to 9 from the media list.

2.2.3. Column Experiments-Phase III

After identifying the top two filtration media, the columns were emptied out, cleaned, and filled with these two media (6 columns of each) to test the vegetation impact. Three native plants – Pink Muhly (Muhlenbergia capillaris), Inland Sea Oats (Chasmanthium latifolium) and Frogfruit (Phyla nodiflora) – were added to the columns to determine if and to what extent plant uptake assists in pollutant removal.

2.3. Synthetic Stormwater

The influent pollutant concentrations were based on a study of bioretention performance for stormwater quality improvement in Texas (Li et al. 2010). The synthetic stormwater was made using deionized (DI) water and chemical salts as shown in Table 2- 1. The requisite volume of pollutant stock solution was added to the designated volume of DI water to attain the targeted influent concentration (C_{in}^{Target}). The concentrations of all the pollutants in the stock solution were tested prior to the experiments.

Table 2- 1. Targeted concentration (mg/L) of pollutants, required volume of stock solution for 5 gallons DI water and chemicals used in manufacturing the stock solution.

Pollutant	Target Concentration C_{in}^{Target} (mg/L)	Stock Solution (mL)	Chemicals (salts)			
TSS	100		Solids (<150 μm)			
Nitrate (NOX) as N	0.3	1.89	Potassium Nitrate (KNO ₃)			
Total Kjeldhal Nitrogen (TKN) (Org N + NH3-N)	1.85	189.27	Nicotinic Acid (C ₆ H ₅ NO ₂) Ammonium chloride (NH ₄ Cl)			
Total Phosphorus (TP)	0.2	1.89	Mono-potassium phosphate (KH ₂ PO ₄)			
Total Copper (TCu)	0.02	1.89	Copper(ll) Sulfate (CuSO ₄)			
Total Zinc (TZn)	0.13	1.89	Zinc Chloride (ZnCl ₂)			
Total Lead (TPb)	0.08	18.93	Lead Nitrate (PbNO ₃)			
Buffer (M)	0.05 M	0.189	Sodium carbonate anhydrous (Na2CO3)			

The solids used in the synthetic stormwater were collected from the accumulated sediments in one of the UTSA sand filter basins' pre-treatment chamber, which drains 6.5 ha (16 acres) including a parking lot, two avenues and a natural area. A pH of 7.4 was used for the synthetic stormwater in accordance to previous stormwater data at UTSA main campus (Zarezadeh et al. 2018), using a 0.5 M carbonate buffer and adjusting with sodium hydroxide (NaOH) or hydrochloric acid (HCl) as needed.

2.4. Experimental Procedure

The column experiments mimic a rainfall event with total depth of 30 millimeters (1.2 inches) and duration of 4±0.5 hours, which is the median duration of such rainfall events in San Antonio, Texas. The median duration was estimated from 40 years of rainfall records, in 15-minute time intervals from the weather station (COOP: 417422) located at the Randolph Air-Force Base at Universal City. The injection volume was calculated based on the column volume considering the porosity of all column layers. The injection rate was calculated as 150 mL.min⁻¹ for all columns and the injection duration was adjusted for each column considering the injection volume calculated based on the porosity of media.

The pumping apparatus consisted of a 30.2 L (8-gallons) feed tank, agitator engine and propeller, peristaltic pump with 10 mm (3/8 in) tubing, and distributing gutters. The synthetic stormwater was constantly mixed by the propeller in the feed tank to maintain homogeneity and was delivered to the columns by the peristaltic pump. A distributing gutter with two orifices was used to inject two columns of same media simultaneously. The water level in the gutter and the orifices' flowrate were monitored throughout the experiment to maintain consistency, and the feed

tank was refilled to sustain the desired injection rate and total volume of 150 mL/min and ~38 liters (10 gallons), respectively.

Column runs were performed in triplicates for the first phase and duplicates for the second phase for each media type. Two influent samples (300 mL) and ten timed effluent samples (300 mL) were collected. After collecting the initial effluent sample, samples were taken every 15 minutes for the first hour, and every 30 minutes for the remaining run time. A total of 12 samples per column were collected and stored at 4 °C.

2.5. Water Quality Analysis

The collected influent and effluent samples were tested for following water quality parameters: Total Suspended Solids (TSS) [mg/L]; Orthophosphate (P) and Total Phosphorus (TP) [mg/L of PO₄³⁻]; Nitrate (N) and Total Nitrogen (TN) [mg/L as NO₃⁻-N]; Dissolved and Total concentration of metals including Copper, Zinc and Lead [µg/L]. The sample preparation, storage and analysis complied with the Standard Methods for the Examination of Water and Wastewater (APHA, AWWA, WEF 2012). The instruments and methods used for analyses are listed in Table 2- 2. The persulfate method (SM4500P, SM4500N) was used for digesting the samples to determine the total nutrient concentration. After digestion, colorimetric methods (Table 2- 2) were used to determine total phosphorus and total nitrogen concentrations.

The mean influent and effluent concentrations were determined to calculate the removal rate using following equation:

$$RR(\%) = \frac{\bar{C}_{in} - \bar{C}_{out}}{\bar{C}_{in}} \times 100 \tag{1-1}$$

where \bar{C}_{in} and \bar{C}_{out} are the mean influent and effluent concentrations for a particular pollutant.

Table 2-2. Water quality parameters, units, methods, instrumentation, and detection limits.

Parameter	Units	Method	Instrument	Detection limit
TSS	mg/L	US EPA gravimetric method	Desiccator, furnace	NA
Phosphorus	mg/L	PhosVer 3® ascorbic acid method (SM4500-P)	HACH® DR 2800	0.02 to 2.5
Nitrogen	mg/L	NitraVer® 5 cadmium reduction method (SM4500-NO ₃ ⁻)	HACH® DR 2800	0.3 to 30.0
Heavy metals	μg/L	Acid digestion/preparation	PerkinElmer NexION 350 ICP-MS	0.0005 and 0.001*

^{*} Detection limit of 0.0005 μ g/L for lead (Pb) and copper (Cu), 0.001 μ g/L for zinc (Zn)

2.6. Statistical Analysis

To examine the removal efficiencies of each type of media and to determine whether the mean influent and effluent concentrations are statistically different, t-tests and non-parametric Wilcoxon test were performed at a confidence level of 95% (p<0.05). Significance of differences between mean effluent concentrations was examined at same confidence level (p<0.05). Shapiro-Wilk test was performed to determine normality of the dataset. F-test was performed to test the variances and to determine the type of t-test for each dataset (Bartlett F-test for normal and Levene's F-test for non-normal distribution).

2.7. Results and Discussion

2.7.1. Media Physical and Chemical Properties

The sieve analysis results showed the recycled glass blend (R.G.+Biofilter) had the coarsest particle size distribution, whereas Biofilter433 had the highest percentage of fine media (72.32%) resulting in slower water movement and the lowest hydraulic conductivity of 19.3 mm/hr (0.76 in/hr) (Table 2- 3). The recommended bioretention soil media specification requires an infiltration rate of 12.7-152.4 mm/hr (0.5-6 in/hr) and suggests 25.4-50.8 mm/hr (1-2 in/hr) for comprehensive pollutant treatment and better hydrologic benefit (Dorman et al. 2013). As for size distribution, the

manual requirements are 85-88% sand passing through 6.35 mm (1/4 in) sieve, 8-12% fines passing through #270 sieve (0.053 mm) and 2-5% of organic matter (Dorman et al. 2013). All the bioretention soil media meet the infiltration rate criteria except for Biofilter433MS and R.G.+Biofilter with hydraulic conductivity of 344 and 616.2 mm/hr, respectively. As for the chemical composition, SPLP (Synthetic Precipitation Leaching Procedure) results (Table 2-3) indicated the highest nutrient content in Biofilter532 and Biofilter-433 and 433 MS, as well as higher copper content compared to the other soil media. It should be noted that the initial SPLP pollutant content corresponds to leaching and mobility of these pollutants under rainfall and does not match to the total pollutant content of the media samples.

Table 2-3. Physical and Chemical properties of the tested filtration media

Media [(No#) Name]	Si Distrib		Organic Matter	Hydraulic Conductivity	pН	Total P	Total N	Total Cu	Total Pb	Total Zn
[(No#) Name]	270	1/4	(%)	in/h		mg/kg	mg/kg	μg/kg	μg/kg	μg/kg
(1) Regular Sand	0	100	0	14.8	7.7	0.8	14.4	42.0	30.8	581
(2) Manufact. Sand	0	100	0	43.1	9.0	2.6	11.4	44.8	16.4	401
(3) Biofilter532	23.9	100	5.8	2.4	8.3	56.6	59.4	299	23.2	745
(4) R.G.+Biofilter	1	96	2.9	24.3	8.3	35.4	27	187	14.4	466
(5) Lime-Mix	22.0	100	5.0	2.4	9.4	9.8	43.4	117	7.8	419
(6) Blend#1	38.0	100	1.4	1.4	8.9	6.8	29	57.6	10.4	458
(7) Blend#2	38.0	100	1.4	1.3						
(8) Biofilter433	72.3	100	3.9	0.8	8.4	23.1	81.6	190	21.4	602
(9) Biofilter433MS	30.9	100	3.7	13.5	8.6	23.6	88.8	160	17.6	382

^a (%) passing through sieve 1/4in (6.35 mm) and #270 (0.053 mm)—Not measured, should be same as Blend#1.

2.7.2. Water Quality Analysis

This section presents the water quality results for all performed column tests in terms of mean influent and effluent concentrations and removal rates for TSS, P and TP, N and TN, and dissolved and total copper, zinc and lead. The boxplots represent the median (central line), first and third quantile (box), minimum and maximum concentrations (whiskers), outliers (red plus) and the

mean influent (green circle) and mean effluent (blue diamond) concentrations of pollutant for each media.

Column Experiments – Phase I

The mean influent and effluent concentrations of the collected samples and the removal efficiencies for the four media tested in phase one are shown on Table 2- 4 and Table 2- 5 and in Figure 2- 2 and Figure 2- 3. The results indicate high TSS removal rates ranging from 91.6% (p=0.005) to 84.6% (p=0.0003) for Sand, Man.Sand and Biofilter532, respectively (Table 2- 5). The high standard deviation of influent TSS concentrations (Table 2- 4) reflect fluctuations in the influent TSS, which was caused by the partial accumulation of sediments inside the distributing gutter as well as the natural difference in the matrix of solids that were used in the preparation of each batch of the synthetic stormwater. The large variations between the median (central line) and mean influent concentrations (green circle) in the boxplots (Figure 2- 2) indicate the influent inconsistencies. Subsequently, these TSS fluctuations led to inconsistencies of the influent pollutant concentration for each column test (Table 2- 4).

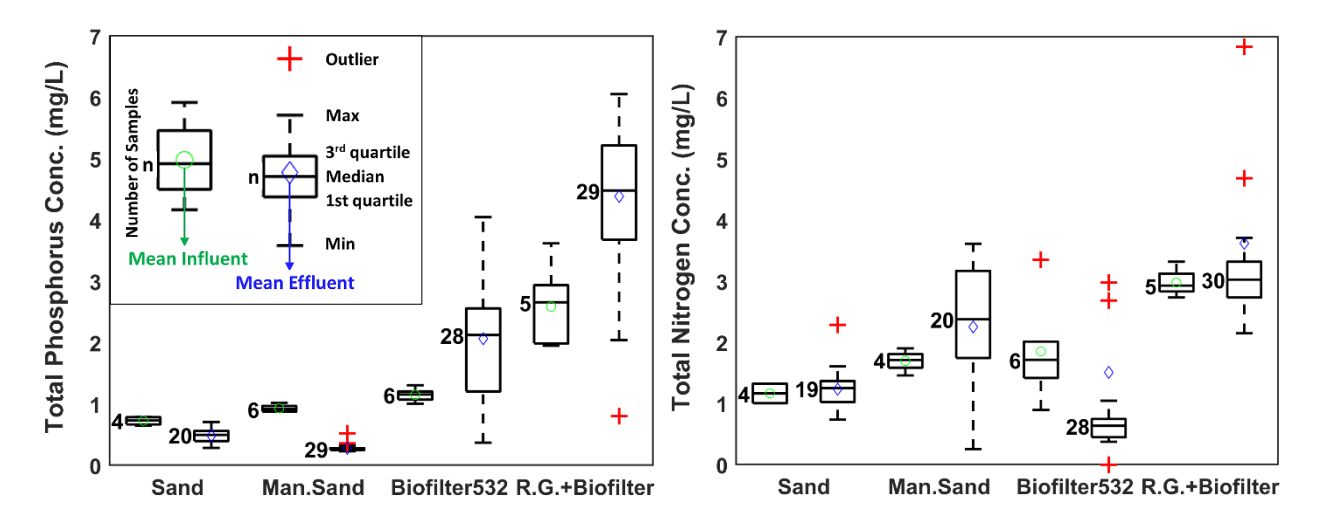


Figure 2- 2. Paired boxplots of influent and effluent concentration for TP and TN (mg/L)

The nutrient removal rates varied greatly for different media (Table 2- 5 and Figure 2- 2). Several measurements were not obtained for nitrate and orthophosphate (Table 2- 4) due to color interference in the colorimetric measurements. A dark yellowish color in the effluent samples was observed, likely due to high dissolved organic matter or iron content in the Biofilter532, leading to unreliable measurements. Due to inaccuracies caused by color interference in the colorimetric measurements, TP and TN are more reliable water quality indicators for further assessments (Figure 2- 2). The highest P and TP removal rate of 93.1% and 70.3% was achieved by limestone sand (Man.Sand) (p=0.0001, p=0.0001). Sand performed poorer for treatment of both dissolved and total phosphorus with removal rate of 49.8% and 46.1%, respectively (p<0.0001 and p=0.003). On the other hand, negative removal rates of TP for Biofilter532 (p=0.038) and R.G.+Biofilter (p=0.009) indicate leaching of phosphorus (Table 2- 5).

Biosolids make up the 5.84% organic matter content of Biofilter532 resulted in a soil mixture with high phosphorus content of 108.96 ppm, which led to TP export and greater effluent concentrations (Figure 2- 2). Although the recycled glass mixture (R.G.+Biofilter) has half phosphorus content of the Biofilter532, higher mean effluent TP concentration was recorded (Figure 2- 2) due to higher inlet TP concentration. However, the removal efficiencies are greater for the R.G.+Biofilter that could be explained by ten times smaller hydraulic conductivity of the Biofilter532 (Table 2- 3) resulting in desorption of phosphorus through the effluent.

The concentration of nitrate in the sand effluent samples was significantly higher than in the influent (-108.3%, p=0.002), which was similar to the observations made in Austin sand filters (Barrett 2003). Man.Sand results also showed higher effluent nitrate concentration but with no significant difference (-35.4%, p=0.119) (Table 2- 5). Considering the TN concentrations, only Biofilter532 is removing 12.3% of the total nitrogen (p=0.003) while other media show increased

effluent TN concentration (Figure 2- 2) (p=0.675, p=0.112, p=0.782 for Sand, Man.Sand and R.G.+Biofilter, respectively). Nitrate removal is achieved through denitrification processes which require an anaerobic environment (saturated zone) (Barrett et al. 2013; Chen et al. 2013; Davis et al. 2010; Dorman et al. 2013). Therefore, fast water movement and short contact time does not provide the suitable environment for denitrification and leads to poor nitrate removal, except for Biofilter532. Its small hydraulic conductivity (61 mm/hr, Table 2- 3) allowed saturation and longer contact time, which promoted denitrification and nitrate removal accordingly.

The recorded heavy metal concentrations indicated higher removal rates for total metals compared to dissolved metals for all four media (Figure 2- 3,Table 2- 5), likely caused by high removal of particulate contaminants through sedimentation and filtration (Davis et al. 2010). The boxplots show large variations between the median (central line) and mean influent concentration (green circle) values (Figure 2- 3), which indicate the inconsistencies caused by the varying TSS of the influent and consequently the concentration of heavy metals. The removal of dissolved metals on the other hand, occurs through biological and chemical mechanisms and is highly dependent on the adsorption capacity of the filtration media (Davis et al. 2010).

The total lead had the smallest mean effluent concentrations (p<0.005), ranging from 0.14 to 3.58 μ g/L, indicating highest removal efficiencies (98.6% average removal rate) of the three examined metals. Total zinc concentrations indicated an average removal rate of 93.3% (p<0.03) representing the second-best treatment among the metals with no significant difference between the effluent concentrations except for R.G.+Biofilter (p<0.04). On the contrary, significant difference is observed in copper removal rates and effluent concentrations (p<0.0001) (Table 2-3, Table 2-5) with highest mean effluent total copper concentration of 55.14 and 46.54 μ g/L for Biofilter532 and R.G+Biofilter, respectively (p=0.0002, p=0.34) (Figure 2-3).

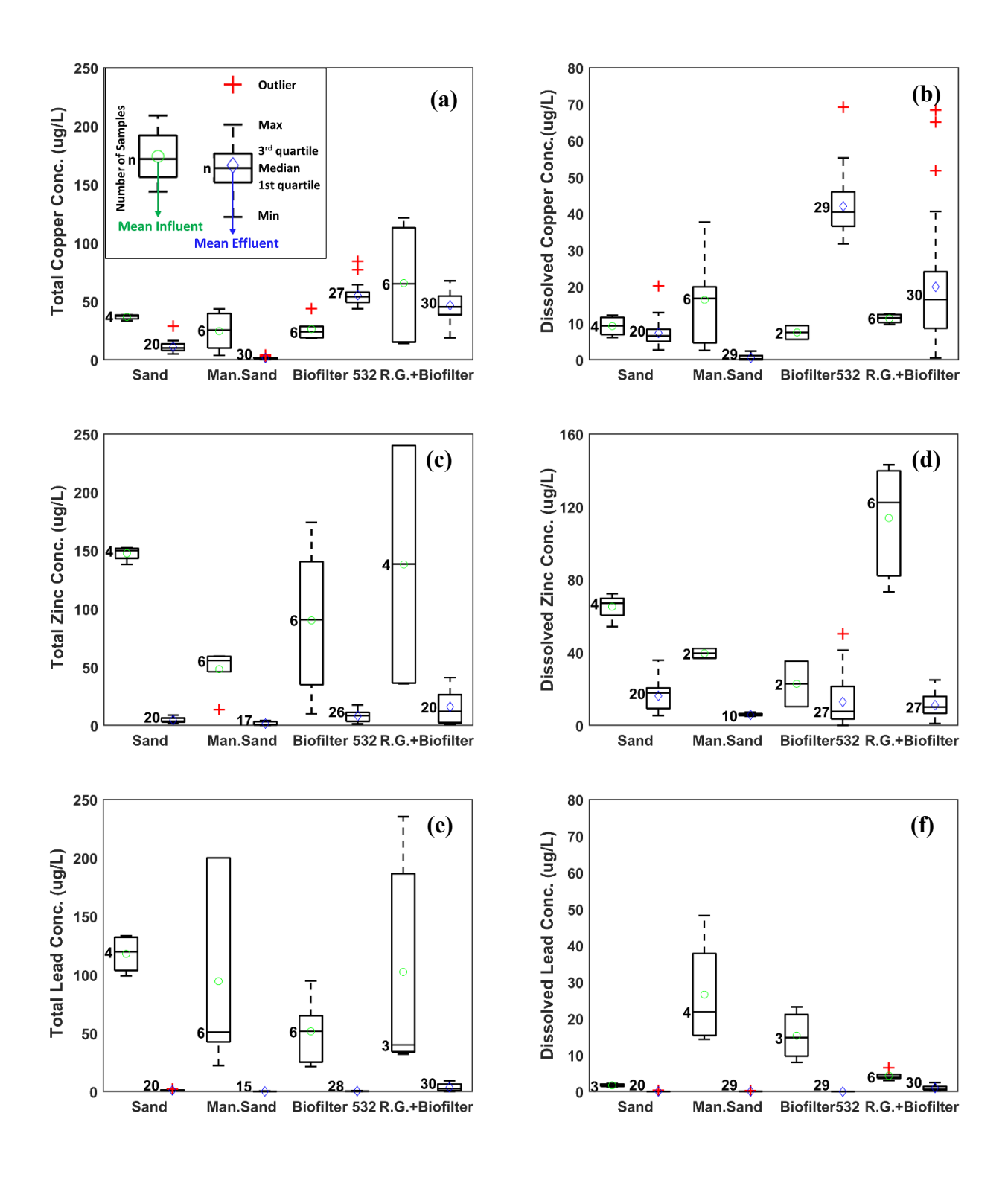


Figure 2- 3. Paired boxplots of influent and effluent concentration for dissolved and total heavy metals including (a,b) Copper (μ g/L), (c,d) Zinc (μ g/L) and (e,f) Lead (μ g/L) – Phase I.

Leaching of copper by bioretention media has also been reported by previous studies (Li and Davis 2008; Li Houng and Davis Allen P. 2009; Wang et al. 2019) indicating that association of copper with organic matter leads to more copper in the effluent. Since higher organic matter is correlated with phosphorus content and export, copper and phosphorus concentration are intercorrelated subsequently.

Removal efficiencies for dissolved metals show greater discrepancies between the tested media (Figure 2- 3, Table 2- 3). Similar to the total copper measurements, poor dissolved copper treatment of 20.3%, -461.3% and -77.3% is achieved for Sand, Biofilter532 and R.G+Biofilter, respectively (Table 2- 5). Biofilter532 had the highest dissolved copper concentration with significant difference from the influent (p=0.022), whereas Sand and R.G+Biofilter showed no significant difference (p = 0.1631 and 0.4323). Man.Sand reached superior treatment performance for all dissolved heavy metals compared to Sand (p<0.05) (Table 2- 5).

The Man.Sand performed best at removal of dissolved and total heavy metals with significantly lower effluent concentration for all measured elements (p<0.03). On the contrary, recycled glass addition to the Biofilter532 led to lower removal efficiencies for lead (p<0.0001) and total nitrogen (p<0.0001) due to its coarse particle size and fast water movement. Thus, Limestone sand was selected as the substitute media to generate the enhanced bioretention soil mixture.

Column Experiments – Phase II

Phase II of the experiments tested five bioretention mixes including four limestone blends and one standard bioretention mixture (Table 2- 5). The TSS measurements of the tested media in phase two was in agreement with the results of phase one, indicating overall high removal efficiency (≈90%). The boxplots in Figure 2- 4 show TP and TN removal for limestone mixtures, standard bioretention mixtures and Sand.

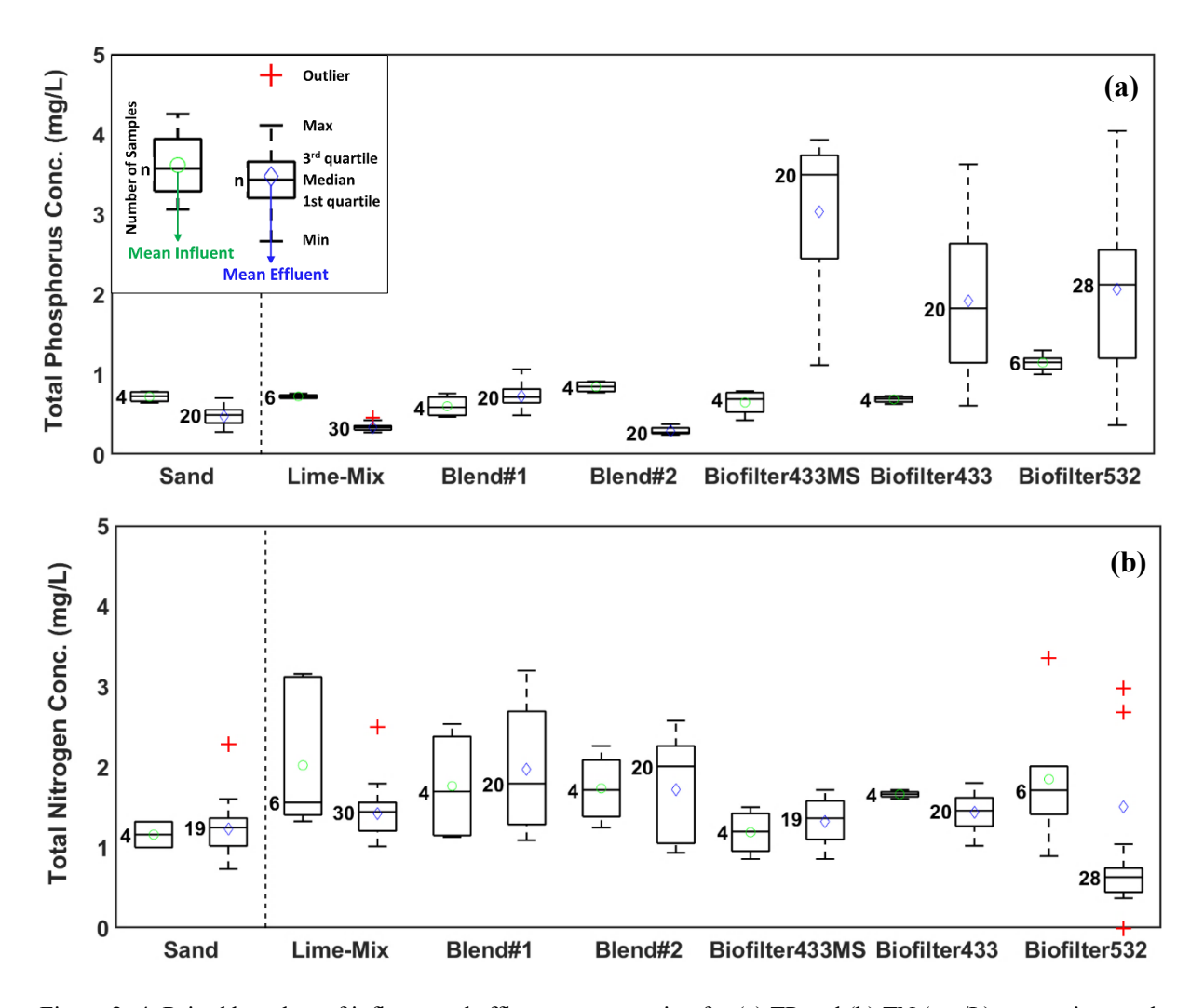


Figure 2- 4. Paired boxplots of influent and effluent concentration for (a) TP and (b) TN (mg/L) comparing sand to the standard and customized bioretention soil mixtures (phase I and II).

The four customized limestone mixtures showed considerable improvement in treatment of TP, and relatively smaller mean effluent concentration, except for Biofilter433MS (APPENDIX, Table A1). The Lime-Mix and Blend#2 had the highest TP removal efficiencies of 53.2% and 65.2%, respectively (p=0.0001, p=0.0021), while Blend#1 showed relatively similar influent and effluent concentrations (p=0.13) with slight leaching of 29.7% (Table 2- 5). The Biofilter433 showed slightly reduced effluent TP concentration compared to Biofilter532 (p=0.457), which indicated that use of green-waste instead of biosolids in Biofilter433 was helpful and the organic matter and

phosphorus content was reduced to 3.9% and 23 mg/kg, respectively (Table 2- 3). Although the effluent TP concentration is smaller for Bifilter433, lower removal rate is achieved that is due to smaller influent concentration compared to the Biofilter532 (Table 2- 5). Addition of limestone sand to the soil mixture enhanced the TP removal up to 65.2% for Blend#2, however Blend#1 and Biofilter433MS still leached phosphorus with significantly different effluent concentrations (p<0.0001).

Moreover, bigger boxplots and longer whiskers for Biofilter433MS, Biofilter433 and Biofilter532 indicate greater discrepancy in the effluent concentrations over time, while the limestone mixtures show more consistent results (Figure 2- 4). As shown in Figure 2- 4, no significant difference was evident between the influent and effluent TN concentrations for all limestone mixtures (p=0.1, 0.392, 0.907, 0.289), with slight removal for Lime-Mix and Blend#2 (29.7% and 1%, respectively). The Biofilter433- similar to Biofilter532 - removed 13.3 % of TN (p=0.0008) and 59.3% of N (p=0.0029) due to its smaller infiltration rate (19.3 mm/hr, Table 2- 3) that provides the required saturated zone for denitrification processes.

The total metals influent and effluent concentrations were significantly different with high removal efficiencies of 99%, 95% and 68% on average for lead, zinc and copper, respectively. The boxplots of the dissolved heavy metal measurements are presented in Figure 2- 5 showing relatively higher dissolved effluent copper concentration compared to other metals. However, the limestone mixtures showed reduced values compared to the tested media in phase one (p<0.0001), which is indeed correlated with phosphorus removal. All tested bioretention mixtures in phase two performed better than Sand in removal of dissolved zinc (Figure 2- 5) with mean removal rates of 85.8%, while Sand only removed 75.2% of the dissolved zinc (p=0.002) (Table 2- 5).

Blend#1 and Biofilter433 were selected as the two top performing media for Phase three. Blend#1 was selected since (1) Lime-Mix is not reproducible and (2) potential impacts of additive iron (Blend#2) on groundwater quality were not studied; and Biofilter433 was the best bioretention soil mixture.

Table 2- 4. Mean influent and effluent concentration and standard deviation of measured water quality parameters - Phase I

		Mean Concentration ± Standard Deviation								
Water Quality Parameter	Sar	nd	Man.	Sand	Biofilt	er532	R.G.+B	iofilter		
	Influent	Effluent	Influent	Effluent	Influent	Effluent	Influent	Effluent		
TSS (mg/L)	85.50±8.99	7.35 ± 17.29	78.81±40.5	7.35 ± 13.68	69.00±42.25	13.38 ± 9.33	206.80±88.67	12.87±16.38		
Orthophosphate (mg/L)	0.50 ± 0.08	0.25 ± 0.09	0.69 ± 0.05	0.05 ± 0.05			2.33 ± 0.60	2.86 ± 1.13		
Total Phosphorus (mg/L)	0.72 ± 0.06	0.48 ± 0.11	0.93±0.16	0.28 ± 0.06	1.14 ± 0.06	2.06 ± 0.60	2.58±0.64	4.38 ± 0.74		
Nitrate (mg/L)	0.87 ± 0.05	1.81 ± 1.04	0.80 ± 0.18	1.08 ± 0.52						
Total Nitrogen (mg/L)	1.16 ± 0.16	1.24 ± 0.34	1.69±0.16	2.25 ± 1.14	1.86 ± 0.75	1.51 ± 4.06	2.98 ± 0.21	3.64 ± 1.62		
Dissolved Lead (µg/L)	1.69 ± 0.38	0.02 ± 0.08	26.58±13.44	0.07 ± 0.06	15.33±6.22	0*	4.35 ± 1.1	0.98 ± 0.67		
Total Lead (µg/L)	117.90 ± 14.61	1.09 ± 0.45	94.46±75.24	0.17 ± 0.14	51.57±24.63	0.35 ± 0.18	102.44±93.99	3.58 ± 2.99		
Dissolved Copper (µg/L)	9.24 ± 2.45	7.36 ± 3.88	16.42±11.53	0.57 ± 0.69	7.49 ± 1.88	42.02 ± 7.87	11.28±1.15	20.01 ± 16.96		
Total Copper (µg/L)	36.65 ± 2.00	11.18 ± 5.12	24.62±14.32	1.54 ± 0.81	26.30±8.76	55.14 ± 9.00	65.61±42.31	46.54 ± 11.92		
Dissolved Zinc (µg/L)	65.14 ± 6.67	16.16 ± 8.02	39.55±2.70	5.83 ± 0.68	22.78±12.49	12.87 ± 13.22	113.79±27.1	11.15 ± 6.53		
Total Zinc (µg/L)	147.56 ± 5.68	4.44 ± 2.13	48.21±16.15	1.61 ± 1.67	90.04±56.4	8.00 ± 5.52	138.11±101.9	15.89 ± 13.23		

^{*} Under detection limit considered as zero -- Missing values are due to color interference

Table 2-5. Removal efficiencies (%) of water quality parameters – Phase I and Phase II

Water Quality Parameter	Removal Efficiency (%)									
water Quanty Farameter	Sand	Man.Sand	Biofilter532	R.G.+Biofilter	Lime-Mix	Blend#1	Blend#2	Biofilter433MS	Biofilter433	
TSS (mg/L)	91.6	91.6	84.6	85.2	94.9	87.3	86.0	75.7	86.6	
Orthophosphate (mg/L)	49.8	93.1		-22.7	77.4	-32.9	89.1	-583	-266	
Total Phosphorus (mg/L)	46.1	70.3	-80.8	-69.4	53.2	-20.5	65.2	-380	-178	
Nitrate (mg/L)	-108	-35.4			4.0	-7.2	-3.7	-12.7	59.3	
Total Nitrogen (mg/L)	-6.25	-32.9	12.3	-22.2	29.7	-11.8	1.0	-11.3	13.3	
Dissolved Lead (µg/L)	98.9	99.9	100	77.4	95.9	100	100	95.0	99.8	
Total Lead (µg/L)	99.1	99.8	99.3	96.5		100	100	99.4	98.5	
Dissolved Copper (µg/L)	20.3	96.6	-461	-77.3	10.0	-71.5	-10.1	-28.4	-162	
Total Copper (µg/L)	69.5	93.8	-102	29.1	69.2	63.6	79.2	64.4	75.9	
Dissolved Zinc (μg/L)	93.2	95.9	64.9	90.2	89.7	92.1	98.3	93.8	87.0	
Total Zinc (µg/L)	89.0	87.9	85.7	88.5		94.6	87.8	91.7	96.2	

⁻⁻ Missing values are due to technical issues with colorimetric methods and ICP-MS

Column Experiments - Phase III

The treatment performance of Blend#1 and Biofilter433 was tested after plant addition to the columns to assess the impact of plant uptake on removal efficiencies and to determine whether different plant species (Inland Sea Oats, Frogfruit and Pink Muhly) impacted treatment performances differently. The water quality analysis results (Table 2- 5 and Table 2- 6) showed increased solids (TSS) in all effluent samples compared to phase two (p<0.0001). The mean TSS removal rate was reduced from 88% to 32% and 30% for Blend#1 and Biofilter433, respectively. This might be due to added mulch layers at the top of the columns, and transportation of solids through plant root canals within the media. Several previous studies have also reported higher TSS removal rates for non-vegetated bioretention cells compared to the vegetated ones (Wang et al. 2019). The Sea Oats columns showed smaller effluent TSS concentration (55% removal rate) compared to Frogfruit (35% and 20%) and Muhly (6 and 16%) for Belnd#1 and Biofilter433, respectively (p<0.0001, p=0.019) (Table 2-6).

On the other hand, there was significant improvement in nutrient removal, especially for Blend#1. Figure 2- 6 compares the P and TP concentrations for Blend#1 and Biofilter433 in phases two and three. The mean effluent concentrations indicated decreased phosphorus content to 0.08-0.12 (mg/L) and 0.3-0.35 (mg/L) for orthophosphate (p<0.0001) and total phosphorus (p=0.0015) of Blend#1 after addition of plants, respectively. No significant difference was observed between performances of different plants in removal of total phosphorus (p=0.095), whereas Muhly effluents had slightly higher orthophosphate concentration (p<0.0001). Conversely, the boxplots of Biofilter433 (Figure 2- 6) do not show any improvement in phosphorus removal and increased effluent phosphorus concentration with no significant difference between plants was observed (p=0.597, p=0.353 for P and TP respectively).

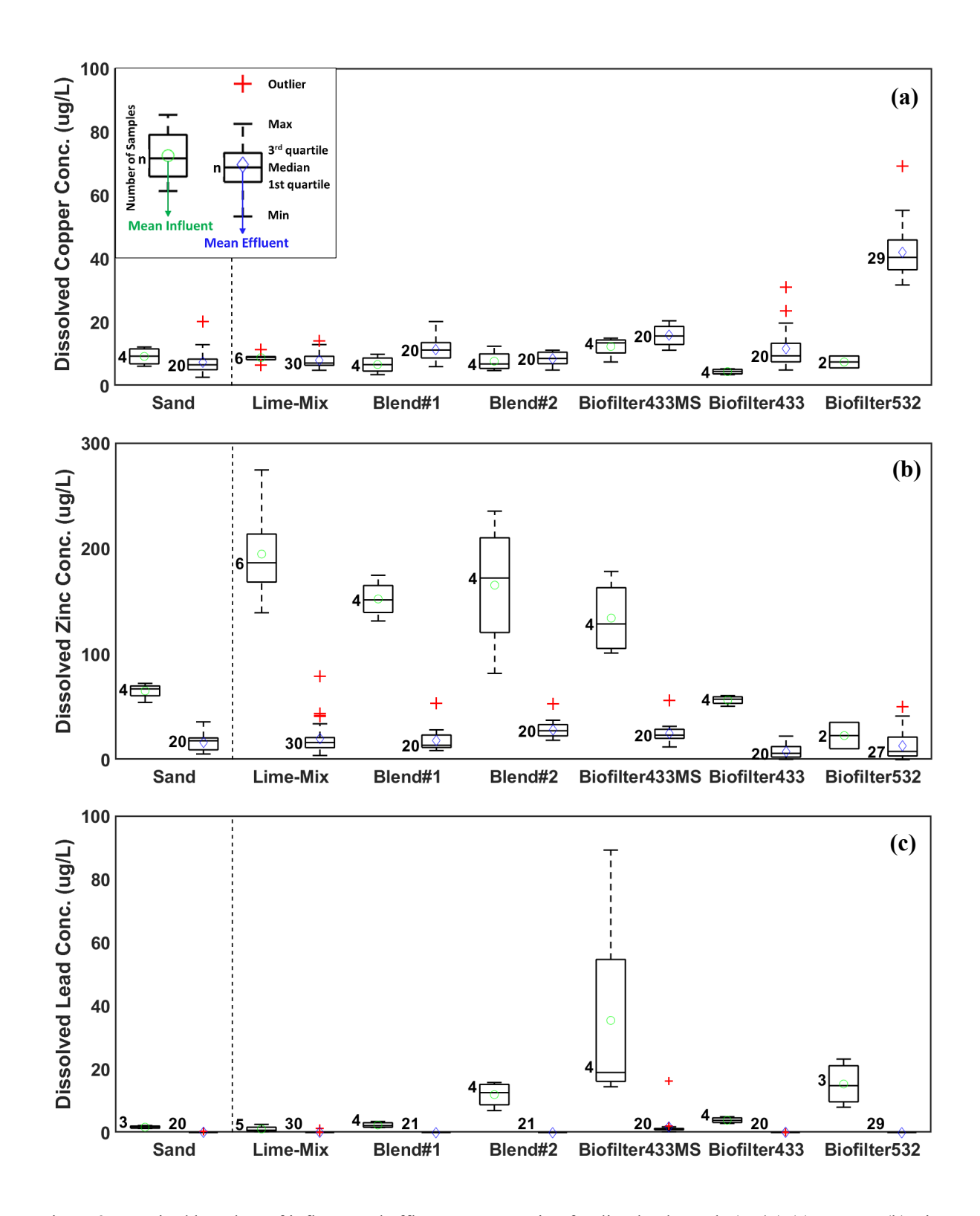


Figure 2- 5. Paired boxplots of influent and effluent concentration for dissolved metals (μ g/L) (a) Copper, (b) Zinc, and (c) Lead, comparing sand to the bioretention soil mixtures.

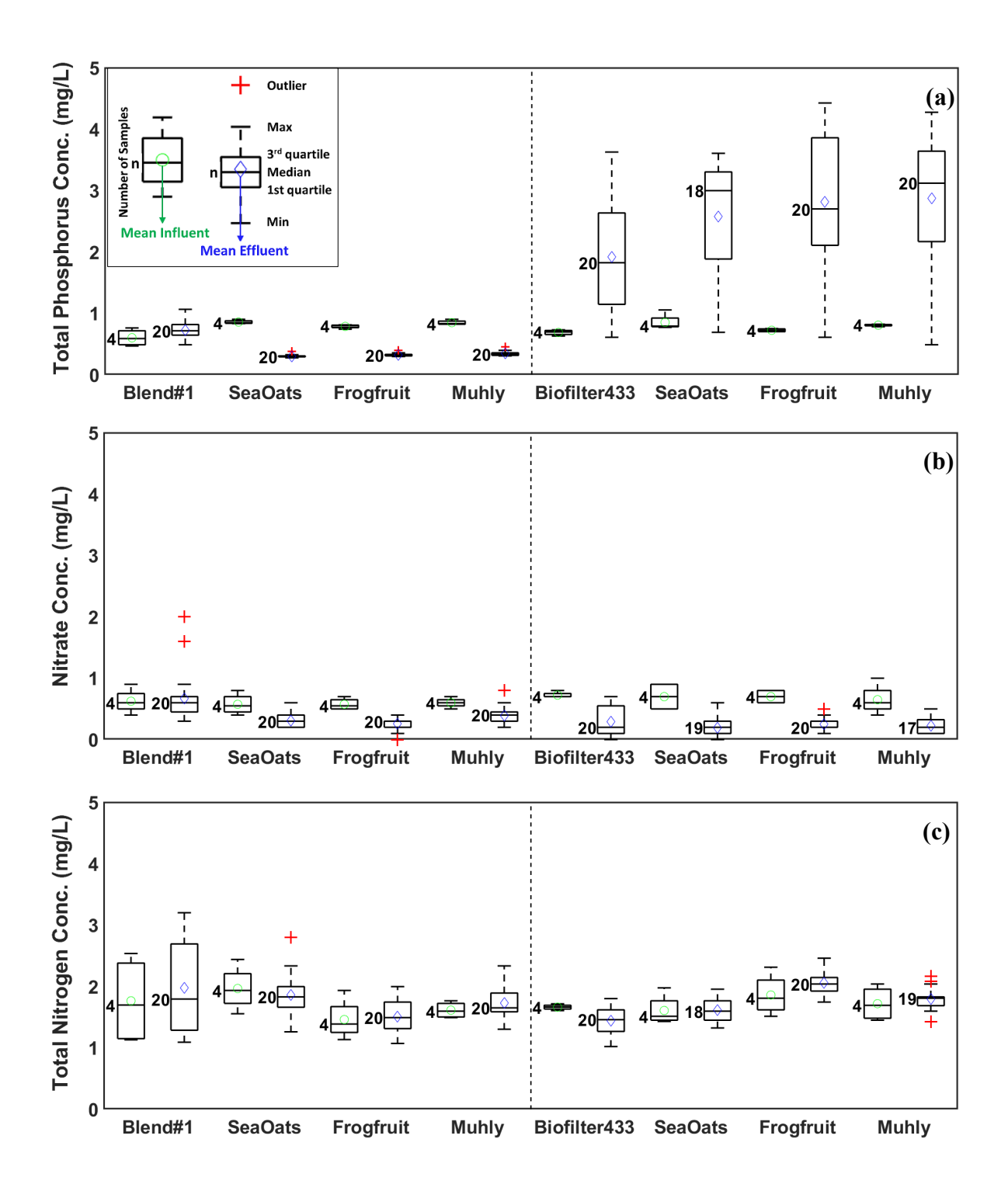


Figure 2- 6. Paired boxplots of influent and effluent concentration (mg/L) for (a) TP, (b) N, and (c) TN, comparing phase II and phase III.

The nitrogen measurements, represented in (Figure 2- 6), suggested that plant uptake enhanced nitrate removal in all columns to 35-56% and 64-73% for Blend#1 and Biofilter433, respectively (Table 2- 6). Similar to phosphorus results, plants impact on nitrate removal was more significant in Blend#1 (p<0.0001) compared to Biofilter433 (p=0.364). The mean nitrate removal rate was increased to 46% for vegetated columns from -7.2% (leaching) for Blend#1 in the second phase of the experiment, whereas Biofilter433 showed only up to 13.6% enhancement with no significant difference of performance (p=0.244).

There was no significant improvement in total nitrogen removal from plant addition, and slight leaching was evident (Figure 2- 6), which might be associated with the increased washed off solids in the effluent samples. Slightly greater total nitrogen removal of Sea Oat columns (5.5% and -0.4% for Blend#1 and Biofilter433, respectively) is in accordance with greater TSS removal rate, as well (Table 2- 6). The concentration of heavy metals and the corresponding removal rates indicated no significant difference before and after plants addition, except for copper. The dissolved copper removal was enhanced significantly after plant addition (p<0.0001) (-71% to 57%), which is correlated with enhanced phosphorus removal rate, whereas total copper effluent concentrations were similar (p=0.06). Due to increased concentration of solids in the effluent, slightly lower overall total metals removal was observed.

Comparing the water quality parameters and removal efficiencies of phase two and three indicated nutrient removal enhancement, particularly for Blend#1 after addition of plants (Figure 2-6). The mean orthophosphate removal was increased to 83.8% from -32.9% (p<0.0001), while mean total phosphorus removal rate was increased to 61.0% from -29.7% (p=0.0015) (Table 2-6). Enhanced nitrate removal was achieved for both media in phase three (Figure 2-6) with overall increase of 52.8% and 8.3% for Blend#1 and Biofilter433, respectively (p<0.0001 and p=0.363).

The heavy metal removal efficiencies were relatively similar for all columns, except for dissolved copper with overall enhanced removal of 129% and 87% for Blend#1 and BioFilter433 (p<0.0001 and p=0.3067), respectively (Table 2- 6). Overall, the results confirmed that vegetation enhances some pollutant removal (nutrients and dissolved copper) in bioretention systems.

Table 2-6. Removal efficiencies (%) of water quality parameters before & after plant addition- Phase III

			%)						
Water Quality	Phase III with plants Phase II								
parameter		Blend#1		I	Biofilter433		No	Plants	
	Sea Oats	Frogfruit	Muhly	Sea Oats	Frogfruit	Muhly	Blend#1	Biofilter433	
TSS	55.2	34.6	6.0	55.0	19.9	15.6	87.3	86.6	
Orthophosphate	87.9	82.8	80.8	-275	-420	-355	-32.9	-266	
Total Phosphorus	64.7	59.0	59.2	-202	-289	-255	-20.5	-179	
Nitrate	46.1	55.7	35.0	72.9	64.3	65.6	-7.2	59.3	
Total Nitrogen	5.5	-2.9	-7.3	-0.4	-10.6	-4.7	-11.8	13.3	
Dissolved Lead	84.3	100	98.5	71.3	100	68.5	100	99.8	
Total Lead	98.2	97.9	98.8	99.2	97.7	97.7	100	98.5	
Dissolved Copper	44.0	64.6	63.8	-17.8	-169	-39.1	-71.5	-162	
Total Copper	47.4	77.0	73.2	68.5	73.4	71.1	63.6	75.9	
Dissolved Zinc	86.8	96.3	94.7	88.7	89.8	91.5	92.1	87.0	
Total Zinc	95.7	95.6	90.1	93.9	86.0	87.9	94.6	96.2	

2.8. Conclusions

A series of column experiments were performed to assess treatment efficiencies of nine different media. All media demonstrated good filtration capacity and high TSS removal (≈90%), which also translated into a high removal of particulate contaminants. The removal of dissolved pollutants is highly dependent on the adsorption capacity of the soil media and infiltration rate. For that reason, limestone sand showed the best treatment performance (orthophosphate and dissolved heavy metals, particularly) due to its high adsorption capacity, whereas the use of recycled glass in the bio-retention mixture did not provide any significant improvements. Accordingly, lime-stone sand was used as a substitute of regular sand in the bioretention soil

mixtures, and as expected, enhanced removal efficiencies were achieved compared to the standard bioretention soil mixtures and sand. Excess nutrient content was a major observed disadvantage of bioretention soil mixtures, resulting in greater effluent nutrient concentrations (phosphorus) than the influent. This issue was addressed by adding vegetation in the third phase of the column tests, where significant improvement in the removal of dissolved nutrients was achieved, indicating the positive effect of plant uptake on the pollutant removal in the bioretention systems.

In this study, we used accumulated solids in a sand filter basin's inlet chamber as TSS in the synthetic stormwater, to better represent actual stormwater of urban areas. However, this approach led to inconsistent influent pollutant concentration among all different media batches, and it can be highlighted as a weakness in our methodological approach. On the other hand, solids influents differences were not significant to impair our major findings and the conclusions of this experimental study. Further research is required on the plant–soil interactions to better understand the role of plants in pollutant removal and find the potential causes of the increased effluent TSS and poor treatment of Biofilter433 even after the addition of plants. Moreover, the clogging of LID systems causes a major limitation on their hydrologic and treatment performance that needs to be prevented for a reliable effective operation in the long term. A future study is underway where the two bioretention systems alongside limestone sand are tested in a full-scale LID testbed. The monitoring of the LID testbed will provide us with a better understanding on the long-term performance of a regular bioretention, a lime-stone-based bioretention, and a sand filter basin operating under the same conditions on the field scale.

CHAPTER THREE: FIELD TEST - LOW IMPACT DEVELOPMENT TESTBED

This Chapter describes the field test, incorporating the full-scale LID testbed filled with the selected top performing media from the pilot test. Continuous monitoring of the LID testbed provides an extensive dataset that enables us to better understand the performance of LID systems while comparing performance of (1) sand filter basins vs. bioretention basins, (2) different bioretention media and impact of limestone sand usage in the bioretention soil mixture, and (3) lined vs. unlined systems and the potential impact of impermeable liner on the effluent water quality. This extensive dataset also serves the data and model development needs for further assessment of these systems.

3.1. Introduction

The international stormwater Best Management Practices (BMP) database contains over 700 BMP studies including treatment performance analysis results. The 2020 report of the international BMP database (Clary et al. 2020) provides a summary statistic of various BMP (e.g. bioretention, bioswales, sand filters and porous pavement) performance for total suspended solids (TSS), bacteria, nutrients and heavy metals. Considering Sand filter basins (media filter) and bioretention systems, the results suggest lowest effluent TSS concentration for both systems - with median of 10 mg/L for bioretention and 7.2 mg/L for sand filter basins - indicating effective particulate pollutants removal of 79% and 84%, respectively (p<0.05). Bacteria measurements are limited and highly variable and show no significant removal in any of the studied BMPs, except for detention ponds, bioretentions and media filters. Removal of particulate nutrients and heavy metals is correlated with effective TSS removal efficiencies, whereas removal of dissolved forms is challenging. Bioretention data shows export of orthophosphate (-800%, p<0.05) and nitrogen (-22%) that is significantly reduced in BMPs with permanent pools (e.g., wetland basin/retention

pond with removal rate of 37% and 59%, p<0.05), which indicates positive impact of internal water storage on nutrient removal efficiencies particularly for nitrate. Sand filters, on the other hand, show slight removal of orthophosphate (40%, p<0.05) and export of dissolved nitrogen (-41%, p<0.05). Dissolved heavy metal removal rates is highly variable in different BMPs and is impacted with the influent concentration. Significant export of copper (-10%) is evident in the bioretention systems (p<0.05), while both BMPs perform well in removal of dissolved zinc (40% and 78%, p<0.05). Total metal treatment, on the other hand, are relatively higher for all BMPs as the particulate pollutant removal is associated with TSS removal (Clary et al. 2020).

Assessing the performance of sand filter basins has been the focus of several studies in the past decade. It has been shown that sand filter basins perform well in reducing the peak flow and runoff volume and removing particulate pollutant. However, they are not effective in the removal of dissolved pollutants (Barrett 2003; Shahrokh Hamedani et al. 2019; Zarezadeh et al. 2018). Barrett (2010) conducted a comprehensive study to evaluate the performance of five sand filter basins located in city of Austin from 1985-1997. He found similar effluent pollutant concentrations in all five basins, indicating slight impact of design factors. Water quality analysis suggested that the removal of particulate pollutants is directly correlated to the particle size of the sediments and filtration media. Zarezadeh et al. (2018) evaluated the performance of a sand filter basin located at the University of Texas at San Antonio's (UTSA) main campus and observed congruent results indicating effective particulate contaminant removal through physical processes of sedimentation and filtration. The results, however, indicate poor removal of dissolved pollutants such as metals and nutrients (Zarezadeh et al. 2018).

Bioretention systems, also referred to as rain gardens, are LID stormwater control measures characterized by shallow landscaped depressions that detain, store and filter stormwater runoff

through layers of mulch, plants and soil media. Bioretention systems have the potential to improve the removal of dissolved pollutants because of chemical and biological processes that occur within the soil media and plants, including adsorption, biotransformation, bioaccumulation and biouptake (Davis et al. 2010; Dorman et al. 2013; Hsieh and Davis 2005b; US EPA 2007). One limitation of bioretention systems is the high nutrient content of the bioretention soil mixtures that can lead to high concentration of nutrients in the effluent (TCEQ 2005). According to the International Stormwater BMP database, the removal of particulate nutrients and heavy metals is correlated with effective TSS removal efficiencies, whereas removal of dissolved forms can be challenging. Among the nutrients, phosphorus in stormwater is found to be mainly particulatebound and thus high removal of particulates (solids) provides high total phosphorus removal efficiencies as well. Nitrogen, on the other hand, is transported in both particulate and dissolved phases and its treatment efficiencies varies greatly for various forms of nitrogen due to the differences in their respective removal processes. Overall, nitrogen cycle is strongly impacted by the soil moisture (wetting and drying cycles), plant-soil interactions and the microbial community (Skorobogatov et al. 2020; Søberg et al. 2021) Similar to phosphorus, effective total metal treatment aligns with high particulate pollutant removal, whereas dissolved heavy metal removal varies substantially amongst BMPs and is significantly impacted by the adsorption capacity of the filtration media (Clary et al. 2020).

Furthermore, along with the characteristics of the filtration media, design elements such as depth, inlet and outlet structures, and liner types are crucial factors for LID's effective performance too. Impermeable liners are required to restrain infiltration and ground water contamination (San Antonio River Authority 2015; TCEQ 2005), which prevents fully restoration of the hydrologic flow regime and recharging the aquifers. Furthermore, partial infiltration through the subsoil in

unlined systems can be an effective mechanism to not only enhance the volume reduction, but also to naturally remove pollutants that pose minor risks to groundwater (e.g. phosphorus) (Clary et al. 2020). There are limited studies on the impact of liners and contaminant transport from LIDs to groundwater. Reck et al. (2021) investigated the seepage metal concentrations beneath long-term operated bioretentions and found that the soil's metal concentrations declined with depth, indicating high retention of dissolved metals and filtration of particulate metals in the upper layers. Thus, the seepage metal concentrations were all below the water quality thresholds, suggesting efficient treatment performance and no risk of groundwater degradation. Edwards et al. (2022) also studied the transport of stormwater contaminants to groundwater through dry wells, and found no evidence that stormwater contaminates could degrade groundwater quality, as none of the studied contaminants reached concentrations at human health risk levels.

3.2. Low Impact Development (LID) Testbed

Following the results of the column experiments, two top performing media and sand were implemented in the LID testbed. The LID testbed provides the opportunity to compare the performance of sand filter basin alongside two different bioretention designs under same conditions. The LID testbed is installed in the UTSA main campus, behind the Margaret Batts Tobin Laboratories (Latitude: 98°37'48.4001"W Longitude: 29°35'1.3943"N). It drains approximately 2.67 acres of parking lots, rooftops and landscapes with overall runoff coefficient of 0.69 and time of concentration of 21.5 minutes (Figure 3- 1). Currently this drainage area is not being treated by any stormwater method.

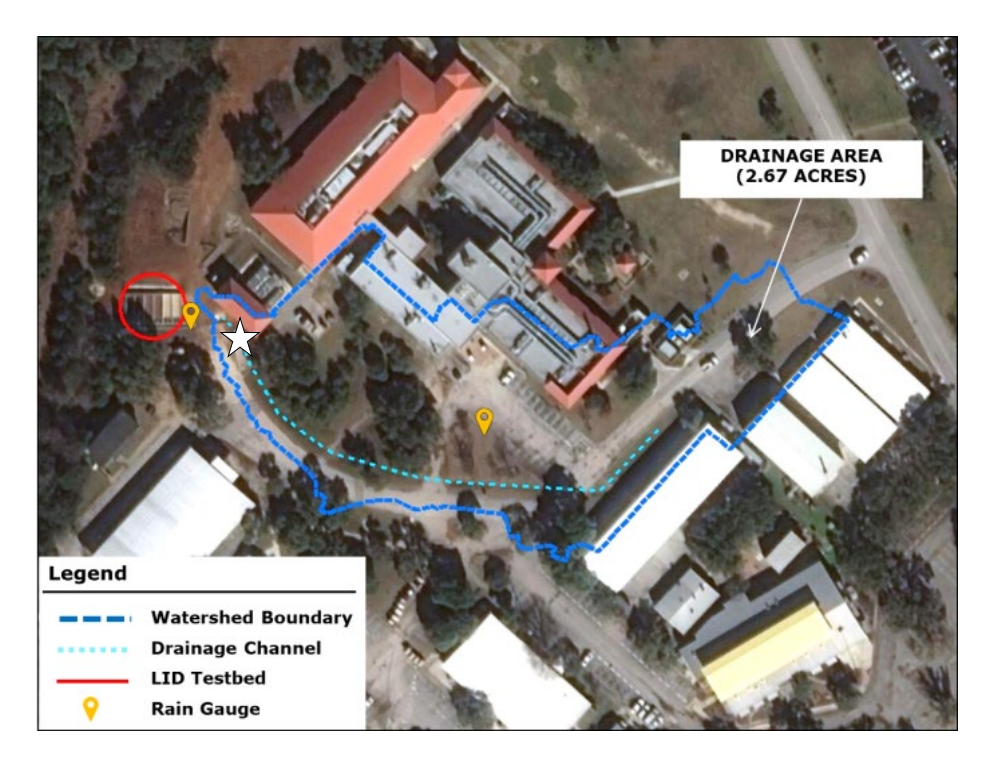


Figure 3-1. LID testbed drainage area, white star is the pre-implementation monitoring location

The LID testbed is composed of six parallel cells (9ft×30ft×4.5ft) containing the three media in duplicates - with and without impermeable liner - to study the potential impacts of direct infiltrations on water quality and quantity control, and changes in the aquifer recharge rate in particular. The aerial view of the testbed including the water movement, monitoring and sampling locations is shown in Figure 3- 2. Cells 1 and 2 contain the custom limestone blend (Blend#1), cells 3 and 4 are the standard bioretention media (Biofilter433) and cells 5 and 6 are the regular sand filter basins filled with limestone sand (Table 3- 1). Cells 1, 3 and 5 are lined with a concrete bed that does not allow any infiltration to the sublayer (Figure 3- 3). Three native plants of frog fruit, inland sea oats and pink muhly are planted in the bioretention cells (1-4). The surface area of each cell is 270 ft². By dividing the drainage area (2.67 acres) to the total surface area of the LID testbed results in a ratio of 3.7%.

The stormwater runoff enters the inlet channel (4.5ft×60ft) through two 15inch culverts. The level rises to 4 inches to reach the inlet of the cells and then the runoff starts flowing equally to all

six cells. A 13ft long 1ft high and 6in wide level spreader is installed in the first half of inlet channel to allow flow to uniformly distribute, ensuring that water reaches to the end of the inlet channel, and that the water surface elevation is horizontal. The level spreader can be seen on Figure 3 – 4. The overflow channel (5ft×26ft) transfers the excess water in the inlet channel to mitigate overflowing of the cells in case of extreme events.

Table 3-1. Physical and chemical Properties of the LID testbed media

Media	Siz Distrik 270	oution	Uniformity Coefficient (Cu)	Organic Matter	Hydraulic Conductivity mm/hr		Total P	Total N	Total Cu	Total Pb	Total Zn
Limestone Sand	0	100	5.8	0	1095.8	9.0	2.6	11.4	44.8	16.4	401
Limestone-Mix	38.0	100	5.6	1.45	35.1	8.9	6.8	29	57.6	10.4	458
Bioretention-Mix	72.3	100	2.7	3.9	19.3	8.4	23.1	81.6	190	21.4	602

^a (%) passing through sieve 1/4in (6.35 mm) and #270 (0.053 mm) (fines). The uniformity coefficient (Cu) is defined as the ratio of D60 to D10. If 4<Cu<6 soil is well graded and Cu<4 corresponds to poorly graded or uniformly graded soil.



Figure 3-2. Aerial view of the LID testbed, water movement and monitoring locations

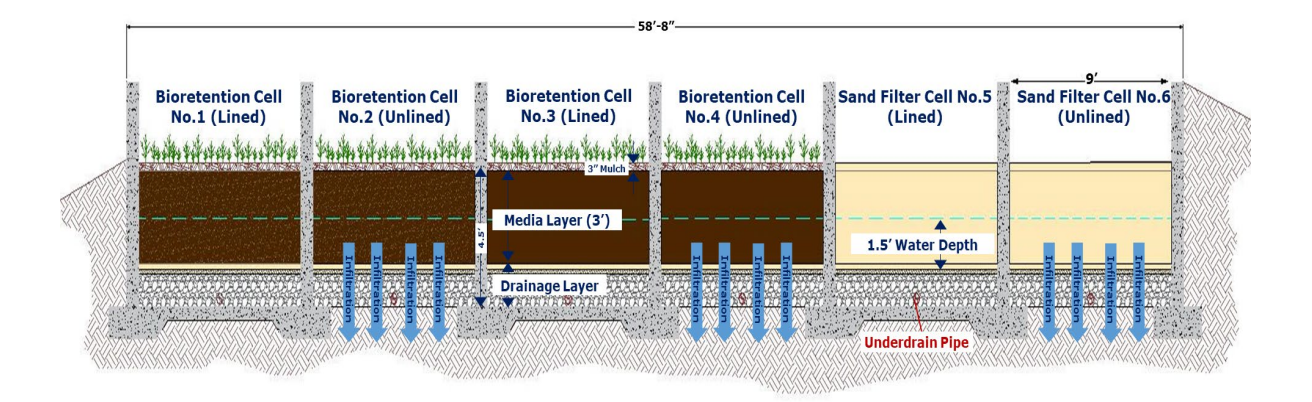


Figure 3- 3. Cross-section profile view of the LID testbed cells, blue arrows show water infiltration to the sublayer through unlined cells. Cell 1 and 2 contain Limestone-Mix media, Cells 3 and 4 Bioretention-Mix, and Cells 5 and 6 Limestone Sand.

3.3. Field Monitoring

The performance of all LID testbed cells is assessed in terms of quantity and quality control by monitoring the rainfall, flowrate, water level and moisture content; and collecting flow-paced stormwater samples at the inlet and six outlets of the testbed. For the pre-implementation period (year 1), only one location was monitored at the upstream culvert of the LID testbed inlet. For the post-implementation period (year 2-4), seven locations are being monitored: one inlet and six outlets (Figure 3- 2). The post-implementation monitoring consists of two main periods: (1) 22 months of monitoring (June 2019 – April 2021) with a bottom slotted underdrain and no internal water storage (IWS) and (2) 20 months of monitoring (April 2021- December 2022) with elevated outlet and internal water storage layer (Figure 3- 3). All the water quality analysis is performed at the UTSA Environmental Engineering Laboratory and some samples were sent to external certified laboratory to validate the results and the laboratory testing protocols.

3.3.1. Hydrologic Performance

To monitor the hydrologic performance of the testbed, the flow level and discharge is measured in a 5-minute time interval using bubbler flow meters at the inlet and six outlets (Figure 3- 2) using ISCO TIENETTM signature bubbler flow modules connected to 6in and 15in v-notch weirs in the

Rainfall is monitored using a tipping bucket rain gauges (TE525-WS) with resolution of 0.01 inch the inlet monitoring point. Total of eight pressure transducers (In-Situ-Rugged Troll 100) are recording the water level in the inlet channel and cells (Figure 3- 4). Six sensors are placed inside of 2in×7ft PVC pipes and secured to the concrete wall of the cells, and two are placed inside 2in×2.5ft PVC pipes secured to the wall of the beginning and end of the inlet channel. All the pressure transducers are positioned touching bottom of the cells and inlet channel. The atmospheric pressure transducer (In-Situ - Rugged BaroTroll) was kept at the shed by the testbed to record the atmospheric pressure (Pressure Baseline) that is used for correcting the measurements made by the submerged ones. Moreover, soil moisture content of each cell is recorded by the soil moisture sensors that are installed in middle of the cells at 1.5 ft deep (STEVENS HydraProbe).

The recorded data is used to generate hydrographs and hyetographs to get a better understanding of the flow regime within the drainage area and also to assess hydrologic performance of each LID cell. Moreover, the water balance of the testbed is estimated to describe the water movement within the system considering all the components.

Simple presentation of water balance equation is:
$$P = R + ET + I + \Delta S$$
 (3-1)

where P is the precipitation (input), R, E, I and ΔS are the outputs of the system referring to runoff, evapotranspiration, infiltration and changes in soil storage, respectively. The interrelationships between components and variations with time needs to be considered for an accurate representation. The water balance for the testbed could be defined as follows:

$$R_{IN} + \sum_{i=1}^{6} P_i \times A_c = \sum_{i=1}^{6} R_{Ci} + \sum_{i=1}^{6} I_{Ci} + \sum_{i=1}^{6} ET_{Ci} + \sum_{i=1}^{6} \Delta S_{Ci}$$
 (3-2)

where the input includes the total inflow volume (R_{IN} , cf) and the direct rainfall on each cell (cf), as the output sums up the outflow, infiltration, evapotranspiration and soil moisture changes

for all six cells (i=1-6). The rainfall, inflow and outflow, and soil moisture content are measured directly, whereas the infiltration and evapotranspiration could be estimated using the recorded data.

$$VR_{j} = \frac{\sum_{i=1}^{n} V_{INi} - \sum_{i=1}^{n} \sum_{j=1}^{6} V_{iC_{j}}}{\sum_{i=1}^{n} V_{INi}} \times 100$$
(3-3)

For each storm event, recorded hydrologic characteristics of the inlet and outlets were used to determine the total volume reduction (VR), peak flow reduction (QR) and reduction ratio (R_{peak}), as well as the lag time between the inlet and outlet peak ($t_{j, j=1-6}$) for each LID cell (Braswell, Winston, & Hunt, 2018).

$$QR_j = \frac{Q_{PIN} - Q_{PC_j}}{Q_{PIN}} \tag{3-4}$$

$$R_{Peak_j} = \frac{Q_{PIN}}{Q_{PC_i}} \tag{3-5}$$

$$t_j = t_{C_j} - t_{IN} \tag{3-6}$$

$$Hydrograph\ Centroid = \frac{\sum Flow \times Time}{\sum Flow}$$
 (3-7)

where Q_P represents the peak flow and V_{IN} is the total inflow accounting for the runoff and the direct rainfall on each cell. The lag time was estimated considering the (1) delay between the start of the inflow versus the outflows, and (2) the centroid of the inlet and outlet hydrographs. The time of the hydrographs' centroid (gravity center of the hydrograph) was computed as the weighted-mean of the flow based on time (equation 3-7). The alternative time gages instead of the time to peak (t_p) was used to avoid negative lag times caused by multiple-peak hydrographs.





Figure 3-4. Field monitoring equipment and sensors at the LID testbed

3.3.2. Treatment Performance

ISCO 3700 autosampler coupled with signature flow meter was used to collect flow-paced samples at the seven sampling locations (Figure 3- 2). The flow volume pace was estimated for collecting average of 12 samples (600ml) for water quality volume of approximately 716 ft³ for each cell. The water quality volume was calculated considering mean porosity of 35% for the media layer and 40% for the drainage layer which adds up to equivalent depth of 2.95 ft.

The treatment performances were evaluated by analyzing the measured water quality parameters including the total and volatile suspended solids (TSS, VSS) (mg/l), orthophosphate and total phosphorus (mg/l of PO₄³⁻), nitrate and total nitrogen (mg/l of NO₃⁻-N), dissolved and total concentration of heavy metals including copper, zinc and lead (μg/l), conductivity (μs/cm), dissolved oxygen (mg/l of O₂), total and fecal bacteria (CFU/100ml) and pH.

Table 3-2. Water quality parameters, units, methods, instrumentation, and detection limits.

Parameter	Units	Method	Instrument	Detection limit
TSS	mg/L	US EPA gravimetric method	Desiccator, furnace	NA
VSS	mg/L	US EPA gravimetric method	Desiccator, furnace	NA
DO	mg/l of O_2	SM 4500-O	HACH® sensION156	0-22
pН	-	SM 4500-H+B	HACH® HQ40D	0-14
Conductivity	μs/cm	SM 2510 B	HACH® HQ40D	0.01-100
Total & Fecal coliform	CFU/100 ml	Membrane filtration (SM 9222)	Vacuum filtration, Incubator	NA
E. Coli****	CFU/100 ml	HACH method 10029	Vacuum filtration, Incubator	NA
Nitrate	mg/L NO ₃ -N	Ion chromatography	Metrohm 850	0.04
Orthophosphate	$mg/L PO_4^{3-}$	(SM 4110)	Professional IC***	0.01
Total Phosphorus	mg/L PO ₄ ³⁻	PhosVer3® ascorbic acid method (SM 4500-P) **	HACH® DR 2800	0.02-2.5
Total Nitrogen	mg/L NO ₃ -N	TNT plus 826 (SM 4500-NO ₃ -N)	HACH® DR 2800	1.0-16.0
Heavy metals	$\mu g/L$	EPA 6010, SM 3125	PerkinElmer NexION 350 ICP-MS	0.001*

^{*} Detection limit of 0.001 µg/L for lead (Pb) and copper (Cu) and zinc (Zn).

Collected samples were transferred to the UTSA Environmental Engineering Laboratory (Figure 3- 5). The conductivity, Dissolved oxygen (DO) and pH measurements were recorded using HACH mustimeters (HQ40D, SensION156) while the samples were being prepared and stored for further analysis following the guidelines of the Standard Methods for the Examination of Water and Wastewater (APHA, AWWA, WEF 2012). The instruments and methods used for water quality analysis are listed in Table 3- 2. Similar to the column experiment water quality analysis, persulfate digestion method was used for total phosphorus and total nitrogen measurements.

^{**}The persulfate digestion method (SM4500P) coupled with HACH colorimetric methods were used to determine total phosphorus.

^{***} For Phase II, EPA method 300 and Shimadzu - Nexera series LC-40 was used with detection limits of 0.01 and 0.075 mg/L for nitrate and phosphate, respectively.

^{****} Starting April 2020, switched from fecal coliform to E-Coli using HACH method 10029, following TCEQ Revised Total Coliform Rule (RTCR), Title 30 of the Texas Administrative Code (TAC), Chapter 290.



Figure 3- 5. Sample collection and laboratory analysis, TSS samples and digested samples for Total Metals (TM) showing the first flush effect and reduced solids for consecutive samples

Mean event concentration (EMC) was calculated for measured pollutant for each storm event.

The EMC represents flow proportional average concentration of a particular pollutant for the corresponding storm event. After calculating the influent and effluent EMC, EMC efficiency was calculated to determine the removal rate for each particular pollutant.

$$EMC = \frac{\sum_{i=1}^{n} V_i C_i}{\sum_{i=1}^{n} V_i}$$

$$EMC_{Efficiency} = \frac{EMC_{inf} - EMC_{eff}}{EMC_{inf}} \times 100$$
(3-7)

$$EMC_{Efficiency} = \frac{EMC_{inf} - EMC_{eff}}{EMC_{inf}} \times 100$$
 (3-8)

where V_i is the volume of flow during period i; C_i is the concentration associated with period i; and n is the total number of measurements taken during an event. EMC_{inf} and EMC_{eff} are the influent and effluent event-mean concentration (mg/L or µg/L). Boxplots (2.4) are used to represent the average EMC for each pollutant and its statistical summary including the median, first and third quartile and the maximum and minimum values. Moreover, pollutant loading (L) and percent load removals were calculated assuming equal load input $\binom{L_{inlet}}{6}$ into each cell (Equation 3-9).

$$L = \sum_{i=1}^{n} V_i C_i \qquad \text{\% Load Removal} = 100x \frac{L_{inlet}/6 - L_{outlet}}{L_{inlet}/6}$$
(3-9)

3.3.3. Statistical Analysis

Statistical analysis was performed to determine if the removal rates are significant, and also to investigate if there is a significant difference between performances of LID cells. We conducted ttests (normal distribution) and Wilcoxon rank-sum test (non-parametric) at a confidence level of 95% (p<0.05) to examine the removal efficiencies of each LID cell and to determine whether (1) the mean influent and effluent EMCs and (2) the mean effluent EMCs of six cells are statistically different. Shapiro-Wilk test (confidence level of 95%) was performed to determine normality of the dataset.

Regression Analysis

Subsequently, to compare the results of the LID testbed with previous literature records, regression analysis was performed between the LID testbed monitoring data and the international stormwater BMP database (Clary et al. 2020). We exported the paired influent and effluent EMC records for bioretention and media filter (sand) systems worldwide. The number of reported EMCs were different for each water quality parameters ranging from 50 to 500 records. Total and fecal/e-Coli Coliform and VSS were excluded from the regression analysis due to lack of adequate data on the BMP database. The linear regression model represents the relationship between the recorded influent and effluent EMC for a particular BMP.

$$EMC_{eff} = m \times EMC_{inf} + b \tag{3-10}$$

where m is the slope of the regression line, EMC_{inf} and EMC_{eff} are the influent and effluent event-mean concentration (mg/L or μ g/L); and b is the intercept. The confidence and prediction intervals of effluent EMC at a level of 95% will be estimated according to:

$$s_{\hat{y}} = s \sqrt{\frac{1}{n} + \frac{(x - \bar{x})^2}{\sum_{i=1}^{n} (x_i - \bar{x})^2}}$$
(3-11)

$$s_{pred} = s \sqrt{1 + \frac{1}{n} + \frac{(x - \bar{x})^2}{\sum_{i=1}^{n} (x_i - \bar{x})^2}}$$
(3-12)

where $s_{\hat{y}}$ is standard deviation of the measured EMC; s_{pred} is standard deviation of the predicted error; s is the standard error; n is number of paired data points; x is influent EMC of interest; \bar{x} is the average measured inflow EMC; xi is measured influent EMC at time i. The upper and lower confidence (EMC_{eff}^{conf}) and predicted (EMC_{eff}^{pred}) lines are drawn based on the standard deviations and the t-value for the particular probability (95%) and degrees of freedom (n-2):

$$EMC_{eff}^{conf} = EMC_{eff} \pm t_{0.05} s_{\hat{y}} \tag{3-13}$$

$$EMC_{eff}^{pred} = EMC_{eff} \pm t_{0.05}S_{pred} \tag{3-14}$$

Correlation Analysis

Impact of Storm Regime on Water Quality

The collected data on the hydrology and water quality of the testbed were investigated to find trends and potential impacts of hydrological conditions on the water quality parameters. This analysis aims to answer if and how the storm regime impacts the pollutant load and removal rates. Multivariate correlation analysis is performed to test for correlation between hydrologic characteristics and water quality parameters. For normally distributed data, Pearson correlation coefficient (r) must be greater or smaller than the critical value for 95% confidence level to indicate a significant correlation. If the data is not normally distributed, Spearman's rank correlation is performed, where the p value must be smaller than the 0.05 significance level for significant correlation.

Relationship between various pollutants and potential co-pollutants

Lastly, to explore correlations between various pollutants and identify potential co-pollutants, we generated the correlation matrix for 16 measured water quality parameters by conducting the Non-Parametric Spearman's rank correlation at significance level of 95% (p<0.05). The Spearman's rank correlation is a non-parametric measure of the monotonic association between two datasets. Spearman's correlation coefficient (rho) ranges between -1 and 1 with 0 implying no correlation. Rho values of -1 and +1 indicates positive (direct) and negative (inverse) exact monotonic relationship, respectively.

3.4. Soil Core Sampling

One of the concerns to LID performance is the pollutant removal capacity of filtration media and accumulation of pollutants in LIDs over time, and its consequent impact on their short and long-term performance and maintenance needs (Costello et al. 2020; Jones and Davis 2013; Paus et al. 2014). Soil core sampling is conducted to measure the accumulated retained pollutants on the filtration media, explore spatial patterns, and to assess their removal capacity and hydraulic performance over time. Multiple studies have examined pollutant retention in bioretention cells through soil-coring at different locations and depths for heavy metals, phosphorus and nitrogen, and found most pollutant accumulation near the inflow and surface layer (5-10 cm) of media (Jones and Davis 2013; Kandel et al. 2017; Paus et al. 2014). Following the methodology of reviewed literature, core samples were collected at 6 locations for each cell of the LID testbed using the AMS soil core sampler (2.5 in x 6&12 in) to further investigate the treatment processes and determine the retained pollutants in each cell. Two samples (R1, L1) towards the inlet, two in the middle (middle R, middle L) and two towards the end of the cells (R2, L2) - at two different depths of 0-6inch, 6-18 inch - were collected (Figure 3-6). Only surface sample (0-6 inch) were collected in bioretention cells, as the plants and the media characteristics did not allow it. Due to high sand ratio in the media compositions, intact soil core sample collection were not feasible and disturbed samples were collected. The mulch layer and debris (~ 1 cm) were removed from the surface before sample collection, samples were stored in cold room at 4°C before analysis. In addition to the collected samples, initial pollutant content of soil media was tested by analyzing soil media samples from before implementation in the LID testbed.



Figure 3-6. Soil sampling locations at the LID testbed

Collected samples were weighted and sieved though a 2 mm Mesh to remove roots and leaves from the sample. Samples were dried in oven at 105°C for 24 hours (Li and Davis 2008). The sample extracts were made with 1:10 (weight/Volume – 4g/40ml) slurry of soil in ultra-pure water. The slurry was mixed for 5 minutes on a tube revolver at 25 rpm, and then for 16 hours on a shaker table (Hathaway and Hunt 2011; Kandel et al. 2017). The extract was then digested for TN using the TNT plus 826 HACH kit, and for TP following the persulfate digestion method (SM4500P) coupled with HACH colorimetric methods (PhosVer3® ascorbic acid method) (Table 3- 2). Total metal analysis was conducted by an external certified laboratory following the EPA method SW-6010B with method detection limits (MDL) of 0.24, 0.59 and 1.27 ppm for zinc, copper and lead.

Moreover, for quality control of our TN and TP measurements, sample duplicates were analyzed by the external certified laboratory using methods M4500 for TN and TP (MDL = 50, 2.5 ppm), respectively.

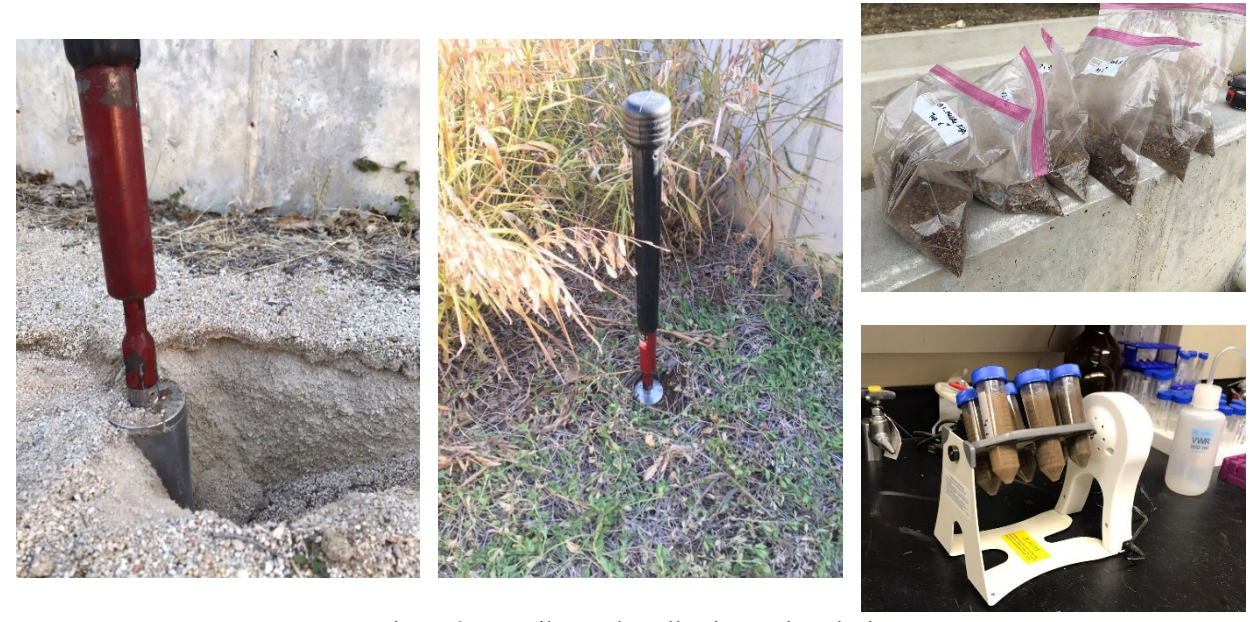


Figure 3-7. Soil sample collection and analysis

3.5. Results and Discussion

3.5.1. Pre-implementation Monitoring

The upstream culvert of the LID testbed was set as the preconstruction monitoring site (Figure 3-1). The flow level and discharge and velocity were measured in a 5-minute interval using ISCO TIENET® 350 area velocity sensor installed in the 15inch concrete culvert. The ISCO 3700 autosampler was programmed to start sampling once the water level in the sampling culvert reaches 1 inch and then collect samples every 15 minutes for the first hour – to investigate the first flush effect- and then every 30 minutes for the remaining time after 45 minutes delay. Total of 16 storm events were captured in one-year period starting from January 2018 to May 2019 (Table 3-

3). From April to August 2018, the upstream culvert was blocked due to constructions in site, which prevented runoff from reaching to the sampling location. Therefore, the samples for the two first storm events in May and July 2018 were collected manually. The measured mean runoff and peak flow for these two events are also very small due to this blockage issue.

Table 3-3. list of pre-implementations monitored storm events January 2018-May 2019

No.	Event Date	Rainfall Duration (min)	Total Rainfall Depth (in)	Maximum Intensity (in/hr)	Total Runoff Volume (ft3)	Peak Flow (cfs)	Antecedent Dry Periods (days)
1	05/04/2018	420	1.24	2.76	-	0.007*	1
2	07/07/2018	45	0.18	0.48	-	0.004*	1
3	08/11/2018	215	0.41	0.72	503	0.12	4
4	08/12/2018	185	0.96	3.6	581	0.25	1
5	09/03/2018	65	0.89	2.64	1141	0.23	22
6	09/04/2018	290	3.81	3.24	12699	1.75	1
7	09/09/2018	445	2.03	2.04	7108	0.68	5
8	09/14/2018	190	0.52	0.24	617	0.10	5
9	09/22/2018	235	1.24	2.04	2851	0.23	8
10	09/30/2018	40	0.45	1.8	66	0.01	8
11	10/09/2018	100	0.65	1.2	783	0.15	9
12	10/24/2018	240	0.49	0.36	307	0.03	6
13	12/07/2018	670	1.50	1.08	7465	0.21	28
14	12/27/2018	175	1.05	1.68	2004	0.52	19
15	04/24/2019	145	0.62	0.96	53	0.02	6
16	05/03/2019	135	1.43	3.84	1827	0.85	9

^{*} Blocked upstream culvert

The pollutant EMC and load were calculated for each storm event, the median EMCs for the qualified storm events are reported in Table 3- 4. The qualified representative storms were identified considering the 72-hour interval from the preceding measurable storm event (EPA)

1983), quality of data (missing/faulty data due to equipment malfunction) and sampling (number and frequency of collected samples). Accordingly, storms 1, 2, 4 and 6 were disqualified.

Table 3-4. Median pollutants' EMC and loading, pre-implementation monitoring

	$\begin{array}{c} \textbf{Median EMC} \\ (mg/L)^a / \\ (cfu/100ml)^b / (\mu g/L)^c \end{array}$	Mean EMC (mg/L) ^a / (cfu/100ml) ^b / (μg/L) ^c	Total Loading (Kg) ^a /(log(cfu)) ^b /(g) ^c
рН	7.6	7.6	
Total Suspended Solids (TSS) ^a	98.2	133.1	69.6
Volatile Suspended Solids (VSS) ^a	15.1	26.3	8.3
Orthophosphate (P) ^a	0.06	0.09	0.09
Total Phosphorous (TP) ^a	0.15	0.17	0.20
Nitrate (N) ^a	0.51	0.54	0.21
Total Nitrogen (TN) ^a	2.6	1.6	0.96
Total Coliform Bacteria ^b	671914	2152881	133
Fecal Coliform Bacteria ^b	10000	12295	99
Dissolved Copper (DCu) ^c	4.93	5.84	5.43
Total Copper (TCu) ^c	9.68	33.35	12.86
Dissolved Zinc (DZn) ^c	19.82	25.91	14.18
Total Zinc (TZn) ^c	45.13	139.43	36.81
Dissolved Lead (DPb) ^c	0.05	1.54	1.35
Total Lead (TPb) ^c	5.81	8.36	4.39

The results suggested substantially higher concentration of solids (TSS) and heavy metals (especially zinc) in the first flush, while nutrients were relatively consistent with several elevated values that were correlated with rainfall-runoff peaks in the hydrograph (Figure 3- 8). Comparing the first flush mean and the total mean events indicated approximately 69%, 56% higher TSS and VSS for first flush, respectively. Also, greater heavy metal load was observed in the first flush samples, making them on average 28% more polluted (Table 3- 5). As for Nutrients, nitrate concertation was fairly consistent, whereas phosphorus concentration varied by the rainfall-runoff regime.

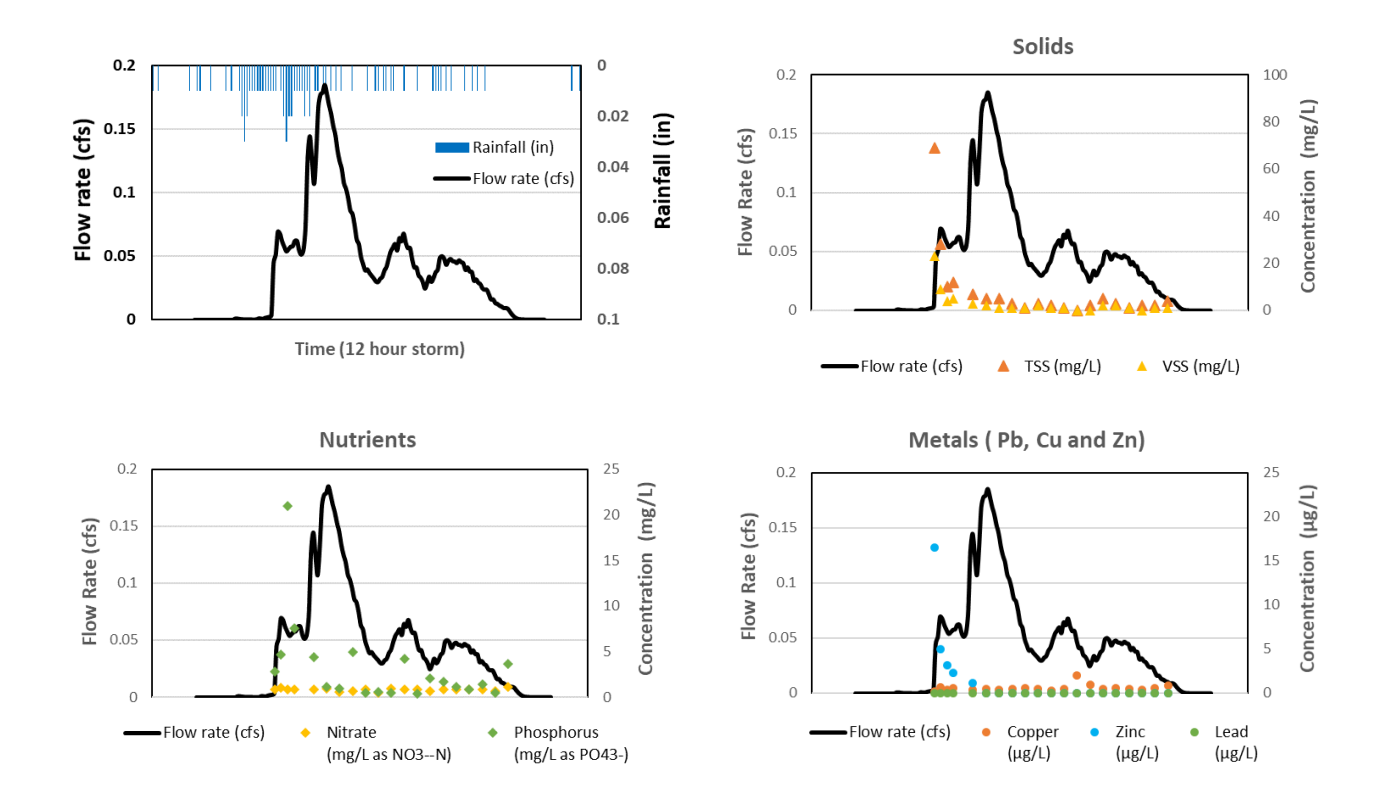


Figure 3- 8. Hydrograph and Pollutographs for selected storm – 12/07/2018

Table 3-5. Mean pollutant concentration of first flush samples vs total collected samples

Mean	Solids (mg/L)	рН		rients g/L)	Me	etals (µg	/L)	Bacteria (log(cfu/	
Concentration	TSS	VSS	PII	TN	TP	Cu	Zn	Pb	Total	Fecal
Total Event	122.9	21.7	7.50	3.35	0.16	21.5	159.9	4.07	6.30	5.23
First Flush	153.0	25.8	7.53	3.15	0.17	25.8	195.5	4.28	6.30	5.27

3.5.2. Phase I: without Internal Water Storage (IWS)

we captured total of 9 paired storm events in 21 months of monitoring (June 2019 - April 2021) (Table 3-6), from which 6 were qualified as representative storms considering the 72-hour interval from the preceding measurable storm event (EPA 1983), quality of data (missing/faulty data due to equipment malfunction) and sampling (number and frequency of collected samples).

Table 3- 6. List of monitored storm events June 2019 – April 2021

No.	Event Date	Rainfall Duration (min)	Total Rainfall Depth (in)	Maximum Intensity (in/hr)	Total Runoff Volume (ft³)	Peak Flow (cfs)	Antecedent Dry Period (days)
1*	06/24/2019	155	1.44	2.04	1556	0.64	7
2*	09/19/2019	60	1.33	5.52	1320	0.92	81
3*	10/24/2019	360	2.32	2.52	18529	3.42	35
4	4/4/2020	290	1.35	1.32	1202	0.43	14
5	5/16/2020	195	1.29	2.16	1428	0.60	42
6*	05/24/2020	285	1.71	3.36	3593	1.73	8
7*	09/03/2020	140	1.17	2.28	728	0.28	94
8*	09/09/2020	90	2.24	3.72	9484	2.88	6
9	11/28/2020	330	1.11	0.96	613	0.29	79

^{*} Representative storm events

Hydrologic Performance

Figure 3- 9 represents the hydrologic performance of the LID testbed, plotting the inflow volume and peak flow versus the outflows for the captured storms. Overall, volume and peak flow reduction is evident for all cells and all storm events, except for the few storms at the beginning of the monitoring period due to the saturated conditions and excess water in cells due to irrigation of the newly planted vegetation.

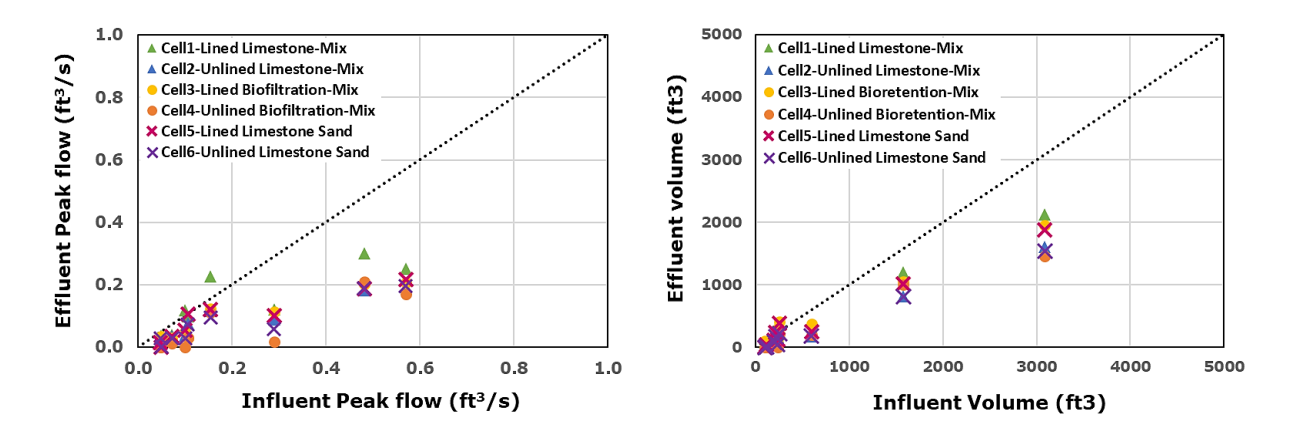


Figure 3-9. Influent volume/peak flow versus the effluent volume/peak flow - Phase I

Mean total runoff volume reduction of 44%, and peak flow reduction of 51% was achieved considering the 9 captured storm events. The results show the clear difference in the outflow peak and volume for the lined and unlined cells. Lined cells (Cells 1, 3 and 5) show higher peak flow and volume compared to the unlined cells (Cells 2, 4 and 6) that allow infiltration and are subjected to seepage loss (Table 3-7).

Table 3-7. Mean hydrologic performance indicators, Phase I – no IWS

	Cell 1 Limestone- Mix Lined	Cell 2 Limestone- Mix Unlined	Cell 3 Bioretention- Mix Lined	Cell 4 Bioretention- Mix Unlined	Cell 5 Limestone Sand Lined	Cell 6 Limestone Sand Unlined
Volume Reduction (VR) *	27%	52%	28%	58%	29%	55%
Peak Flow Reduction (QR)	0.3	0.5	0.5	0.7	0.4	0.6
Peak Flow Reduction ratio (R _{peak})	1.8	2.2	2.6	3.5	1.9	2.5
Lag time (start time)	25	35	31	41	31	37
Lag time (Hydrograph Centroid)	27	20	48	65	29	23

^{*} Assuming equal inflow to each cell

There is a 25-45 minutes delay between the inflow and outflow start time (Table 3-7), with cell 1 and cell 4 as the fastest and slowest outflows, respectively. Longer lag time was observed for the unlined cells, due to portion of inflow infiltrating into the subsoil. Cells 3 and 4 with the bioretention-mix show overall greater lag time, indicating slower water movement which is due to its lower infiltration rate (Table 3- 1), whereas limestone-mix and limestone sand showed relatively similar performance. Considering the hydrograph centroid, cell 4 shows greater lag time than cell 3, indicating wide and flat hydrographs and slow rate effluent. Cells 2 and Cell 6, on the other hand, show smaller lag time than the lined cells (Cell 1 and Cell 5) indicating sharp hydrograph and fast discharge. This suggest that the effluent flow is mainly dominated with the

infiltration rate of the filtration media, and slower water movement provides longer lag times and greater peak flow and volume reduction.

It is important to note that all the captured storm event (Table 3- 6) have rainfall depth of greater than 1 inch. The physical characteristics of the drainage area with many disconnected impervious surfaces, results in high initial abstraction rate requiring at least 1 inches of rainfall to generate adequate runoff that can reach the testbed and generate outflow. In order to diminish this threshold and capture smaller storm events, a pumping system was designed to expand the contributing drainage area by transferring the stormwater runoff from the corresponding drainage culvert to the testbed inlet (Figure 3- 10). The orange area is the added contributing area (3.3 acres) via stormwater transfer lines (yellow lines) to the LID testbed inlet.



Figure 3- 10. Pump system installed in November 2020 to expand the contributing drainage area

Treatment Performance

The EMC boxplots shows the statistical distributions of inlet and outlet EMCs (APPENDIX, Table A 3) highlighting the mean, median, first and third quartile, maximum and minimum and outliers considering the six representative storms (Figure 3- 11). The h values aside the boxplots show the significance of difference between (1) inlet vs outlets, (2) lined vs unlined cell for the three designs, (3) two bioretention soil media and (4) bioretention vs sand filter cells. h-value of 1 indicates statistical difference at significance level of 95% (p<0.05). Overall, no significant difference (h=0) was observed for the TSS removal between cells and against inlet, which indicates relatively poor TSS treatment. The median TSS EMC efficiency ranges from 10-60%, while cell5 is exporting TSS (Table 3- 8). The BMP database suggest relatively lower median influent and effluent TSS EMCs with removal rates of 77% and 84%, respectively (Clary et al. 2020). High effluent EMCs in this study were likely caused by the fines' washoff from cells in the first effluent samples, particularly for limestone sand that is highly soluble (cells 5, Figure 3- 11 [a]). Compared to TSS, higher VSS removal rates with greater improvements for limestone sand and limestone-mix was observed.

As shown in Figure 3- 11 [c, d], the bioretention-mix (cells 3 and 4) shows substantially greater effluent dissolved and total phosphorus than the inlet and other outlets (h=1). The BMP database also reports bioretentions with the highest median effluent phosphorus concentration (total and dissolved) of all BMPs, exporting phosphorus (-25% to -800%, p<0.05), whereas sand filter basins show relatively effective removals (10-45%, p<0.05) (Clary et al. 2020). Limestone-mix and Limestone sand provided enhanced phosphorus treatment with median EMC efficiency of 84-93% and 93-97%, respectively with no significant difference between lined and unlined cells (h=0). This suggests that limestone sand can significantly enhance the phosphorus

removal in LID systems if used as stand-alone or within the bioretention soil mixture, which is congruent with previous studies (Limouzin et al. 2011; Mateus et al. 2012; Shahrokh Hamedani et al. 2021).

Table 3-8. Median EMC efficiency for the various pollutants – Phase I

	Cell 1	Cell 2	Cell 3	Cell 4	Cell 5	Cell 6
EMC Efficiency (%)	Limestone	Limestone	Bioretention	Bioretention	Limeston	Limeston
ENIC Efficiency (70)	-Mix	-Mix	-Mix	-Mix	e Sand	e Sand
	Lined	Unlined	Lined	Unlined	Lined	Unlined
рН	-5	-2	-2	-2	-14	-11
Conductivity (COND)	-106	-186	-513	-629	-40	-40
Total Suspended Solids (TSS)	11	62	29	18	-17	22
Volatile Suspended Solids (VSS)	49	69	36	35	71	80
Orthophosphate (P)	84	93	-103	-36	97	93
Total Phosphorous (TP)	42	56	-118	-77	65	71
Nitrate (N)	21	42	-158	-99	-67	-37
Total Nitrogen (TN)	-17	-10	-72	-84	-24	-11
Total Coliform Bacteria	15	64	-7	29	48	44
E-Coli Coliform Bacteria	62	56	54	20	78	86
Dissolved Copper (DCu)	-51	-16	-288	-215	-19	-4
Total Copper (TCu)	-30	-5	-127	-115	1	20
Dissolved Zinc (DZn)	-79	-175	-24	-72	49	-38
Total Zinc (TZn)	32	3	29	-92	52	15
Dissolved Lead (DPb)	19	19	-110	-82	66	66
Total Lead (TPb)	-4	27	30	0	30	37

Similarly, for nitrate removal, bioretention-mix seems to have the lowest EMC efficiency (Table 3- 8) with significant nitrate export (h=1). Only limestone-mix cells are removing nitrate (21-42%, h=0), while the other two media export nitrate (Figure 3- 11 [e]). As for total nitrogen, influent and effluent EMCs were relatively same (h=1) with greater effluent EMCs for cells 3 and 4, where no significant removal was achieved. However, the BMP database reported statistically significant reduction in total nitrogen for both bioretention and sand filter basins, while nitrate was being exported. Greater TN and TP effluent EMCs in this study might be correlated with the greater effluent TSS EMCs and associated particulate pollutants.

It is important to note that substantially higher (up to 5 times higher) nitrate and total nitrogen effluent EMCs were recorded in the vegetation die-off season and after prolonged dry periods

(Storms 7 and 8 - Table 3- 6), due to plants' dead tissues (nitrogenous solids) washoff together with greater effluent TSS. Therefore, periodic maintenance including pruning vegetation and removal of captured sediments is the key factor in ensuring reliable and effective nitrogen removal (Clary et al. 2020; Herzog et al. 2021; Søberg et al. 2021). Greater nitrogen content of the bioretention-mix (Table 3- 1) also contributes to the leaching of nitrogen into the effluent. Moreover, the reports of the BMP database show that the nutrient export rate can be significantly reduced in BMPs with permanent pools (e.g. wetland basin/retention pond with removal rate of 37% and 59%, p<0.05), which indicates positive impact of internal water storage and longer residence time on nutrient removal efficiencies particularly for nitrate (Clary et al. 2020). Accordingly, we decided to examine the performance of the LID testbed cells with an internal water storage in the second monitoring phase.

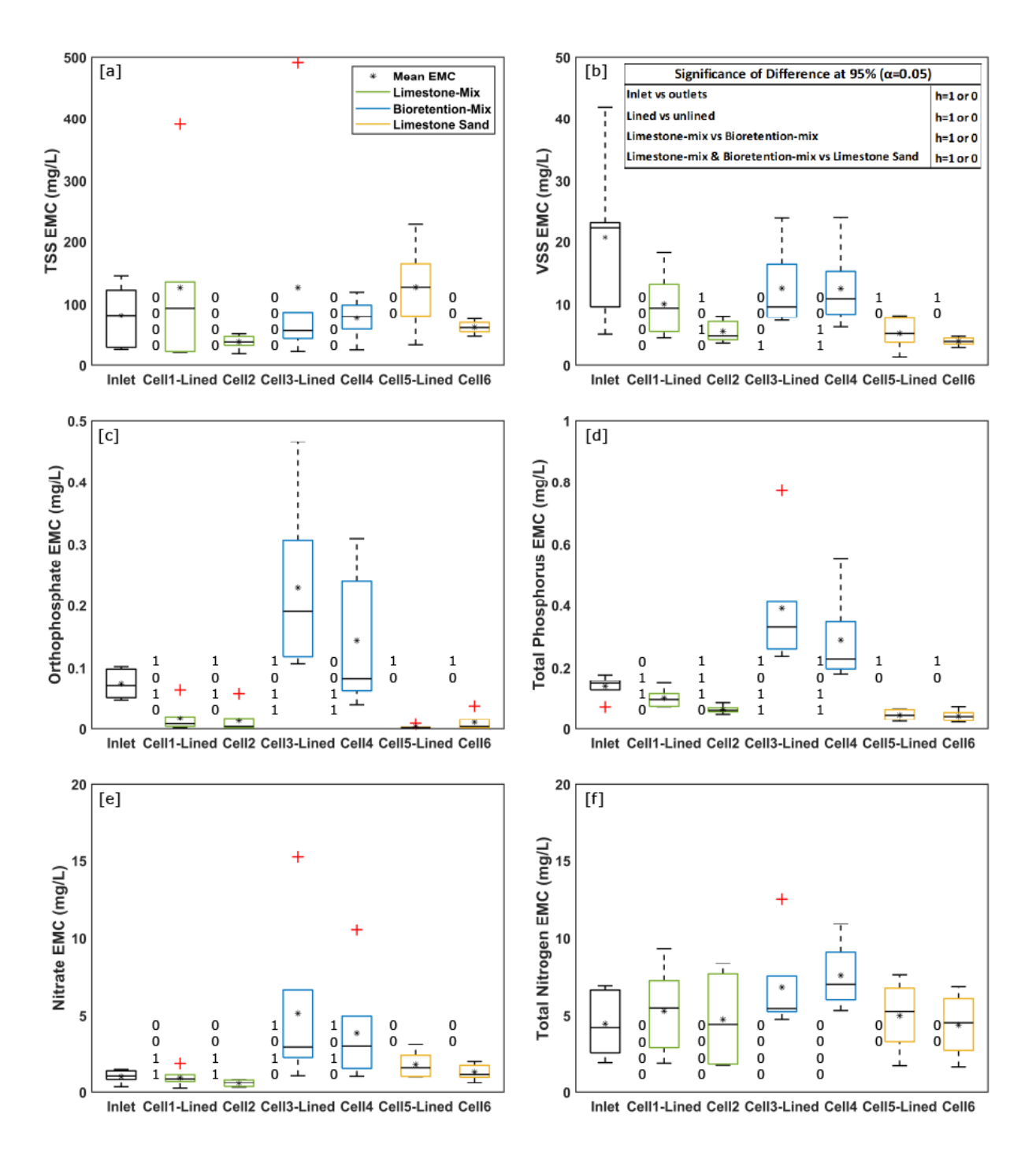


Figure 3- 11. EMC Boxplots, Inlet vs. outlets - Phase I. h-value of 1 indicates significant difference between the median EMCs (p<0.05)

In agreement with literature (Baum et al. 2021; Clary et al. 2020; Davis et al. 2010), the heavy metal EMCs (APPENDIX-Figure A1) show generally greater EMC efficiencies for total metals due to particulate matter removal through physical filtration. Dissolved metal removal, on the other

hand, is highly variable and dependent on the adsorption capacity and retention time. Similar to phosphorus, limestone sand and limestone-mix perform better in removal of copper (Table 3- 8), whereas bioretention-mix had the highest copper effluent EMC with significant difference from the influent (h=1), matching the greater copper content of the media too (Table 3- 1). Previous studies have also reported leaching of copper for bioretentions (Shahrokh Hamedani et al. 2021; Wang et al. 2019). Poor copper removal performance for bioretentions (-10%, p<0.05 - Clary et al. 2020) is found to be associated with high organic matter content of the bioretention soil media (Table 3- 1). Notably, majority of these exported dissolved copper is strongly bound to dissolved organic matter and is therefore less bioavailable to aquatic organisms and less of a threat to aquatic health (Clary et al. 2020). No significant treatment of lead and zinc was observed for any of the cells. It is important to note that low lead removal and similar effluent EMCs (Table 3- 8) is due to the fact that influent concentrations of lead were mostly under detection limit (<0.001 μg/L). All the under-detection limit measurements were replaced by 0.0005 μg/L (half the detection limit), causing no or very small removals due to near equal influent and effluent EMCs.

Total coliform bacteria and E. coli EMCs varied substantially among the LID cells and captured storms. BMP database bacteria measurement are limited and also highly variable for different BMP types and studies. The available data at the BMP database suggests that bioretention, and media filters were able to statistically significantly reduce E. coli, presenting the lowest effluent concentrations, although these BMPs also had the lowest influent concentrations (Clary et al. 2020). We also found positive E. coli EMC efficiencies (Table 3- 8) for all cells, however the medians were not statistically different in any case (Figure 3- 12).

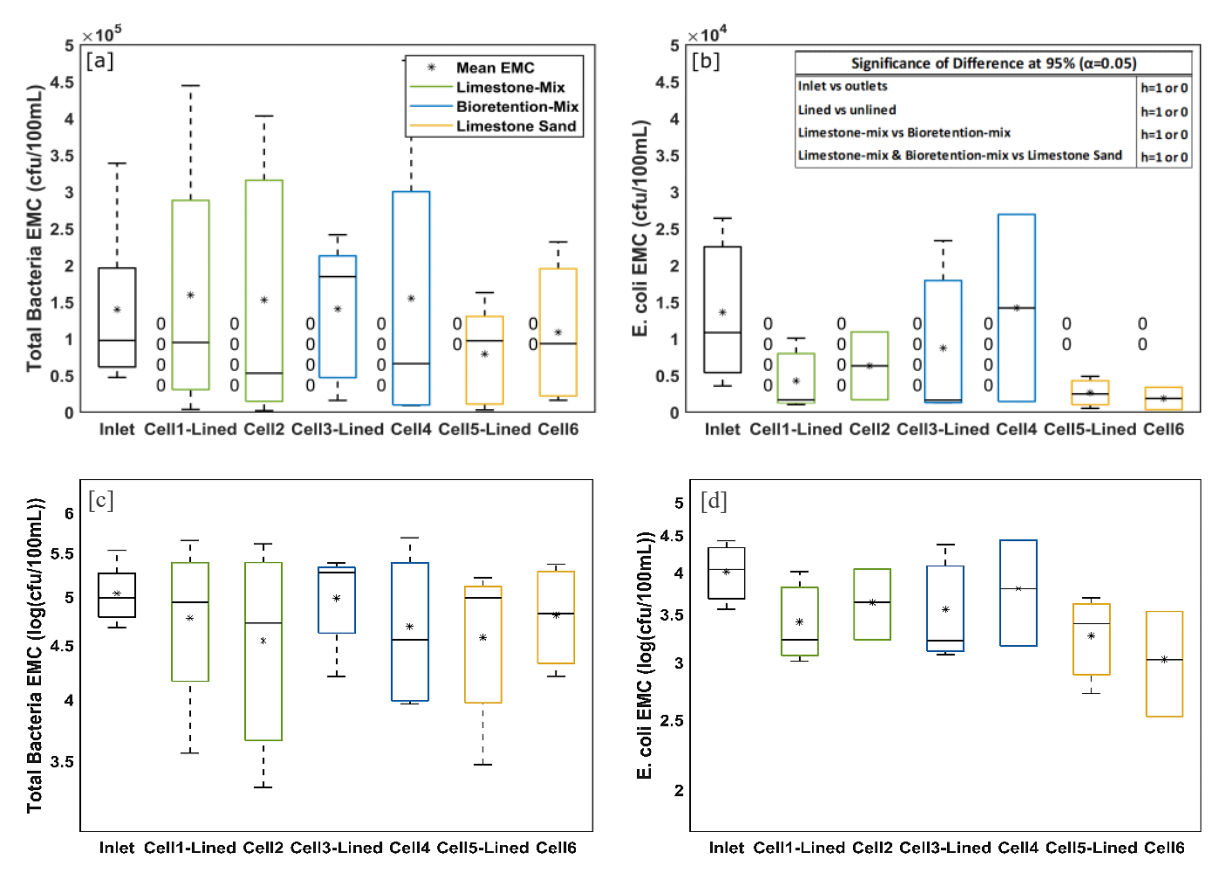


Figure 3- 12. [a, c] Total coliform and [b, d] E. coli bacteria EMC Boxplots, Inlet vs. outlets - Phase I. h-value of 1 indicates significant difference between the median EMCs (p<0.05)

A simple linear regression model was used to generate the regression lines, and confidence and prediction intervals (Figure 3- 13 and Figure 3- 14), and APPENDIX-Figure A2. The LID testbed median EMC were also plotted to demonstrate how our measurements compare to the BMP database. The red circles and triangles on the regression plots represent the four bioretention cells (Figure 3- 13), with relatively greater outlet EMCs for cells 3 and 4 with the bioretention-mix (circles).

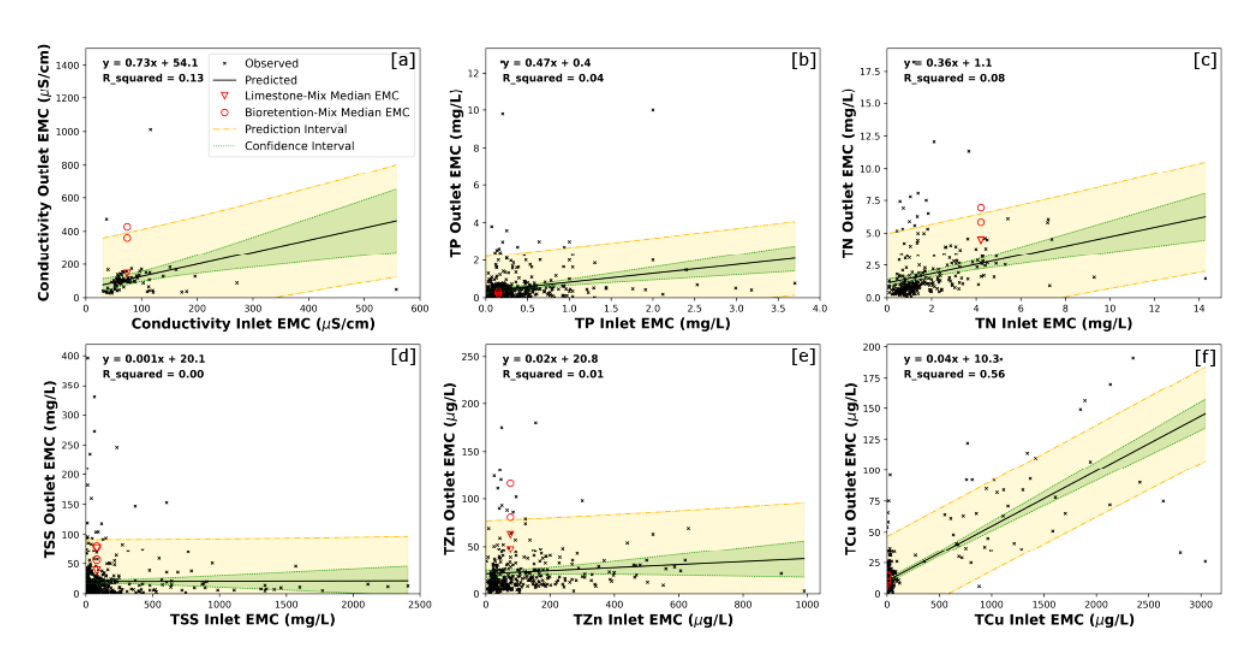


Figure 3- 13. Bioretentions outlet vs. inlet EMC scatter plots (observed), regression lines (predicted), and 95% confidence and prediction intervals

The limestone-mix EMCs mostly fell within the confidence interval, whereas bioretention-mix EMCs were in the margins or out of the prediction intervals indicating greater effluent EMCs than majority of the reported bioretentions on the BMP database. This is likely due to the chemical properties of the bioretention-mix being exceedingly rich in organic matter and nutrients (Table 3-1), which causes leaching of pollutants from the soil itself as well as through washoff of plant tissues from the overly grown vegetation within these cells. Whereas, slightly high TSS and TZn effluent EMCs for the limestone-mix cells (triangles in Figure 3- 13 [d,e]), is likely due to high solubility of limestone sand (Oates 2008) getting washed off into the outlets.

The limestone sand EMC points mainly fell outside the confidence intervals (Figure 3- 14), since limestone sand characteristics and performance vary considerably with a silica-based sand that is commonly used in sand filter basins. Greater effluent pH, TSS and nitrogen EMCs is observed, while phosphorus and copper effluent EMCs are substantially lower than most of the

BMP database reported measurements. For both limestone-mix and limestone sand the phosphorus EMCs fell in the lower margin of the prediction interval, indicating enhanced phosphorus removal.

The LID testbed inlet EMCs fell within the same range as majority of reported data points (BMP database) for a particular pollutant, except for nitrate, total nitrogen and pH that were substantially higher and closer to the upper quartile of the reported inlet EMCs. Overall, the linear equations suggest greater leaching (larger intercept, equation 3-10) for bioretentions than sand filters for all pollutants. Moreover, the wide range of influent EMCs for the reported bioretentions and sand filters demonstrates the diversity of the study conditions making them hardly comparable. This drawback highlights the need for comparative evaluation of LID system under same conditions, which is one of the main objectives of this study.

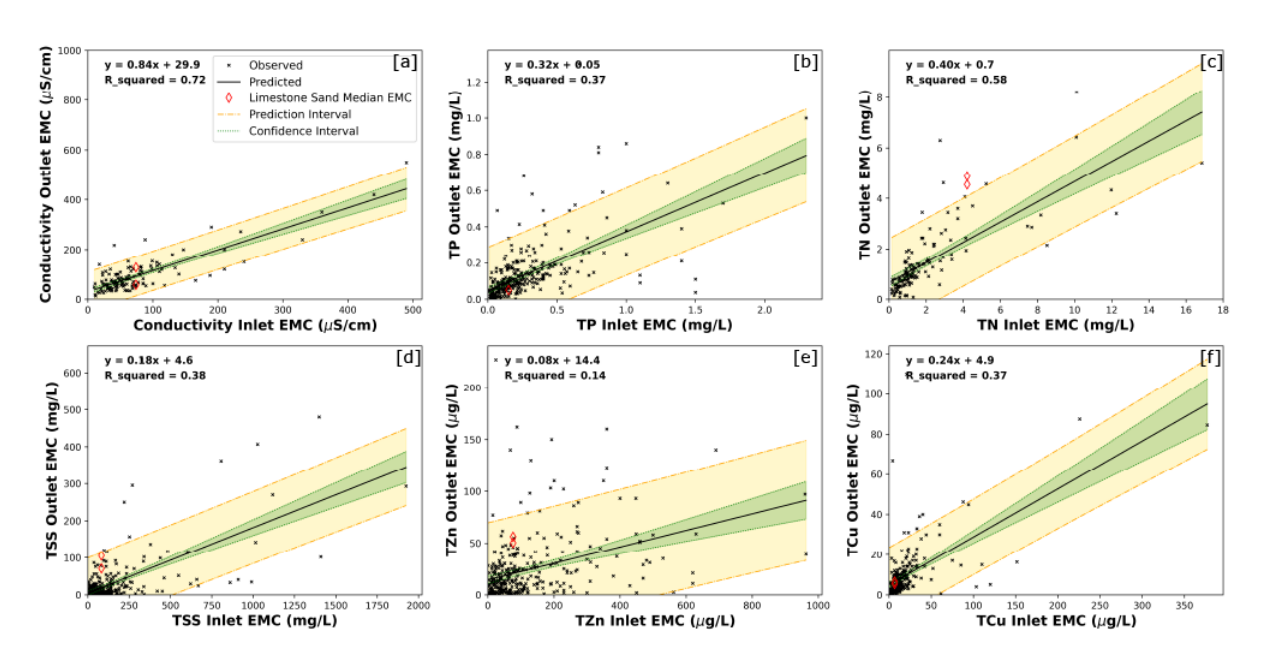


Figure 3- 14. Sand filters outlet vs. inlet EMC scatter plots (observed), regression lines (predicted), 95% confidence and prediction intervals

Moreover, the regression plots show overall poor correlation between the influent and effluent EMCs with the exception of few cases. The wide range of effluent EMCs for comparable influent EMCs accentuates the significance of design features and environmental conditions on the

treatment efficiencies. McNett et al. (2011) also found slight to no correlation between the influent and effluent nutrient concentration (TN and TP) and suggested adoption of new metrics to assess the performance of LIDs while taking a variety of influencing factors into account.

The pollutant loading was calculated (Equation 3-9) for each storm event (APPENDIX, Table A 5), and the median percent load removal is represented in Table 3-9. Overall, greater pollutant load reduction than EMC efficiency was achieved. Pollutant loading is a function of pollutant concentration and volume, hence attained flow reduction in all cells further improves the pollutant load reductions.

Table 3-9. Median percent load removal for various pollutants – Phase I

Percent Load Removal (%)	Cell 1 Limestone- Mix Lined	Cell 2 Limestone- Mix Unlined	-Miv	Cell 4 Bioretention -Mix Unlined	Cell 5 Limestone Sand Lined	Cell 6 Limestone Sand Unlined
Total Suspended Solids (TSS)	56	80	56	65	42	72
Volatile Susp. Solids (VSS)	81	90	50	86	86	92
Orthophosphate (P)	93	96	-81	14	99	97
Total Phosphorous (TP)	55	71	-41	12	79	82
Nitrate (N)	48	60	-139	-44	-36	2
Total Nitrogen (TN)	25	43	-8	23	42	57
Total Coliform Bacteria	64	81	26	84	70	66
E-Coli Coliform Bacteria	81	82	71	65	93	95
Dissolved Copper (DCu)	2	61	-264	-164	20	55
Total Copper (TCu)	-14	33	-55	-23	13	59
Dissolved Zinc (DZn)	2	3	17	3	61	30
Total Zinc (TZn)	37	49	59	67	70	58
Dissolved Lead (DPb)	23	58	-45	14	81	78
Total Lead (TPb)	41	64	55	59	59	68

Considerable pollutant load reduction is observed for most pollutants, where TSS removal is ranging from 40 to 80%, with higher reduction in unlined cells, caused by greater volume reduction in the unlined cells through direct infiltration. Bioretention-mix (cell 3) shows greater phosphorus and nitrogen effluent loads, indicating substantial leaching of nutrients from this media, while limestone sand performs best in phosphorus load reduction. Substantial copper leaching is evident in cells 3 and 4 with the bioretention-mix media, while lead and zinc are being removed in all cells.

Overall, bioretention mix shows poorest load reduction performance compared to the other two media, with highest pollutant load reductions for the limestone sand except for nitrate.

3.5.3. Phase II: with Internal Water Storage (IWS)

We captured total of 6 paired storm events in 20 months of monitoring (April 2021-December 2022) (Table 3- 10), from which 5 were qualified as representative storms considering the 72-hour interval from the preceding measurable storm event (EPA 1983), quality of data (missing/faulty data due to equipment malfunction) and sampling (number and frequency of collected samples). Phase II monitoring period presented more intense storm events than Phase I. The average rain depth for Phases I and II were of 1.55 and 2.74 inches, respectively.

Table 3- 10. List of monitored storm events April 2021 - October 2022

No.	Event Date	Rainfall Duration (min)	Total Rainfall Depth (in)	Maximum Intensity (in/hr)	Total Runoff Volume (ft3)	Peak Flow (cfs)	Antecedent Dry Periods (days)
1	4/28/2021	475	3.08	5.16	3351	1.00	76
2*	4/30/2021	350	2.45	2.04	18644	3.45	2
3	5/1/2021	105	1.6	2.28	20574	5.38	1
4*	5/28/2021	55	1.06	5.4	3723	1.60	4
5*	7/5/2021	205	1.74	3.84	5726	2.47	32
6	7/6/2021	220	5.36	4.08	51332	7.16	1
7*	9/6/2021	240	2.77	3.6	8663	2.20	35
8*	10/13/2021	370	3.87	4.68	29651	6.84	2

^{*} Representative storm events

Hydrologic Performance

The internal water storage resulted in increased reduction of runoff volume and peak flow as represented in Figure 3- 15 and Table 3- 11. Mean total runoff reduction of 62% and peak flow reduction of 75% with addition of the IWS layer.

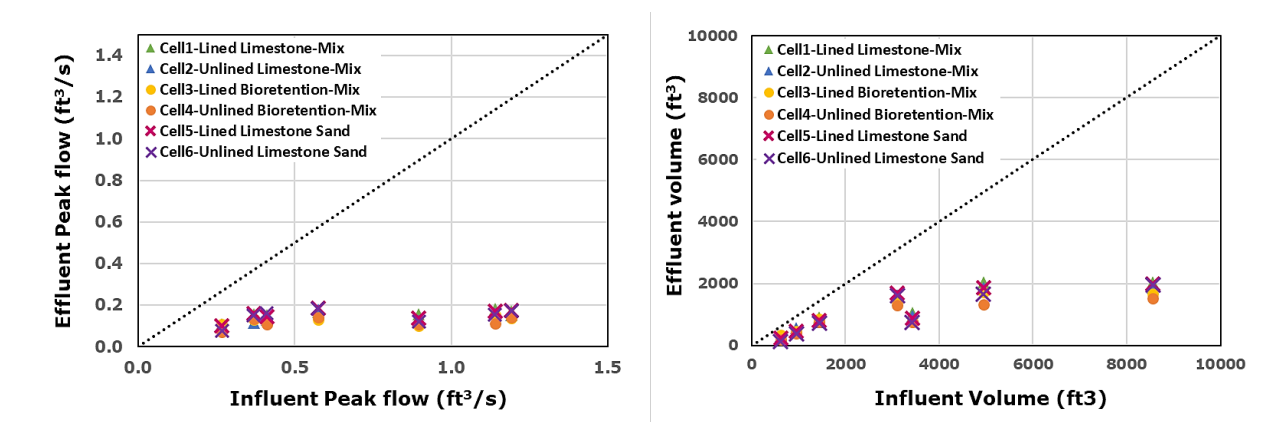


Figure 3-15. Influent volume/peak flow versus the effluent volume/peak flow - Phase II

Although runoff volume and peak flow reduction was significantly increased for the lined cells, performance of the unlined cells was not significantly impacted with the IWS layer. The performance of lined and unlined cells was more similar with the IWS layer (particularly for cells 3 and 4), thus the impact of IWS seems to be more significant on the lined cells than the unlined ones (Table 3- 7 and Table 3- 11). Moreover, the IWS layer leads to longer lag time both considering the start time and the hydrograph centroids, ranging from 30 to 60 minutes. Longer lag time is due to the time it takes for the IWS to be filled with the inflow and reach the elevated outlets for the effluent to start.

Table 3-11. Mean hydrologic performance indicators, Phase II – IWS

	Cell 1 Limestone- Mix Lined	Cell 2 Limestone- Mix Unlined	Cell 3 Bioretention- Mix Lined	Cell 4 Bioretention- Mix Unlined	Cell 5 Limestone Sand Lined	Cell 6 Limestone Sand Unlined
Volume Reduction (VR) *	52%	58%	61%	68%	61%	67%
Peak Flow Reduction (QR)	0.7	0.8	0.8	0.8	0.7	0.7
Peak Flow Reduction ratio (Rpeak)	4.3	4.9	5.4	5.9	4.4	4.7
Lag time (start time)	35	49	40	54	44	54
Lag time (Hydrograph Centroid)	34	46	52	52	41	39

^{*} Assuming equal inflow to each cell

To better visualize the difference of flow movement and outflow volume in lined versus unlined cells, and different LID designs, flow duration curve (FDC) was generated showing the outflow versus percentage of time that a specific outflow were equaled or exceeded (exceedance percentage) for each cell over the 3.5-year monitoring for phase I and II (Figure 3- 16).

The flow duration curve and cumulative volume plot shows evident difference of hydrologic performance and outflow between lined and unlined cells, and different LID designs. As discussed, per storm mass balance calculations indicated greater runoff volume and peak flow in lined cells with no significant difference between different LID designs. The cumulative volume plot for phase I (Figure 3- 16 [a]) represents two discrete groups of lined and unlined cells while the cumulative volume of the three LID designs is relatively similar with cell 1 and cell 4 providing maximum and minimum outflow volume, respectively. The FDC plot (Figure 3- 16 [c]) also demonstrates noticeably greater flows for cell 1 and other lined cells, compared to the unlined ones. Under the phase II with IWS layer, on the other hand, the performance of cells could be classified to three groups with respect to the three different LID designs. The limestone-mix recorded the highest outflows (cells 1 and 2), while the bioretention-mix (cells 3 and 4) flow are the lowest. The reason for these considerable variations might be caused by unequal inflow to cells, which is further investigated in chapter four with the SWMM model. Similar to phase I, limestone-mix and bioretention-mix report the highest and lowest flows, while limestone sand falls in the middle (Figure 3- 16 [d]).

Per-storm runoff control assessment for phase II (Table 3- 11) indicated more equivalent performance of lined and unlined cells compared to phase I. Comparing the cumulative volume plots of two phases, we can also see the same behavior suggesting smaller variations between the lined and the corresponding unlined cell for each LID design in presence of IWS layer (Figure 3-

16 [b]). The ratio of the cumulative outflow volume of unlined cells to lined cells ranges from 0.70 to 0.72 in phase I, whereas phase II ratios range from 0.86 to 0.95 with lowest ratio for the bioretention-mix in both phases indicating greater volume reduction in cell 4. The results suggest that although addition of IWS improves the runoff control of the lined cells substantially, its impact on the performance of unlined cells is not as considerable.

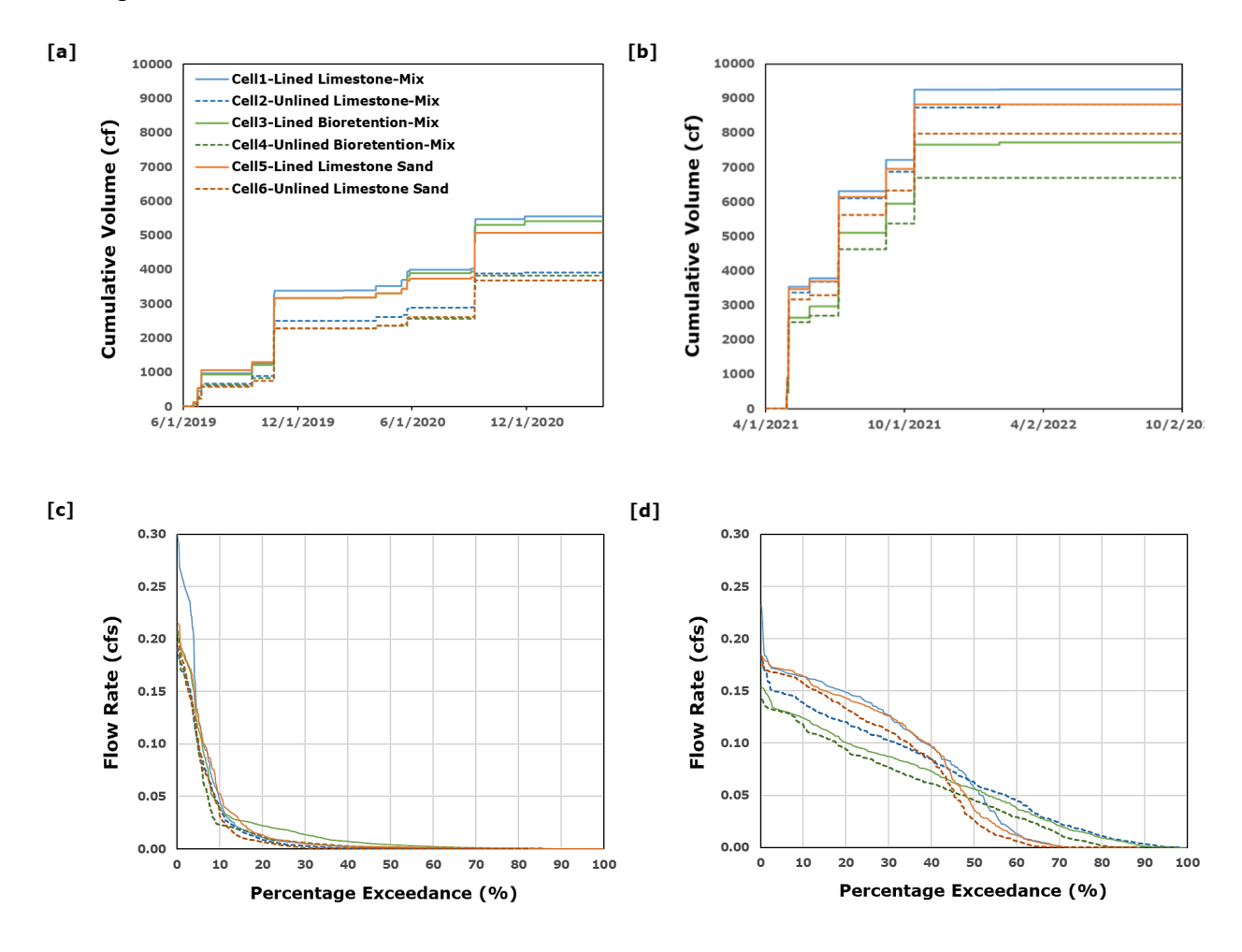


Figure 3- 16. Difference of hydrologic performance, cumulative volume and flow duration curve showing the outflow variations over phase I [a, c] and phase II [b, d]

Over the 3.5 years of monitoring, total of approximately 145,000 cf stormwater runoff was treated with the LID testbed, from which 83,400 cf outflow and 60,785 cf storage were generated.

Assuming equal inflows (total inflow divided by six) to each cell, total volume of 0.29, 0.39 and 0.24 inch of recharge is achieved in cells 2, 4 and 6, respectively (2887, 3811 and 2326 cf).

Treatment Performance

The EMC plots (Figure 3- 15) for the phase II (APPENDIX, Table A 4), indicates enhanced pollutant removals especially for particulate pollutants. Contrary to phase I, significant difference (h=1) between the inlet and outlet TSS EMCs were observed, indicating enhanced TSS removal for all bioretention cells. Greater TSS removal corresponds to greater particulate pollutant removal, resulting in smaller effluent bacteria and total heavy metal EMCs (Figure 3-16 and APPENDIX-Figure A3), in agreement with previous studies suggesting enhanced particulate pollutant treatment with addition of IWS (Afrooz and Boehm 2017; Barrett et al. 2013; Clary et al. 2020).

Table 3- 12. Median EMC efficiency for the various pollutants – Phase II with IWS

	Cell 1	Cell 2	Cell 3	Cell 4	Cell 5	Cell 6
EMC Efficiency (%)	Limestone	Limestone	Bioretention			
Enterency (70)	-Mix	-Mix	-Mix	-Mix	Sand	Sand
	Lined	Unlined	Lined	Unlined	Lined	Unlined
рН	-2	-3	-1	2	-8	-10
Conductivity (COND)	-170	-212	-566	-305	-64	-57
Total Suspended Solids (TSS)	57	58	28	32	45	22
Volatile Suspended Solids (VSS)	50	54	0	28	77	74
Orthophosphate (P)	63	50	-151	-82	75	67
Total Phosphorous (TP)	29	41	-103	-68	31	47
Nitrate (N)	-8	8	-1866	-918	-84	-66
Total Nitrogen (TN)	-20	-12	-839	-795	-51	-28
Total Coliform Bacteria	44	35	56	50	83	84
E-Coli Coliform Bacteria	83	84	85	95	87	76
Dissolved Copper (DCu)	10	-26	-340	-386	21	43
Total Copper (TCu)	-20	-54	-403	-489	-52	-6
Dissolved Zinc (DZn)	36	12	8	34	-22	-1
Total Zinc (TZn)	50	52	39	23	23	-4
Dissolved Lead (DPb)	79	56	25	76	82	91
Total Lead (TPb)	56	66	24	52	59	42

Significant reduction for both total and E. coli coliform bacteria was observed with greater E. coli EMC efficiencies for all cells (Table 3- 12). Dissolved and total heavy metal EMC efficiencies are improved in phase II, providing significant total lead removal in all cells. Zinc removal has also improved, and slight export of dissolved zinc is detected only for the limestone sand cells (Table 3- 12). Copper removal, however, shows wide-ranging EMC efficiencies for different cells with significant leaching of dissolved and total copper for the bioretention-mix cells (h=1, APPENDIX-Figure A3).

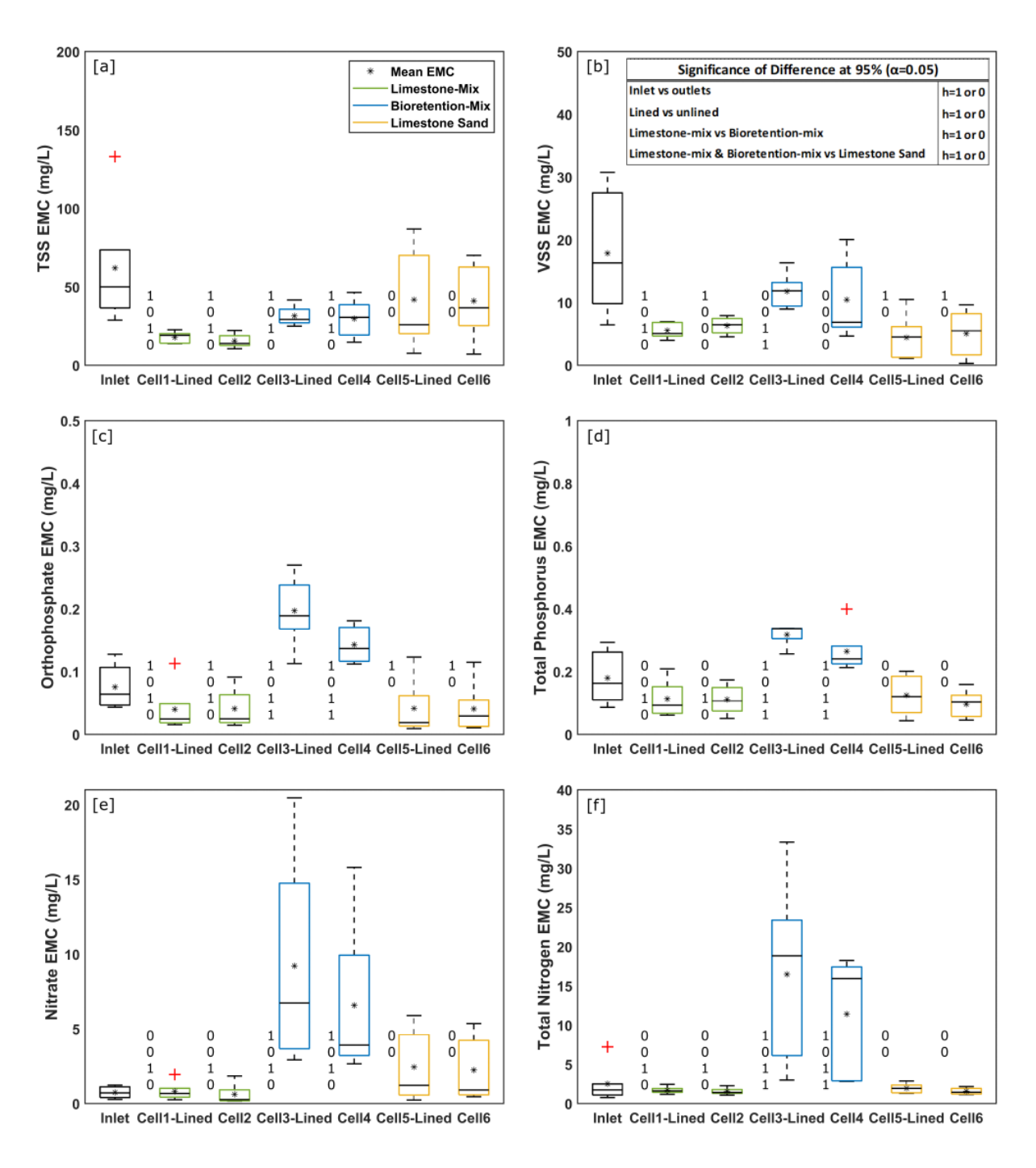


Figure 3- 17. EMC Boxplots, Inlet vs. outlets – Phase II. h-value of 1 indicates significant difference between the median EMCs (p<0.05)

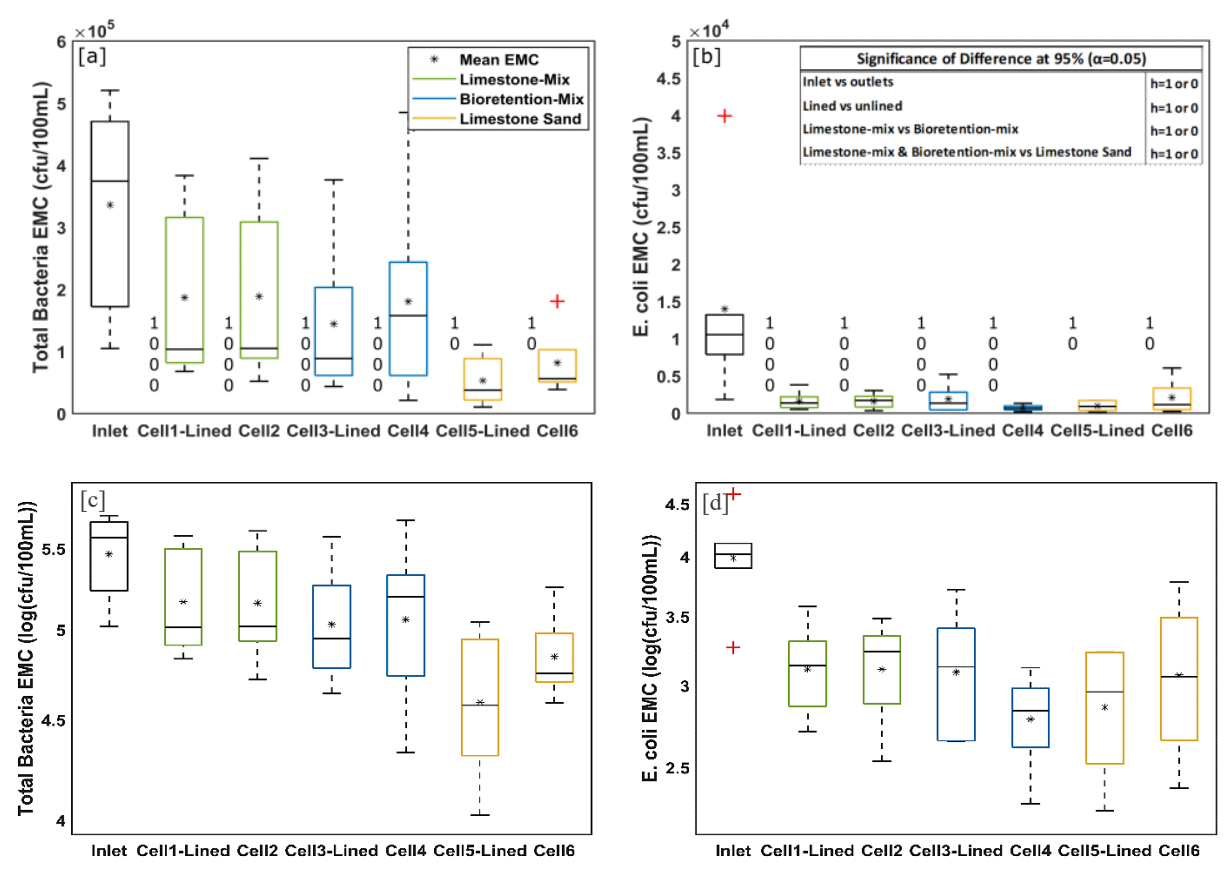


Figure 3- 18. [a, c] Total coliform and [b, d] E. coli bacteria EMC Boxplots, Inlet vs. outlets - Phase II. h-value of 1 indicates significant difference between the median EMCs (p<0.05).

Similar to phase I, no significant difference was observed between the treatment performance of lined and unlined cells for any of the tested pollutants (h=0). Changes to the pH and conductivity EMCs are also consistent through two monitoring phases, where greater effluent pH and conductivity EMC was observed. Cells containing limestone sand (1, 2, 5 and 6) show greater pH than the bioretention-mix due to the carbonate composition of limestone contributing to alkalinity of the outflow. Higher effluent conductivity EMC indicates greater concentration of ions in the outflow, hence higher values for the bioretention cells suggests more dissolved ionic compounds corresponding to greater effluent pollutant EMCs (such as P and DCu) and washed off organic matter (i.e., VSS).

Nutrient removal, on the other hand, is not improved in phase II contrasting the previous literature suggesting enhanced nitrogen removal in presence of saturate zone (Barrett et al. 2013; Clary et al. 2020; Donaghue et al. 2022; Søberg et al. 2021). Similar to phase I, cells 3 and 4 show the poorest performance in phosphorus and nitrogen treatment with significantly greater effluent EMCs (h=1) and leaching of dissolved and total nutrients. Limestone-mix and limestone sand show similar performance with slightly lower effluent EMCs for the limestone-mix. Smaller nutrient EMC efficiencies in phase II (Figure 3- 15) is likely due to longer contact time leading to desorption and washoff of the absorbed pollutants by the filtration media (APPENDIX-Figure A4). Moreover, the greater nitrate effluent EMCs suggests incomplete denitrification processes due to insufficient contact time within the submerged zone, causing excessive leaching of nitrate to the outflow. Also, high nitrate and total nitrogen effluent EMCs (Figure 3- 15 [e, f]) – particularly in the bioretention-mix cells - correspond to the storms during the plants' die-off season (storms 5, 7 and 8 - Table 3- 6) (Figure 3- 19).

Greater nitrogen effluent EMCs is observed after prolonged dry periods and during plant's dieoff season. For instance, the top left chart in Figure 3-19 shows EMC of TN. As we can observe,
concentrations in the beginning of Fall 2020 (9/3/2020) and Fall 2021 (7/5/2021 and 9/6/2021)
were the highest EMCs. According to Table 3-6 and Table 3-10, these events had long antecedent
dry periods (94, 32 and 35 days). High effluent phosphorus and TSS EMCs is caused by media
washoff for the first few captured storms, and then through desorption and excess washoff in
presence of IWS layer. Greater nutrient and copper export in bioretention-mix cells is mainly due
to the media chemical characteristics, where high nutrient and organic matter content of media not
only results in pollutant washoff and leaching, but also causes more plant and weed growth
generating more dead plant tissues and thus greater nitrogenous solid washoff. Figure 3- 20 shows

the evident difference of plant growth between the limestone-mix and bioretention-mix cells, where bioretention-mix feeds overgrown plants and considerable number of invasive plants and weeds. Greater the plant size, greater is the impact of seasonality (dry period) on the effluent pollutant concentration. Greater EMCs were observed in Fall 2021 compared to Fall 2020. This also further emphasizes the significance of maintenance and plant health on effective water quality performance, and that this is a combined effect.

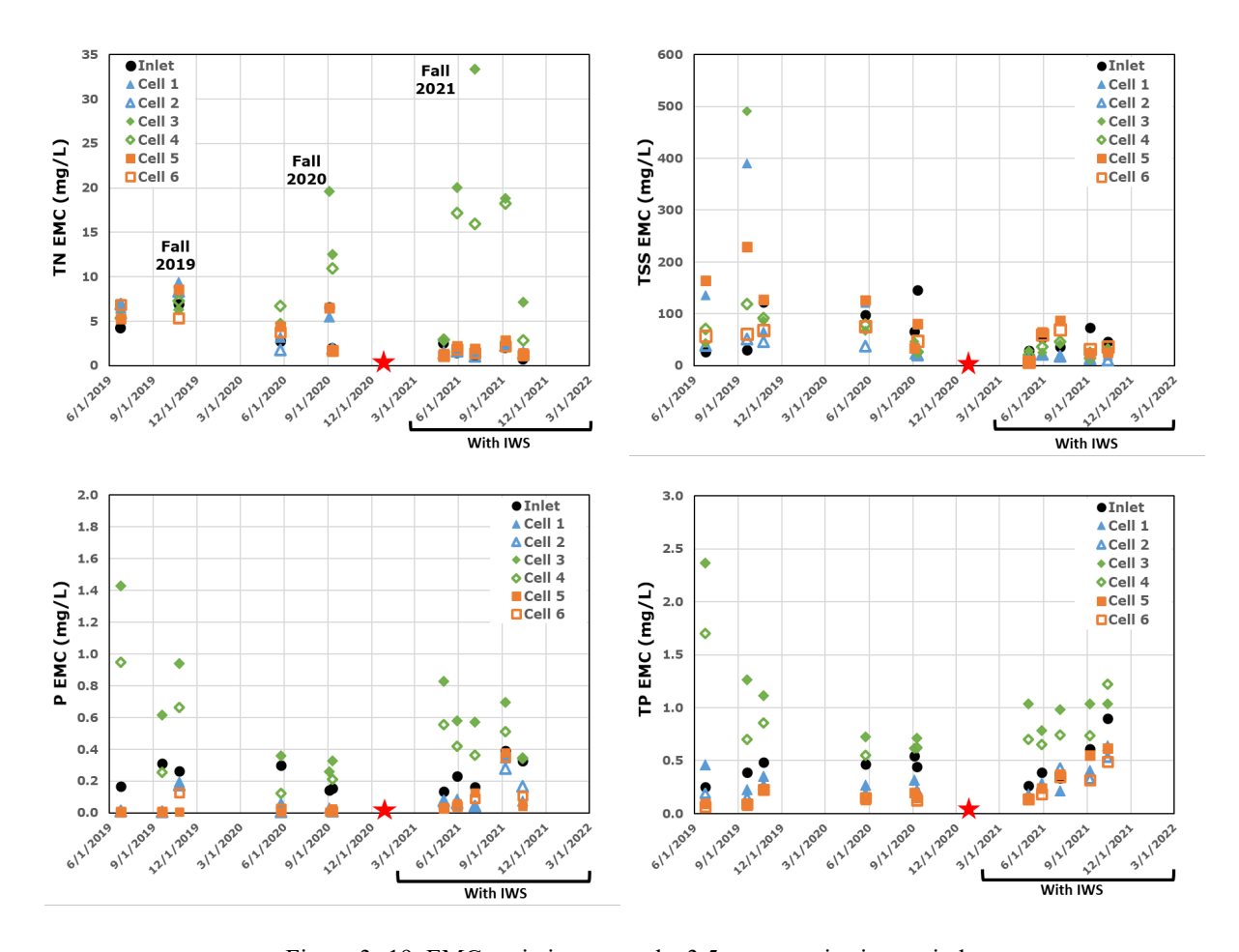


Figure 3- 19. EMC variations over the 3.5-year monitoring period

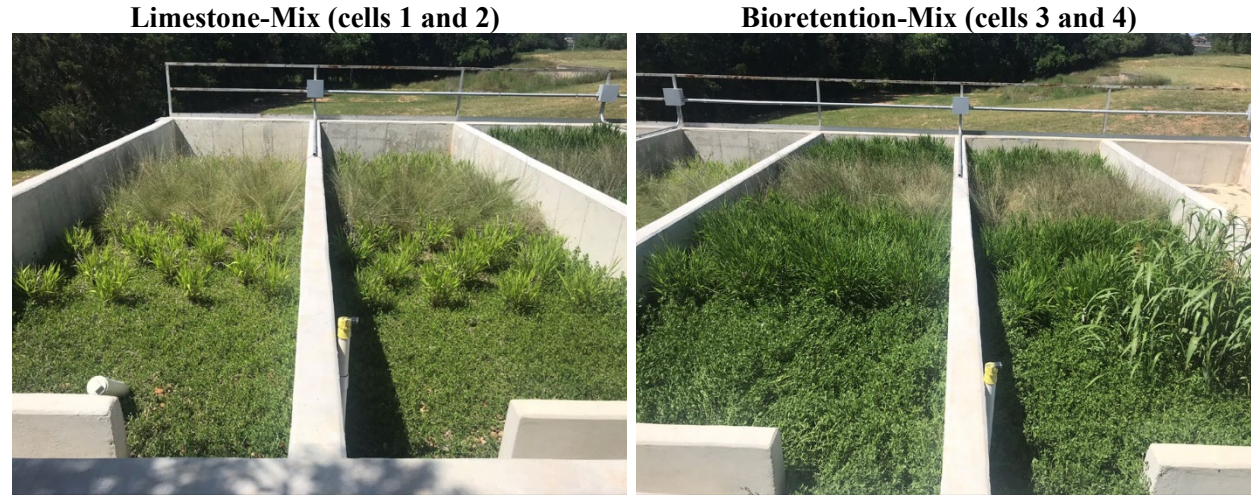


Figure 3- 20. Difference of plant growth in two bioretention designs – 4/29/2020

Red star on the plots (Figure 3- 19) indicate the time the annual maintenance was performed in December 2020. The annual maintenance entailed removal of accumulated sediments, debris and dead plants, and harvesting and pruning the plants (Figure 6- 1). The effluent EMCs for TN were lower for the first storm after maintenance, highlighting the significance of timely maintenance for effective pollutant removal and reliable nitrogen treatment, in particular..

Table 3- 13. Median percent load removal for various pollutants – Phase II with IWS

Dancout Load Dancoual (0/)	Cell 1 Limestone-	Cell 2 Limestone-	Cell 3 Bioretention-	Cell 4 Bioretention-	Cell 5 Limestone	Cell 6 Limestone
Percent Load Removal (%)	Mix	Mix	Mix	Mix	Sand	Sand
	Lined	Unlined	Lined	Unlined	Lined	Unlined
Total Suspended Solids (TSS)	83	79	75	80	79	78
Volatile Suspended Solids	77	77	47	70	89	91
(VSS)						
Orthophosphate (P)	85	81	-33	33	88	87
Total Phosphorous (TP)	67	69	-7	38	73	75
Nitrate (N)	58	63	-641	-182	32	45
Total Nitrogen (TN)	44	42	-454	-304	37	47
Total Coliform Bacteria	65	75	77	85	92	93
E-Coli Coliform Bacteria	91	91	92	98	95	88
Dissolved Copper (DCu)	53	33	-157	-151	70	78
Total Copper (TCu)	51	42	-160	-64	21	65
Dissolved Zinc (DZn)	67	58	52	75	55	66
Total Zinc (TZn)	71	76	74	73	66	74
Dissolved Lead (DPb)	89	79	66	87	90	95
Total Lead (TPb)	74	81	62	75	78	77

The pollutant loading was calculated (Equation 3-9) for each storm event (APPENDIX, Table A 6), and the median percent load removal is represented in Table 3- 13. Overall, greater and significant pollutant load reduction was observed with addition of IWS layer for most pollutants, similar to the EMC efficiencies (Table 3- 12). Bioretention-mix media shows significantly greater leaching of nitrogen and copper with addition of IWS layer, suggesting media and plant tissue washoff and incomplete denitrification in cells 3 and 4. Limestone-mix and limestone sand outperform the bioretention-mix for all pollutants, except for bacteria and zinc, where bioretention-mix shows slightly higher median percent load removal. Figure 3- 21 shows the average percent total load removal (%) among all six cells for Phase I (No IWS) and Phase II (With IWS). For all water quality parameters, it can be observed improved load removals, with exception of the parameters Volatile Susp. Solids (VSS), Nitrate (N), Total Nitrogen (TN), and Total Copper (TCu).



Figure 3- 21. Average among all six cells percent total load removal (%) for Phase I (No IWS) and Phase II (With IWS).

To further investigate the TSS loading and sediment transport within the LID testbed cells, we conducted particle size analysis to compare the particle size distribution (PSD) of the influent and effluent suspended solids (TSS) and to distinguish the particle types, if applicable. To do so, a composite sample was prepared (Li et al. 2005) for the inlet and each outlet for storms 4, 5, 7 and 8 (Table 3- 10) and the particle size distribution was recorded using the SEQUOIA LISST-Portable laser particle size analyzer. The results suggested no significant distinction between the influent and effluent PSD (Figure 3- 22). Sand filter effluents (cells 5 and 6) show greater volume of smaller particle size indicating more fines and overall smaller particle size, while bioretention cells (cells 1-4) show greater volumes towards the end of the plots indicating larger particle size distribution.

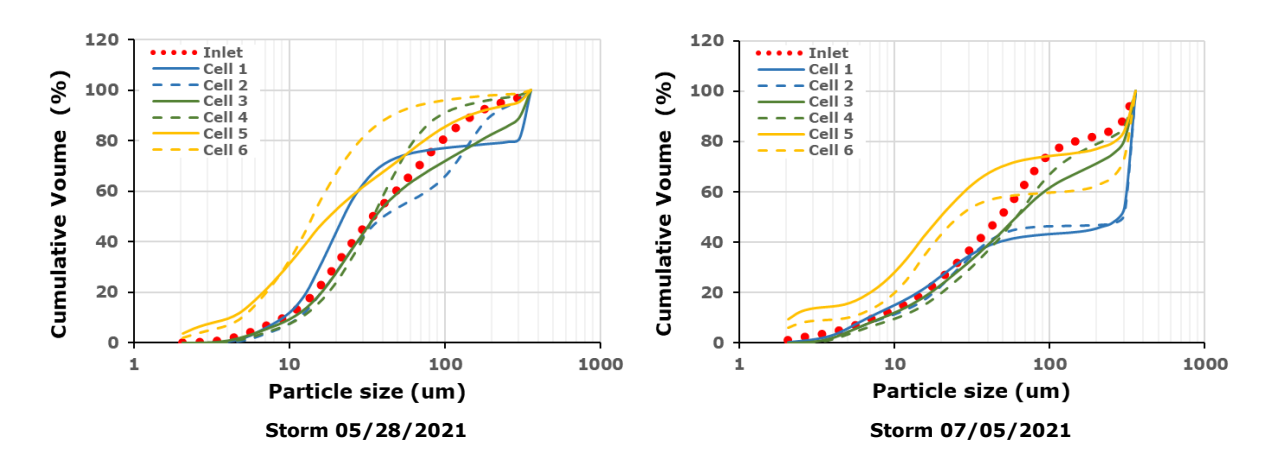


Figure 3- 22. The cumulative volume percent (%) and particle size distribution (μm) of influent and effluent samples - 2 selected storms on 05/28/2021 and 07/05/2021 is shown

3.5.4. Correlation Analysis

Impact of Storm Regime on Water Quality

Correlation analysis was conducted to study the impact of storm regime and environmental conditions on the influent pollutant load. Bedient et al. (1980) explored the pollutant load-runoff relationship in Houston, TX and found strong correlation between the total storm load and peak loads, and total runoff volume and peak flow, respectively. However, other storm characteristics

including the rainfall depth, intensity and duration seem to have little to no effect on the pollutants load (Bedient et al. 1980; Han et al. 2006a). It should be also noted that the final pollutant concentration in the stormwater runoff is a function of complex buildup and washoff processes that are impacted by the source of pollutants and the surface (e.g. road versus roofs) characteristics, dry and wet deposition, rainwater chemistry, and land use type and traffic load leading to various behaviors under same storm characteristics (Göbel et al. 2007).

We examined the correlation between the storm characteristics including the rainfall intensity, depth and duration, antecedent dry period (ADP), runoff peak flow and volume on the influent pollutant EMCs, influent pollutant load, and total percent load reduction for the total of 11 captured storm events (phase I and II). Spearman's correlation coefficient (rho) close to 1 or -1 with p-value smaller than 0.05 indicate significant correlation between the influent EMC the respective storm characteristic (Figure 3- 22). The analysis suggests strong positive correlation between the ADP and nitrogen (0.64 and 0.66, p<0.05) and metal EMCs (copper 0.69, 0.60 and zinc 0.87, 0.77, p<0.05), indicating that longer dry periods cause greater buildup of these pollutants and consequently higher influent EMCs. Han et al. (2006b) also found a modest positive correlation (r=0.7, p<0.01) between antecedent dry days and Total Kjeldahl Nitrogen.

Runoff volume and peak flow, on the other hand, establish a negative correlation demonstrating the dilution effect (-0.48 to -0.85, p<0.05) (Bedient et al. 1980). Rainfall depth and duration also show non-significant negative correlation with dissolved and total zinc and copper EMCs. Han et al. (2006a)'s correlation analysis also suggested that the pollutant EMCs are negatively correlated with total rainfall depth, implying the dilution effect.

Significant positive correlation was observed between the influent pollutant loads versus the runoff volume and rainfall depth, which is to be expected as greater rainfall depth results in greater

runoff volume and accordingly higher pollutant loads. Antecedent dry period was also found to be positively correlated with the inflow pollutant loading. Longer dry periods result in higher pollutant loads through increased pollutant build up and dry deposition on impervious surfaces. To the contrary, peak flow and rainfall intensity showed negative correlation with pollutant loading.

Total percent pollutant load reduction was computed for each storm event considering the sum of outflow pollutant loads for the six cells. Overall, no significant correlations were observed, except for minor instances that cannot be simply explained due to the complex removal processes and many other impacting factors. Weak correlation with storm characteristics for most pollutants suggests that pollutant load reduction is mainly a function of design features and the respective treatment processes within LID systems.

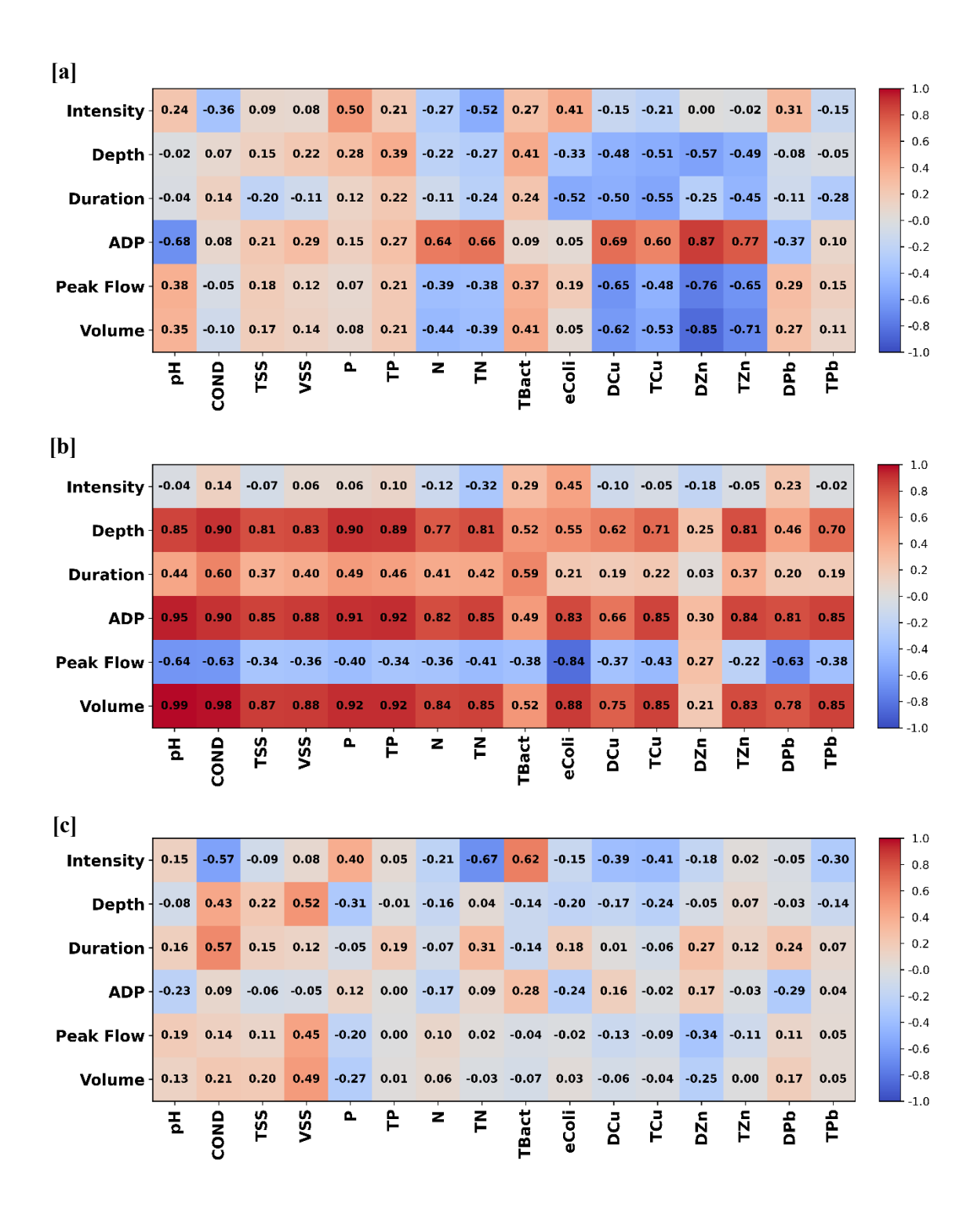


Figure 3- 23. Spearman's rank correlation coefficient matrix – Impact of storm characteristics on [a] influent pollutant EMC, [b] influent pollutant load, and [c] total percent load reduction considering all 11 captured storm events (phase I and II).

Relationship between various pollutants and potential co-contaminants

Correlation analysis was conducted for the 16 water quality parameters considering inlet and (1) all outlets, (2) each individual cell, and (3) lined and unlined cells. The three cases were considered to investigate if there are any difference in the pollutants' composition comparing each cell design (case 2) and lined versus unlined cells (case 3). In other words, we examined how the different cell designs and the subsequent difference in their performance and pollutant removal processes impacts the effluent pollutant EMCs. No change in correlation coefficients between individual cells (case 2) or grouped lined vs unlined cells (case 3) was observed, thus we generated the correlation matrix for inlet and all outlets as shown in Figure 3-23. Previous studies show that the treatment processes of different pollutants can be substantially impacted by the chemistry of stormwater and environment (such as pH and cation exchange capacity), type of pollutants and potential co-contaminants' interactions (Esfandiar and McKenzie 2022; LeFevre et al. 2015).

We found a significant positive correlation (p<0.05) between conductivity and nutrient (0.84 and 0.87 for TP and TN, respectively) and copper (0.95 and 0.88 for dissolved and total) concentrations in the effluent (Figure 3- 23 [b]), indicating cross-correlation of these parameters that is likely associated with the dissolved organic matter content (Clary et al. 2020; Shahrokh Hamedani et al. 2021). Han et al. (2006a) also discovered a strong correlation among conductivity and dissolved and total metals, Total Kjeldahl Nitrogen, and dissolved organic carbon in highway stormwater runoff. Moreover, the results suggested a strong positive correlation between dissolved and total phosphorus, and dissolved and total copper (0.81, 0.8, p<0.05).

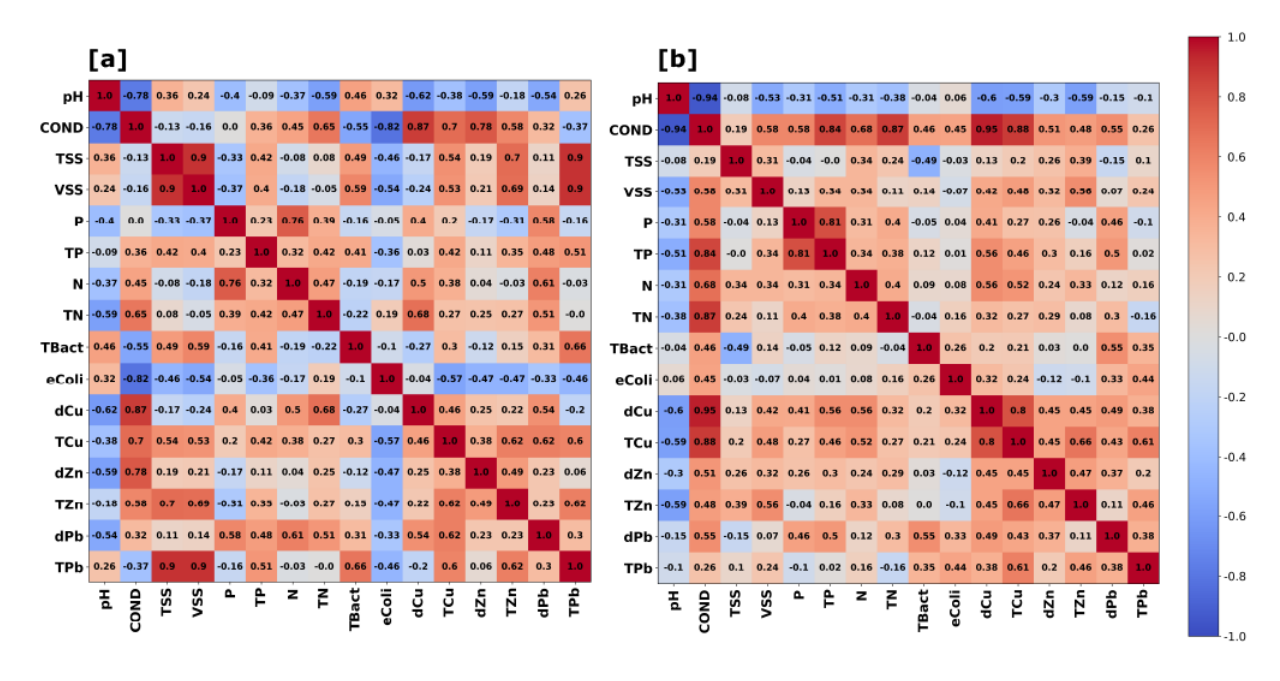


Figure 3- 24. Spearman's rank correlation coefficient matrix for [a] influent and [b] effluents EMCs

For the inlet, on the other hand, stronger correlation (p<0.05) between TSS and VSS, and total metals was observed (Figure 3- 23 [a]). Han et al. (2006a)'s correlation analysis of highway stormwater pollutants demonstrated poor correlation of TSS with most pollutants, even though TSS and VSS were strongly correlated, and relatively good correlation existed between TSS and particulate metals. Additionally, inlet N and P are also strongly correlated (0.76, p<0.05), suggesting uniform sources of nutrients in the inlet stormwater runoff (Göbel et al. 2007; Han et al. 2006b). However, no significant correlation is evident between effluent nutrient concentrations, due to varying removal mechanisms that are dependent on the design, and chemical and physical properties of each cell (Esfandiar and McKenzie 2022).

3.5.5. Soil Core Sampling

The initial pollutant content of the media was subtracted from the pollutant content of the collected soil samples to only account for the retained pollutants. Median pollutant content (Table

3- 14) was relatively similar in the lined and unlined cells with slightly higher values for the lined cells. However, no statistical inferences can be made due to small number of soil samples.

Table 3- 14. Median pollutant content (mg/Kg) in collected samples and initial soil media pollutant content

	Copper (mg/Kg)	Lead (mg/Kg)	Zinc (mg/Kg)	TP (mg/Kg)	TN (mg/Kg)
Cell1 - Lined Limestone-Mix	1.4	0.9	5.5	94	12.2
Cell2 - Unlined Limestone-Mix	1.2	0.9	5.0	79	16.0
Cell3 - Lined Bioretention-Mix	4.4	1.2	11.4	349	14.4
Cell4 - Unlined Bioretention-Mix	2.8	0.5	4.6	101	9.4
Cell5 - Lined Limestone Sand	0.4	< 1.24	2.6	23	1.5
Cell6 - Unlined Limestone Sand	0.6	< 1.24	2.4	23	1.7
Cell5b - Lined Limestone Sand *	< 0.5	< 1.24	1.5	18	0.7
Cell6b - Unlined Limestone Sand *	< 0.5	< 1.24	0.9	12	0.5
Limestone -Mix	2.93	2.88	12.9	174	15.3
Bioretention-Mix	4.64	4.23	18.5	590	25.4
Limestone Sand	<2	<1.5	2.09	16	1.2

^{*} Middle layer sample (6-18inch)

The bioretention cells showed substantially greater measurements for all pollutants compared to the sand filter basins, with highest values for the bioretention-mix (Figure 3- 24). It is important to note that greater pollutant content is not an indicator of higher retention alone; and the pollutant-contributing effects of the accumulated debris and plant tissues in the bioretention cells should also be considered. Contrary to the previous studies suggesting greater pollutant accumulation near inflow, no spatial pattern of pollutant retention was detected in any of the cells (Figure 3- 24 and Figure 3- 25). However, we observed a similar retention pattern and hotspots for the three heavy metals in all bioretention cells (Figure 3- 24), suggesting cross-correlation of lead, zinc and copper and similar removal processes. Although the EMC analysis suggested greater heavy metal removal for limestone sand, no substantially higher heavy metal content was found in the limestone sand samples, and most samples showed metal content below the detection limit (Table 3- 14).

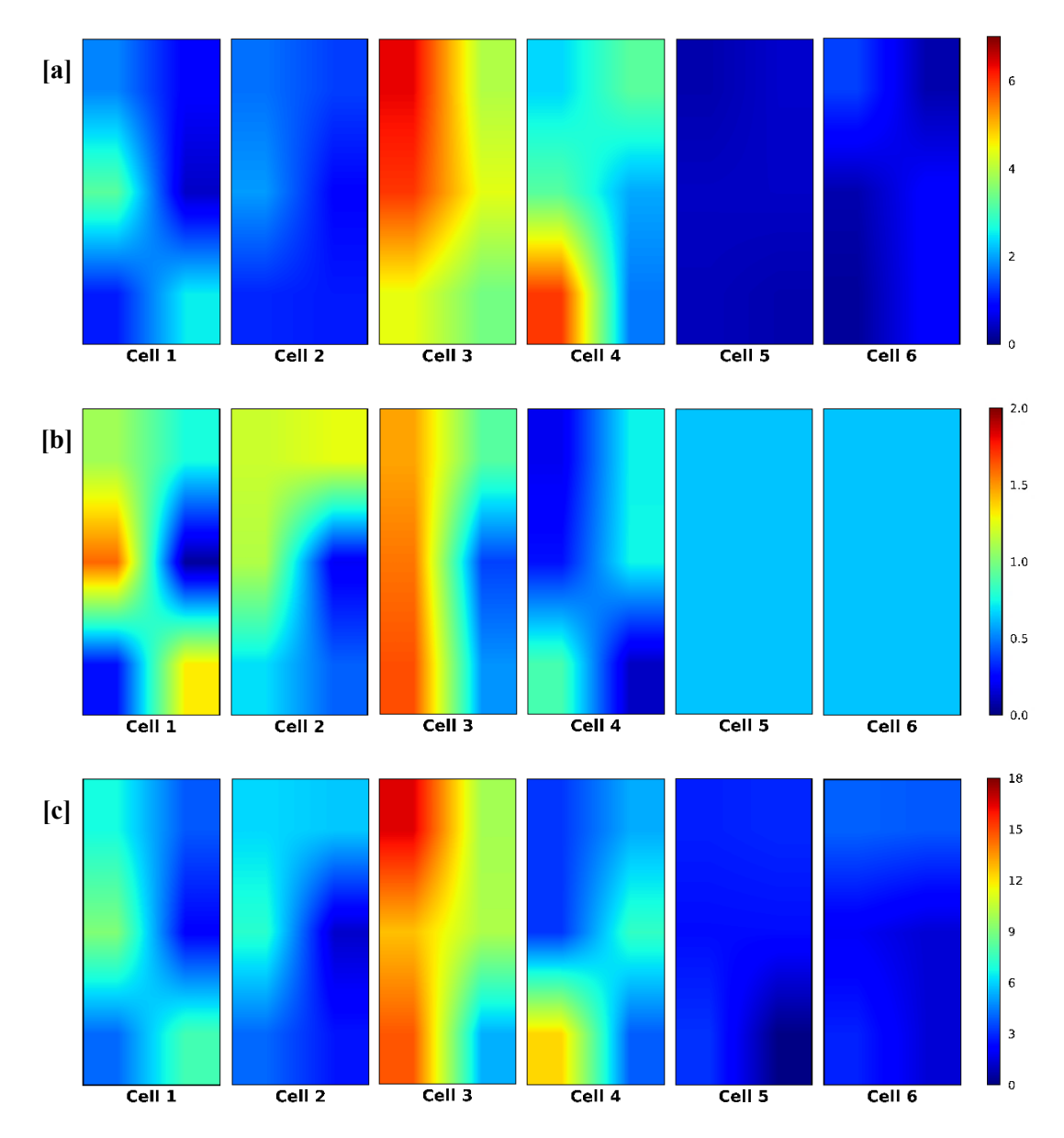


Figure 3-25. [a] Total copper, [b] Total lead and [c] Total zinc content in surface soil samples (mg/Kg)

The nutrient content was significantly higher in bioretention-mix (Figure 3- 25), which correlates with considerable leaching of phosphorus and nitrogen in cells 3 and 4 for both monitoring phase I and II (Figure 3- 11 and Figure 3- 17). In sand filter basins, samples from the middle layer show comparatively lower pollutant content than the surface samples, suggesting

greater accumulation of pollutants on the surface, which is consistent with literature (Jones and Davis 2013; Kandel et al. 2017; Paus et al. 2014).

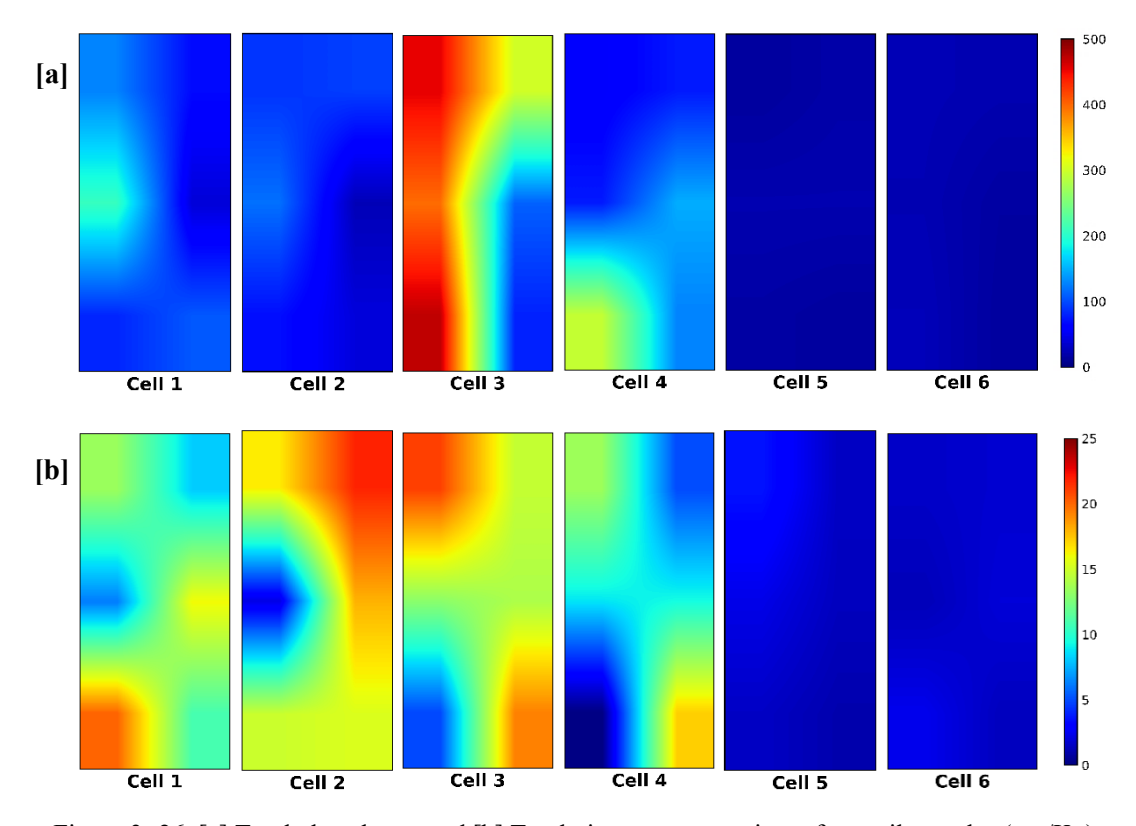


Figure 3- 26. [a] Total phosphorus and [b] Total nitrogen content in surface soil samples (mg/Kg)

It should be noted that assessing various pollutants' species and phases (e.g., organic vs inorganic) can more accurately depict the retention of pollutants while differentiating their sources and forms. A better representation of the soil profile could be achieved by collecting multiple samples at smaller depth increments (for instance: 1-inch, 2-inch, and 6-inch) during winter, when the plant and insect activity is at minimum allowing for deeper sample collection to provide better representation of the soil profile.

3.6. Conclusion

The field monitoring data suggests relatively similar hydrologic performance (APPENDIX, Table A 2) for different filtration media with no significant difference (p>0.05). Assuming equal

inflow to all six cells, Limestone-mix cells seem to show slightly lower runoff volume reduction and peak flow control compared to the other two media, which might be due to its higher infiltration rate (compared to bioretention-mix) and preferential flow paths in the cells. With respect to lined versus unlined cells, greater volume and peak flow reduction was achieved for all three designs, indicating 25-35 % volume difference infiltrating through the subsoil. Through the second monitoring phase, presence of the IWS layer enhanced hydrologic performance by increased runoff volume and peak flow reduction, as well as longer lag times. The impact of IWS was found to be more significant on the lined cells, while no substantial difference was observed in the performance of unlined cells. In the next phase of the study, SWMM model was developed and used to better understand the LID testbed performance, and to evaluate the total volume of treated stormwater, and the infiltration volume in unlined cells over the 3.5 years under a continuous simulation.

Regarding the treatment performance, results suggested overall improved performance for the cells containing the limestone sand - both sand filter (Cells 5 and 6) and bioretention (Cells 1 and 2) cells - compared to the conventional bioretention-mix (Cells 3 and 4). The limestone-mix (Cells 1 and 2) outperformed the bioretention-mix for all pollutants, with statistical significance for orthophosphate, total phosphorus, nitrate and dissolved copper (p<0.05). The export of nutrients and copper from bioretention-mix is mainly due to high organic matter and nutrient content of the soil leaching into the outflow. These findings highlight the importance of filtration media in pollutant removal rates and the subsequent effluent water quality. Maintenance was found to be crucial for reliable pollutant removal, particularly for nitrogen. Greater effluent EMCs after long dry periods and plants die-off season was observed, suggesting washoff of nitrogenous solids into the outflow,

which can be significantly reduced by performing timely maintenance including removal of debris, and harvesting and pruning the plants.

We also discovered a significant positive correlation (p<0.05) between the effluent conductivity and nutrient and copper concentrations, pointing out the association of nutrients and copper with dissolved organic matter in the outflow. We did not observe any significant difference between the water quality performances of sand filter basins vs. bioretention basins, except for the bioretention-mix. Similarly, lined and unlined cells showed various performance for different pollutants, however the differences were not statistically significant (p>0.05). We found our results consistent with previous studies (BMP database) - particularly for the limestone-mix and limestone sand - by conducting regression analysis and plotting the inlet and outlet EMCs, and the corresponding prediction and confidence intervals.

In the second monitoring phase, the IWS layer provided enhanced treatment and hydrologic performance. EMC efficiencies and percent load removal were increased for TSS, total and E. coli bacteria, and heavy metals (lead and zinc), which were significantly lower than the corresponding Inlet EMCs (p<0.05). Similar to phase I, Limestone-mix showed the best treatment performance for most pollutants which was relatively similar to the limestone sand, whereas bioretention-mix showed the poorest performance and great extent of nutrient and copper leaching. The potential reason for reduced removal and increased effluent EMC and loads is the desorption and export of the phosphorus and nitrate from the filtration media and plants. Similar to phase I, no significant difference was observed between the treatment performance of sand filter basins versus bioretention cells and lined versus unlined cells (p>0.05).

The results of the soil sample analysis also demonstrated relatively similar pollutant retention in lined and unlined cells, suggesting matching filtration and removal processes irrespective of the

liner component. Substantially greater pollutant content was measured in bioretention cells compared to the sand filter basins, however further research is required to differentiate the sources of the pollutants and to identify the stormwater-retained pollutants.

CHAPTER FOUR: STORMWATER MODELING - SWMM MODEL

This chapter describes the Stormwater Management model (SWMM) model development process, including the calibration and validation using collected field monitoring data. Then, the model is used to further investigate the hydrologic performance of the LID testbed under continuous simulation to quantify the mass balance and the achieved recharge in unlined cells.

4.1. Introduction

An EPA Storm Water Management Model (SWMM 5.1) is developed to simulate the LID testbed and the corresponding drainage area. SWMM is a dynamic hydrologic-hydraulic water quality model designed primarily for the simulation of runoff quantity and quality in urban areas. SWMM is the standard model in the field of urban stormwater modeling and is being used globally in an array of applications such as design of drainage system components for flood control; sizing detention facilities and their appurtenances for flood control and water quality protection; controlling site runoff using LID practices; and evaluating the effectiveness of BMPs for reducing wet weather pollutant loadings (Rossman and Huber 2015). SWMM represents the physical elements of the water systems by defining objects including subcatchments, junctions, conduits, storage units, weirs, orifices, dividers, outfalls, and rain gauges.

SWMM modeling process is shown in Figure 4-1. SWMM uses a nonlinear reservoir model to estimate the surface runoff from the rainfall input, in which the subcatchments are idealized rectangular planes with a specific width (Guo and Urbonas 2009). The curve number method was used for infiltration calculation and dynamic wave technique for flow routing. As for LID modeling, SWMM contains LID modeling schemes to model different LIDs such as bioretention, green roof, permeable pavement and their constituents. Each LID is a simulated as vertical layers

of surface, soil, and underdrain and can be adjusted based on the specific needs of design (Gironas, J. et al. 2009).

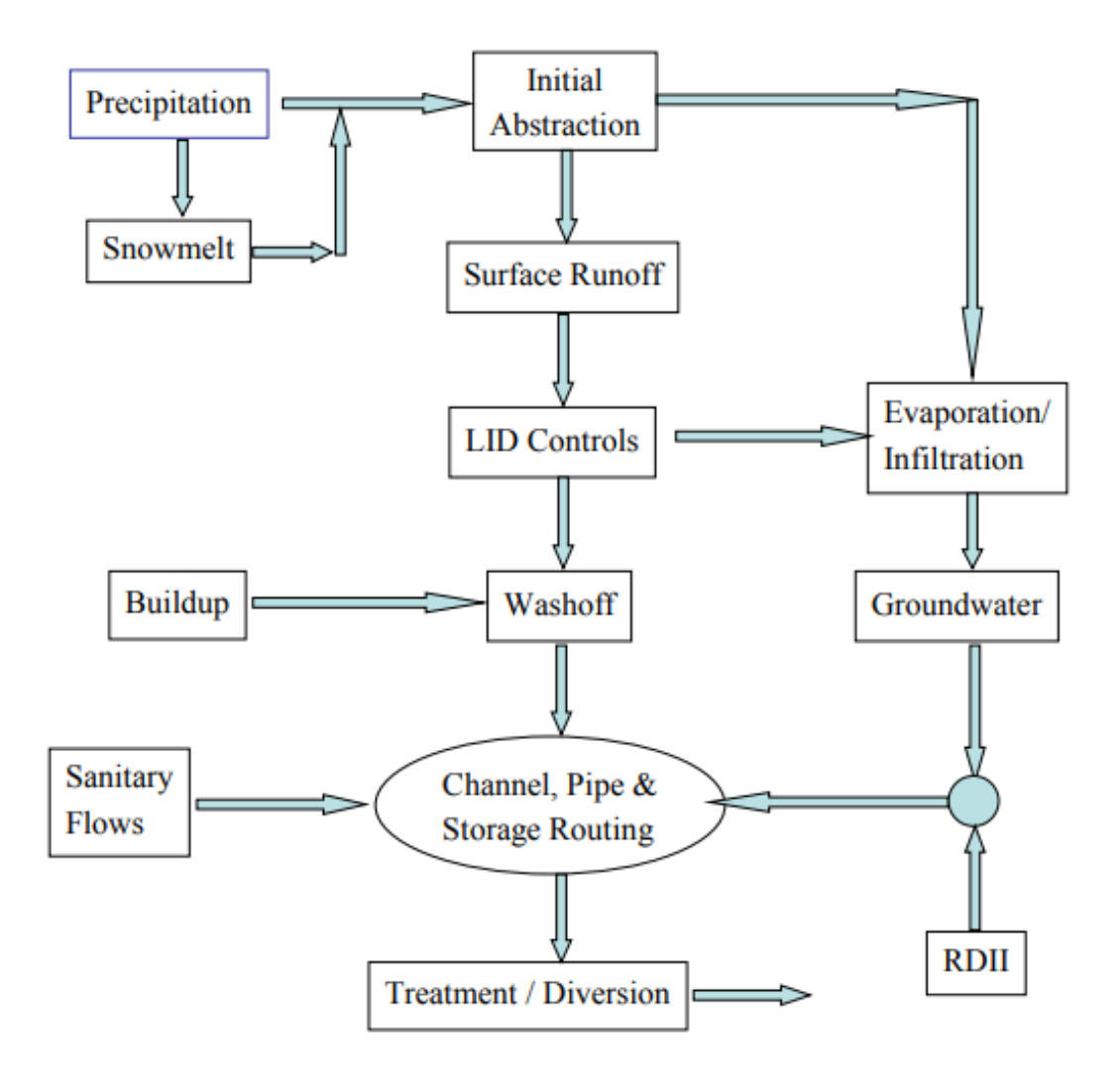


Figure 4-1. Modeling process by SWMM (Rossman & Huber, 2015)

4.2. SWMM Model Development

To simulate the watershed, digital elevation model (DEM) of the watershed and the drainage lines were downloaded from the National Elevation Dataset (NED) and National Hydrography Dataset (NHD), respectively. Land cover and soil map were downloaded from the National Land Cover Dataset (NLCD) and the State Soil Geographic Data Base (STATSGO). Data preparation

including watershed delineation, soil and land use maps, and curve number (CN) grid generation was carried out using ArcGIS10.2 and HEC-GeoHMS and was imported to the SWMM using the inpPINS software. The historical daily temperature data obtained from the San Antonio international airport weather station (GHCND: USW00012921) was used as an input to SWMM to calculate the evaporation rates based on daily minimum and maximum temperatures according to Hargreaves method (Hargreaves and Samani 1985), whereas the recorded field monitoring data were used for rainfall-runoff data.

Table 4-1. Characteristics of the subcatchments in the LID testbed drainage basin

Subcatchment ID	Area (ac)	Slope (%)	Width (ft)	CN	Imperviousness (%)
431	0.08	8.30	10.87	68	20
432	0.18	3.58	2.88	87	38
433	0.11	3.49	5.34	84	20
434	0.24	3.56	8.44	84	20
435	0.08	2.84	8.51	87	38
436	0.11	2.67	3.62	84	20
437	0.06	5.16	3.96	84	20
438	0.14	1.86	2.84	87	38
439	0.04	2.68	2.68	84	20
440	0.15	3.60	2.56	87	38
441	0.13	2.80	2.56	87	38
442	0.21	2.73	3.40	87	38
443	0.13	5.95	5.94	84	20
444	0.08	3.20	2.38	84	20
445	0.10	2.05	2.49	84	20
446	0.03	3.04	0.67	87	38
447	0.11	2.62	3.47	84	20
448	0.02	1.65	0.62	87	38
449	0.11	2.57	2.35	87	38
450	0.20	5.33	5.99	84	20
451	0.10	3.21	2.52	87	38
452	0.01	6.67	0.18	87	38

The CN grid was built using the land cover and soil map data from the National Landcover Dataset (NLCD) and the State Soil Geographic Data Base (STATSGO), which indicated three main districts within three curve numbers of 68, 84 and 87. The study area contains two hydrologic

group soils of type B - that is the silt loam or loam with moderate infiltration rate - and type D that contains clay with very low infiltration rate. The land use of the catchment is divided to two types of residential area with average imperviousness of 38 and 20. The Area (ac), average slope (%) and width (ft) of each subcatchments was calculated and is shown in Figure 4- 2. The widths were calculated by dividing the drainage area per flow length of each subcatchment.

Characteristics of the conduits and junctions including the dimensions and invert elevations were measured at field. SWMM uses a nonlinear reservoir model to estimate the surface runoff from the rainfall input, in which the subcatchments are idealized rectangular planes with a specific width (Guo and Urbonas 2009). The curve number method was used for infiltration calculation and dynamic wave technique for flow routing. The simulation run was performed for 0.1-second routing step, 1-day and 10-second runoff step for dry and wet conditions, respectively.

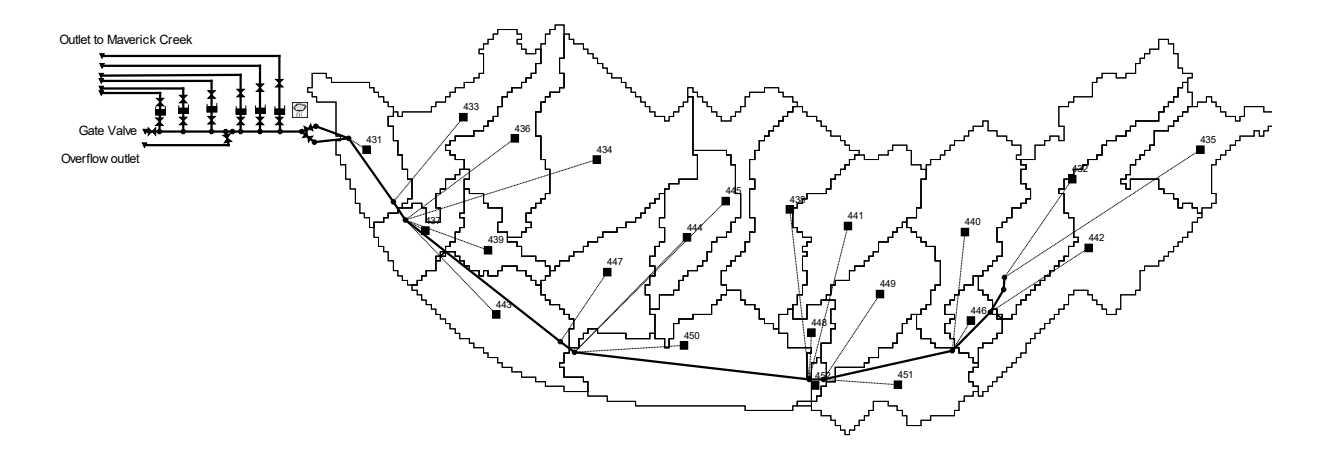


Figure 4- 2. SWMM model – The LID testbed and the drainage area

To simulate the LID testbed, a storage tank was assigned to each cell of the LID testbed. The storage curve was generated by computing the equivalent surface area (ft²) to the water level (ft) considering the porosity of the media within each cell. Outlets were modeled by assigning a unique

rating curve to each cell based on the depth and outflow relationship following the water level and outflow measurements at the field (APPENDIX,

. Physical characteristics of the conduits and junctions including the dimensions and invert elevations were measured using a land survey total station. The Curve Number method was used for infiltration calculation and the Dynamic Wave technique for flow routing.

4.3. Calibration and Validation

Model calibration was performed manually by adjusting the depth of the depression storage on impervious and pervious areas (DStore), Manning's roughness coefficient for impervious and pervious areas (N), percent of impervious area with no depression storage (Zero_Imperv) for the watershed, and by adjusting the rating curve in the LID testbed. The ranges of the calibration parameters were selected based on recommended values by the SWMM manual (Rossman 2015) presented in Table 4- 2.

Table 4-2. Calibration parameters range and final value

Parameter	Range	Final value
Manning's N_Imperv	0.011 - 0.016	0.016
Manning's N-Perv	0.1 - 0.18	0.15
DStore-Imperv (in)	0.05 - 0.15	0.1
DStore-Perv (in)	0.2 - 1.0	0.7
zero_Imperv	0 - 25	5
Curve Number CN	61 - 98	*
Imperviousness	0 - 95	*

^{*} Differs for each subcatchment

The coefficient of determination (r^2) , Nash-Sutcliffe efficiency (NSE), and percent bias (PBIAS) were used to assess the goodness of fit of the simulations. The r^2 value ranges from 0 to 1 with higher values indicating better model performance, whereas the NSE ranges from $-\infty$ to 1 and the values between 0 and 1 indicate acceptable level of performance. PBIAS is an indicator of

over/under estimation and determines the average tendency of simulated data to be greater or smaller than historical series. Smaller PBIAS values (close to 0.0) suggest more accurate model results, while positive and negative values indicate underestimation and overestimation bias, respectively.

$$r^{2} = \left(\frac{\sum_{i=1}^{n} (O_{i} - \bar{O})(P_{i} - \bar{P})}{\sqrt{\sum_{i=1}^{n} (O_{i} - \bar{O})^{2}} \sqrt{\sum_{i=1}^{n} (P_{i} - \bar{P})^{2}}}\right)^{2}$$
(4-1)

$$NSE = 1 - \left| \frac{\sum_{i=1}^{n} (O_i - P_i)^2}{\sum_{i=1}^{n} (O_i - \bar{O})^2} \right|$$
(4-2)

$$PBIAS = \frac{\sum_{i=1}^{n} (O_i - P_i) \times 100}{\sum_{i=1}^{n} (O_i)}$$
(4-3)

where: O_i is the observed flow at time step i, P_i is the predicted flow at time i, \bar{O} is the average observed flow, and \bar{P} is the average observed flow.

4.4. Hydrologic Performance Under Continuous Simulation

The SWMM model enables us to accurately calculate the inflow to each individual cell by compensating for the overflow and standing runoff in the inlet channel before it starts flowing into the cells. Moreover, the continuous simulation accounts for the evaporation in the testbed cells, providing more accurate mass balance to quantify the achieved recharge in unlined cells.

To further assess the long-term hydrologic performance of the testbed and quantify the recharge through unlined cells, A 15-year (1999-2014) continuous simulation was conducted under (1) no internal water storage, and (2) with internal water storage layer. Historical rainfall (15-min) and daily temperature were obtained from the San Antonio international airport weather station (GHCND: USW00012921). Evaporation rates were calculated by SWMM using the daily

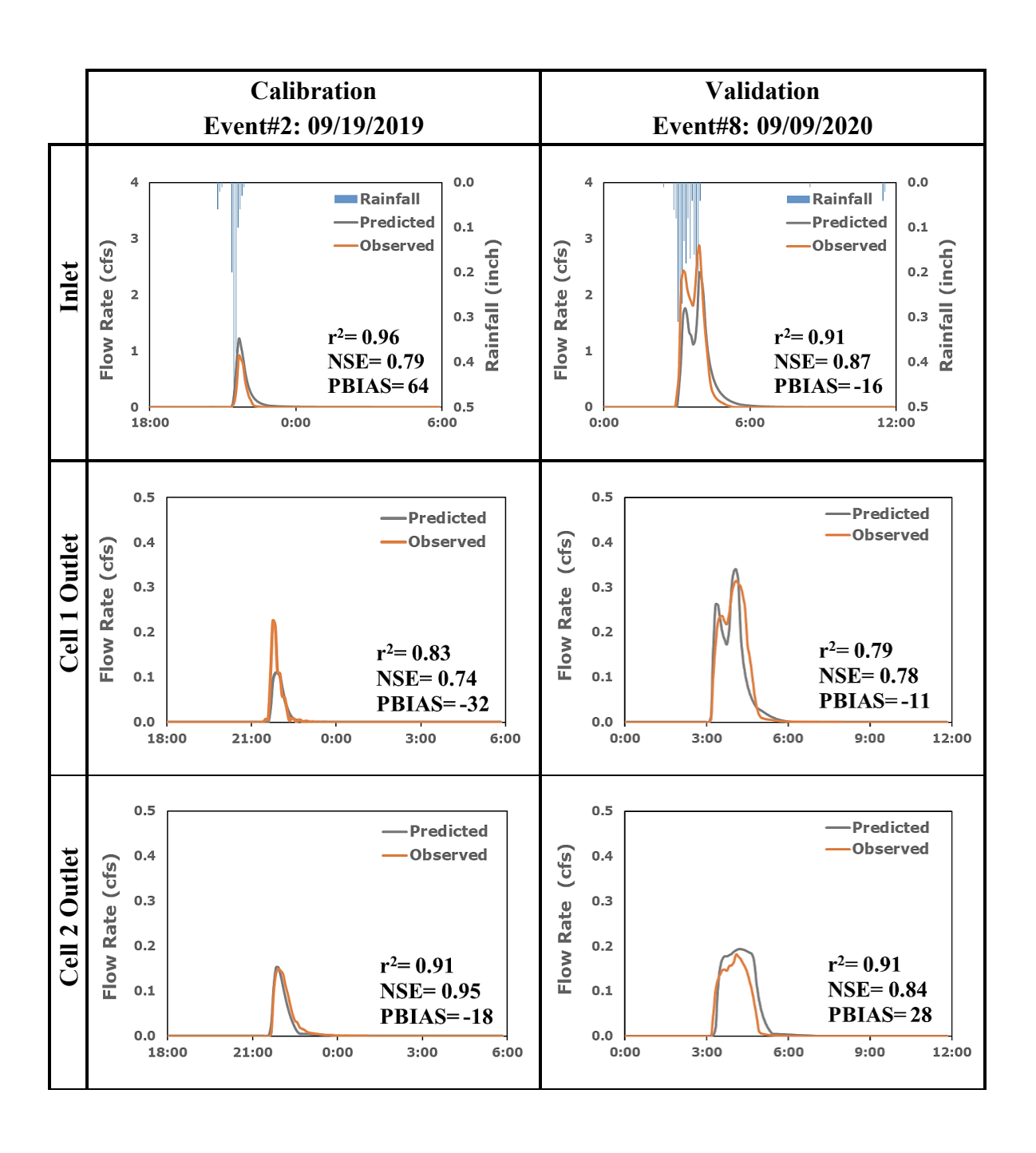
minimum and maximum temperatures according to Hargreaves method (Hargreaves and Samani 1985).

4.5. Results and Discussion

4.5.1. Calibration and Validation

To calibrate the model, the calibration parameters were adjusted manually. The CN number seemed to impact the watershed response to the greatest. The initial run with the acquired CN values from the soil and land cover maps showed great discrepancies with overestimation of the hydrograph. Therefore, the CN value was adjusted for each subcatchment considering the fraction and spatial distribution of the impervious surfaces. For instance, the CN value of two subcatchment (438, 441) with parking lots and rooftops were changed to 98 with 95 imperviousness, and the subcatchment with less than 5 imperviousness were considered as open spaces with good conditions (CN=80) to increase the infiltration in the watershed and reduce the generated runoff consequently. The manning's roughness, the depression storage, and the percent of impervious area with no depression storage were altered accordingly to reach the best performance of the model using visual evaluation, as well as goodness of fit calculations. Overall performance of the model is adequate with better performance for heavy rainfall events, whereas low flows are overestimated (Figure 4- 3). For events with short antecedent dry periods and higher initial soil moisture content, more runoff is generated as a result of saturated soil and decreased infiltration. The predictions, on the other hand, are lower than observed indicating that the model does not accurately account for the changes in the infiltration pattern and its subsequent impact on runoff generation rate. The overestimated prediction of low flows is mainly due to disconnected impervious surface, and high abstraction capacity of the watershed after long dry periods specifically. From the captured events, events number 1, 2 and 5 were selected for calibration and

events 3, 6 and 8 for validation (Table 3-3). Model shows overall good performance in simulating the hydrology and hydraulics of the watershed and the LID testbed. Model performance for one of the calibrated and validate storms is presented in Figure 4-3, illustrating the predicted versus observed inflows and outflows.



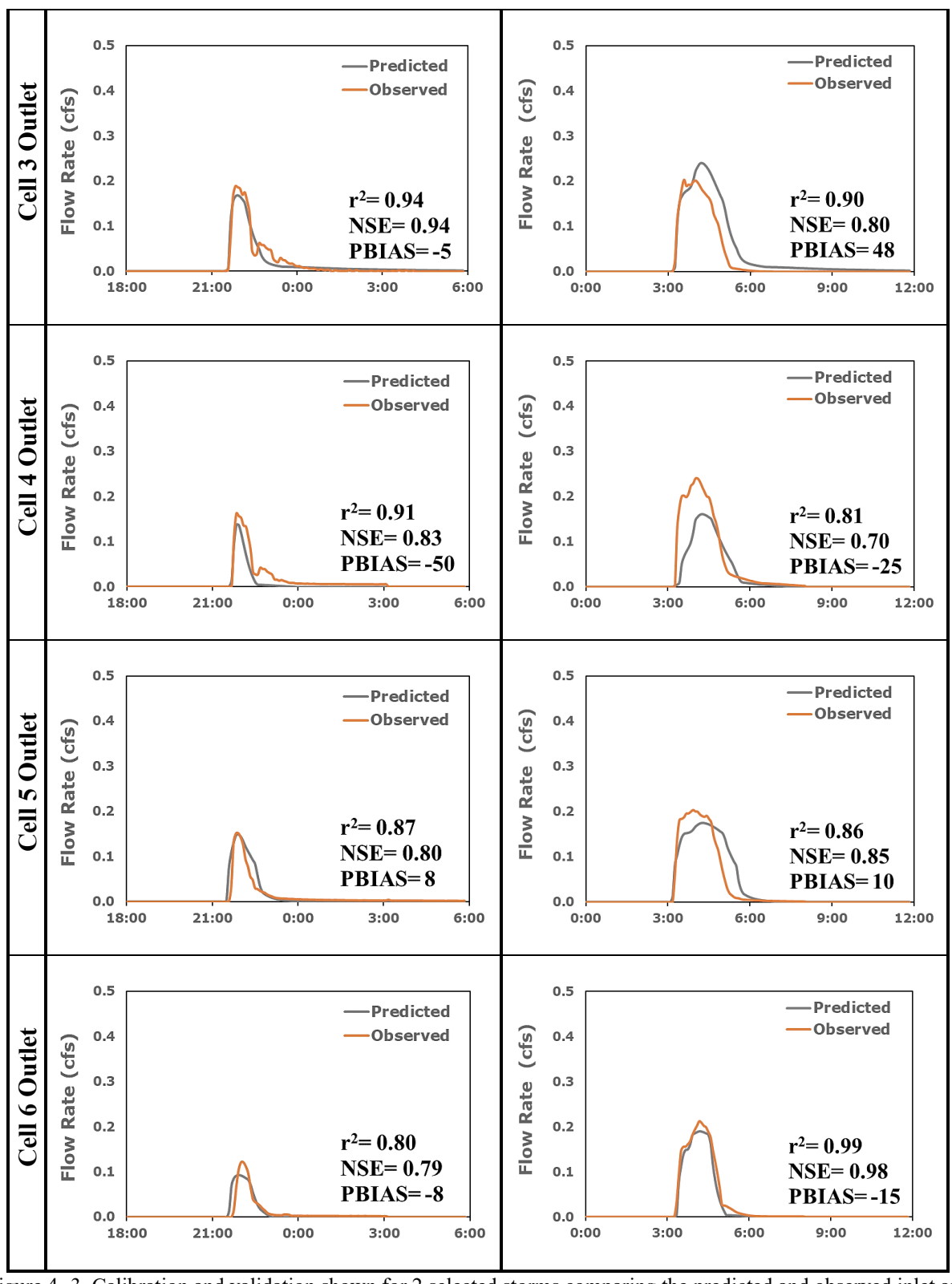


Figure 4- 3. Calibration and validation shown for 2 selected storms comparing the predicted and observed inlet and outlet hydrographs, and the values for goodness of fit indictors

After validating the model for the captured storms, the model performance was also validated for three-year continuous simulation including phase I and II. Model predictions under continuous simulation showed overall good agreement with the observation (Table 4- 3). The continuous simulation incorporates the daily evaporation in each cell, while the changes in storage (soil moisture content) are considered negligible over long time periods. For phase II, the IWS was simulated by increasing the outlet offset and introducing a discharge outlet to drain the lined cells within 48 hours after each storm event, matching the recorded water depths in each cell accounting for plant uptake, soil moisture content and concrete absorbance. The model shows overall good performance in predicting the inflow and outflows for both monitoring phases with relatively insignificant overestimation (10-30%).

Table 4-3. Validation of the model under continuous 5-min simulation.

				Goodn	ess of Fit – SV	VMM model		
			Cell 2 Limestone -Mix Unlined	Cell 3 Bioretention -Mix Lined	Cell 4 Bioretention -Mix Unlined	Cell 5 Limestone Sand Lined	Cell 6 Limestone Sand Unlined	
I	r ²	0.74	0.75	0.81	0.85	0.83	0.85	0.84
Phase	NSE	0.65	0.70	0.68	0.74	0.70	0.75	0.74
Ы	PBIAS	16	24	32	23	28	28	33
П	r ²	0.74	0.85	0.92	0.91	0.91	0.82	0.80
Phase	NSE	0.65	0.83	0.90	0.89	0.90	0.81	0.80
Ph	PBIAS	16	21	12	20	9	21	10

4.5.2. Hydrologic Performance

The continuous mass balance for the LID testbed and its drainage area is presented in Table 4-4 and Table 4-5. From the total received rainfall, 18% is evaporated, 65% and 46% is infiltrated, and 16% and 37% generated surface runoff, for phase I and II respectively. The greater runoff volume and smaller infiltration in phase II is due to consecutive large storms that saturate the soil

infiltration capacity and generate more surface runoff consequently. During phase I, on the other hand, more frequent small storms provide more infiltration and less runoff.

Regarding the mass balance within the LID testbed, the model shows that the inflows to each individual cell are not equal. Cell1 towards the end of the inlet channel seems to be receiving approximately 4% greater inflow than other cells, which can explain larger outflows that were observed for the captured storms. These inflow volume variations were found to be larger in case of big storm events with overflows, hence greater inflow variances in phase II with three big storms that caused overflow of the inlet channel (storms 3, 6 and 8, Table 3- 6).

Table 4-4. Watershed response under continuous simulation for phase I and II

	Rainfall (inch)	Evaporation Loss (inch)	Infiltration Loss (inch)	Surface Runoff (inch)
Phase I (6/2019-4/2021)	34.72	6.40	22.68	5.54
Phase II (4/2021-10/2022)	47.78	8.67	22.15	17.79

Table 4-5. Hydrologic performance of the LID testbed, 3.5-year continuous simulation

		Inlet	Cell 1 Limesto ne -Mix Lined	Cell 2 Limestone -Mix Unlined	Cell 3 Bioretention -Mix Lined	Cell 4 Bioretention -Mix Unlined	Cell 5 Limestone Sand Lined	Cell 6 Limestone Sand Unlined
	Inflow (in)	4.85	0.77	0.73	0.74	0.73	0.74	0.72
Phase I	Outflow* (in)	0.28+0.1 6	0.76	0.59	0.72	0.55	0.72	0.57
Ph	Storage** (in)	-	34.73	34.85	34.74	34.90	34.74	34.87
	VR (%)		11%	27%	12%	32%	12%	29%
	Inflow (in)	17.11	1.83	1.81	1.65	1.64	1.74	1.72
Phase II	Outflow* (in)	6.81+0.2 5	1.13	0.93	0.95	0.71	1.05	0.90
Ph	Storage** (in)	-	48.4	48.6	48.4	48.6	48.4	48.6
	VR (%)		42%	52%	46%	59%	43%	51%

^{*} Outflow for inlet indicates the overflow + standing water in the inlet channel below the cells' orifice

^{**} Storage = Inflow+Rain-Outflow, refers to storage + infiltration (in unlined cells)

Total volume reduction was calculated by subtracting the volumes of overflow and standing water in the inlet channel below the cells' inlet orifice (0.4 ft). Total volume reduction of 23% and 48% was achieved in phase I and II, indicating the evident impact of IWS in improved runoff control. The difference of storage volume between lined and unlined cells, corresponds to the subsurface direct infiltration volume in unlined cells. Total of 0.62, 0.72, and 0.48 recharge (inch) was achieved for cells 2, 4 and 6, respectively. Thus, cell4 provides the greatest infiltration volume which is caused by its lower infiltration rate providing slower water movement and more time for water to infiltrate. The model results suggest greater recharge considering the impact of evaporation, particularly in phase II with IWS. In presence of IWS layer, all the stored runoff in the lined cells contribute to evaporation, soil moisture content increase and plant uptake. In the unlined cells, on the other hand, infiltration plays the major role in storage release. While it takes 36-48 hours for the lined cells to drain fully through evaporation, soil moisture increase, and plant uptake, unlined cells drain fully in less than 12 hours. Therefore, less recharge is estimated based on field monitoring data, where the storage components was considered equal.

The cumulative volume plots for the continuous simulation under phases I and II were relatively similar to the observed data, with 10-30% overestimation (Figure 4- 4). Although the SWMM model showed overall good performance (Table 4- 3), it did not fully capture the difference of performance between different media in the presence of IWS layer, particularly for the bioretention-mix cells. This varied performance might be due to the impact of aging and plant growth that is not well simulated by the SWMM model.

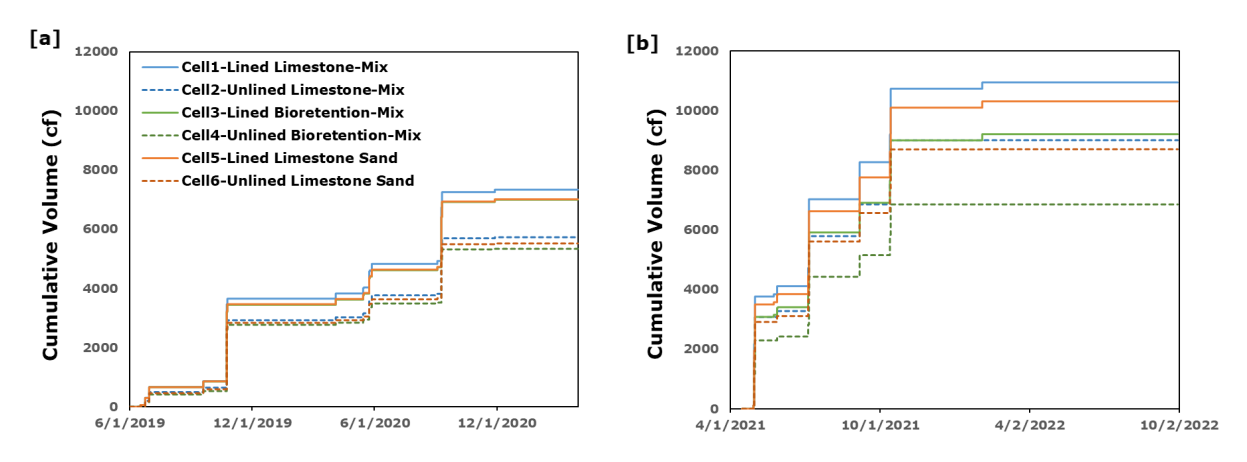


Figure 4- 4. Difference of hydrologic performance, Modeled cumulative volume - phase I [a], phase II [b]

After obtaining acceptable model performance under event-based as well as continuous simulation, the long-term hydrologic performance of the LID testbed with and without IWS was examined under a 15-year continuous simulation to evaluate the impact of IWS on its hydrologic performance. Table 4- 6 shows the watershed response including the total precipitation (PRCP), evaporation (EVP) and infiltration (INF) loss, generated surface runoff and storage. The LID testbed inflow accounts for 88% of the total surface runoff, emphasizing the disconnected impervious surfaces and flat slopes in the channels hindering all runoff to reach the testbed inlet. From the total rain, 14% and 34% evaporation and infiltration loss, and 52% surface runoff was generated.

In the 15 years of continuous simulation total of 252 storm events - with total volume greater than 0.1 cf and separation time of six hours - were captured. The sum of the total inflow through each LID testbed cell, and the outflows with and without IWS layer was computed for the 15-year period (Table 4- 6). The mass balance calculations suggest greater runoff volume and peak flow control, and greater recharge in presence of IWS. Total volume reduction ranging 4-32% without IWS, and 27-60% with IWS could be achieved in 15 years, corresponding to total outflow of 127, and 85.4 inches, respectively. Median peak flow reduction of 0.65 without IWS, and 0.82 with

IWS was achieved. Recharge volume of 6.7, 7.1 and 6.6 inch without IWS, and 9.5, 10 and 7.8 inch with IWS was achieved for cells 2, 4 and 6, respectively. The IWS increased the total recharge volume by 20% for the sand filter basin, and 40-45% for the bioretention cells.

Table 4- 6. Long-term hydrologic performance of the LID testbed under 15- year period

15-year continuous	PRCP (inch)	EVP loss (inch)	INF loss (inch)	Surface runoff (inch)	Storage (inch)	Inflow LID Testbed
simulation	409.7	55.8	139.4	214.8	0.05	189.1
(1999-2014)	Cell 1 Limestone -Mix Lined	Cell 2 Limestone -Mix Unlined	Cell 3 Bioretention -Mix Lined	Cell 4 Bioretention -Mix Unlined	Cell 5 Limestone Sand Lined	Cell 6 Limestone Sand Unlined
Inflow (inch)	25.1	24.5	24.7	24.6	24.8	24.6
Outflow (inch) - no IWS	25.0	17.9	24.5	17.2	24.6	17.7
Outflow (inch) - IWS	18.6	11.7	16.6	9.3	17.6	11.6
Volume Reduction (%) - no IWS	4%	30%	5%	32%	4%	31%
Volume Reduction (%) - IWS	27%	53%	30%	60%	28%	53%

The frequency plot (Figure 4- 5) shows the 15-year performance variation of the LID testbed with and without IWS layer. Without the IWS layer (Figure 4- 5 [a]), there was a distinct differentiation between the lined and unlined outflows, while no difference was evident between bioretention and sand filter basins. With the IWS layer (Figure 4- 5 [b]), on the other hand, bioretention-mix demonstrated comparably lower outflows for both lined and unlined cells, compared to the limestone sand and limestone-mix that showed rather similar runoff control. The low infiltration rate of the bioretention-mix allows more time for subsurface infiltration in cell 4 (unlined), and for storage increase (soil moisture content and plant uptake) in cell 3 (lined), resulting in smaller outflows.

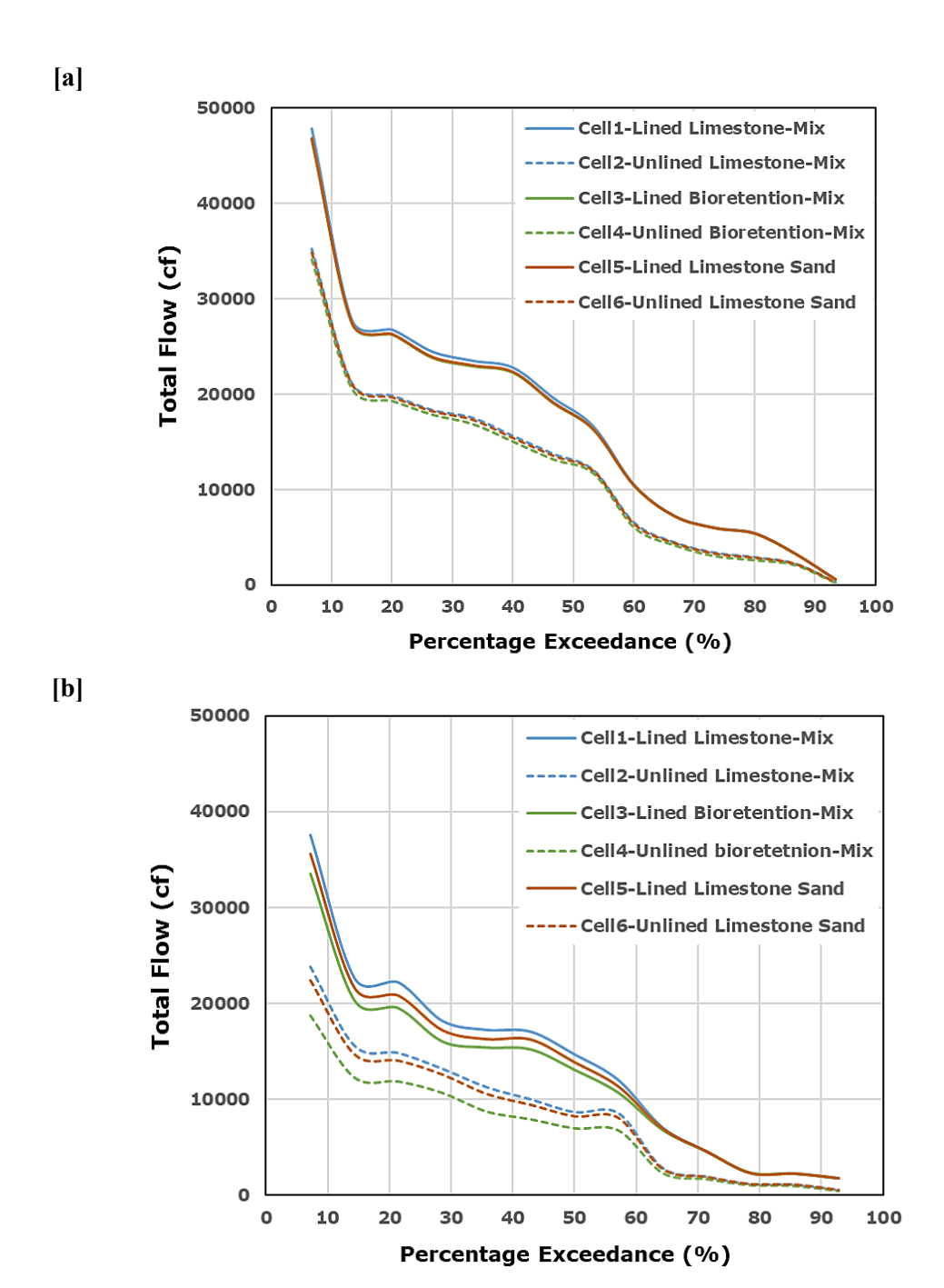


Figure 4-5. Frequency plot, 15-year total outflow with [a] no IWS, [b] IWS

4.6. Conclusion

The SWMM model for the LID testbed and its drainage watershed was generated and calibrated and validated using the field monitoring data. Model showed overall good performance with 10-30% of overestimation. Greater predicted outflow might be due to the varying storage component

(e.g., soil moisture changes and plant uptake) that is not well simulated by the model. Model was used to run a continuous 5-min simulation for phase I without IWS (06/2019-04/2021), and phase II with IWS (04/2021-10/2022). The model results demonstrated unequal inflow to the LID testbed cell, particularly greater inflow was projected for cell 1 (lined limestone-Sand), which explains the observed greater outflows and higher peak flows in the captured storms. It should be noted that unequal inflows also invalidate the equal load input assumption for computing percent pollutant load removal in each cell, thus even greater load reduction can be achieved in limestone-mix cells. Also, the model accounts for the daily evaporation from LID testbed cells, providing more accurate mass balance calculations. The mass balance was recalculated using the inflow and outflows for each individual cell.

Model results suggested no significant difference between the hydrologic performance of bioretention versus sand filter basins, with slightly greater runoff control in the bioretention-Mix. Unlined cells showed approximately 20% reduced outflow compared to lined cells without IWS. Addition of the IWS layer increases the runoff volume and peak flow reduction in both lined and unlined cells and provides greater recharge volume as well.

The long-term performance of the testbed was examined - with and without IWS – to determine the impact of IWS on the LID testbed hydraulic and the recharge volume under the 15-year historical rainfall. Similar to the model predictions for the monitoring period without the IWS layer, distinctive impact of liners was evident and all cells – regardless of filtration media type-function rather similarly. But in presence of the IWS layer, bioretention-mix cells showed quite smaller outflows, while limestone sand and Limestone-mix were more alike. Results of the 15-year continuous simulation suggested 40-45%, and 20% increase in the total recharge volume for bioretention and sand filter basins, respectively.

It should be noted that the developed SWMM model is limited in simulating the storage components including the plant uptake and soil moisture changes. Moreover, the impact of aging on the media physical characteristics - such as the hydraulic conductivity of the media that can change due to clogging (accumulated TSS), plant growth and compaction – is not simulated. For better representation of the system and long-term performance studies, use of process-based models or models with more detailed LID modules, such as GIF-Mod, is required.

CHAPTER FIVE: COST-BENEFIT ANALYSIS

Cost-benefit analysis was carried out following the guidelines by Minnesota Public Works Association (2007). Installation and maintenance cost was estimated for each testbed cell using the average cost suggested by San Antonio River Authority (2015) and the actual project costs. The total operating cost was calculated by summing up the capital cost (installation) and maintenance cost (Table 5- 1). The total volume and pollutant load reduction in each cell was considered as the benefit, and accordingly the cost per unit volume reduction and cost per unit pollutant load was computed and compared to identify the most beneficial media.

Table 5-1. Total capital, maintenance and operating cost for the whole monitoring period

Cost per cell	Capital Cost (\$)	Maintenance Cost (\$)	Operating Cost (\$)
Cell 1 - Lined Limestone-Mix	\$9,304.40	\$6,172	\$15,477
Cell 2 - Unlined Limestone-Mix	\$6,064.40	\$6,172	\$12,237
Cell 3 - Lined Bioretention-Mix	\$9,014.40	\$9,258	\$18,273
Cell 4 - Unlined Bioretention-Mix	\$5,774.40	\$9,258	\$15,033
Cell 5 - Lined Limestone Sand	\$9,070.85	\$1,515	\$10,586
Cell 6 - Unlined Limestone Sand	\$5,830.85	\$1,515	\$7,346

The volume reduction and pollutant removal cost were computed by dividing the total reduced pollutant load and volume over the whole monitoring period (Table 5- 2). Overall, unlined cells were found to be more cost-effective as they provide greater volume and pollutant load reduction at a smaller cost. Amongst the three media, bioretention-mix showed the highest volume reduction and pollutant removal cost, due to its greater maintenance cost and leaching of pollutants. Limestone sand, on the other hand, showed the smallest unit reduction cost and is therefore the most cost-effective. However, this is mainly due to the smaller installation cost of the sand filter cells in the LID testbed (excluding vegetation and mulch layer) as well as subsequent lower

maintenance cost. It should be noted an accurate and inclusive cost-benefit analysis requires inclusion of aesthetics and further environmental benefits of bioretention cells (such as wildlife habitat and biodiversity benefits, and urban heat island mitigation) against sand filter basins.

Table 5-2. Unit volume reduction and pollutant removal cost

Benefits	Cell 1 Limestone -Mix Lined	Cell 2 Limestone -Mix Unlined	Cell 3 Bioretention -Mix Lined	Cell 4 Bioretention -Mix Unlined	Cell 5 Limestone Sand Lined	Cell 6 Limestone Sand Unlined
Volume Reduction Cost (\$/cf)	\$1.8	\$1.0	\$2.1	\$1.2	\$1.2	\$0.7
TSS Removal Cost (\$/Kg)	\$79	\$60	\$94	\$75	\$55	\$37
VSS Removal Cost (\$/Kg)	\$267	\$210	\$322	\$260	\$181	\$125
P Removal Cost (\$/Kg)	\$21,972	\$17,322	\$32,146	\$23,371	\$14,729	\$10,284
TP Removal Cost (\$/Kg)	\$10,010	\$7,775	\$13,288	\$10,173	\$6,744	\$4,617
N Removal Cost (\$/Kg)	\$7,650	\$5,876	\$(19,751)	\$(120,738)	\$5,746	\$3,804
TN Removal Cost (\$/Kg)	\$2,217	\$1,685	\$3,255	\$2,333	\$1,478	\$989
Total Bacteria Removal Cost (\$/CFU)	\$457	\$279	\$779	\$425	\$374	\$205
E-coli Removal Cost (\$/CFU)	\$407	\$275	\$723	\$401	\$362	\$197
Dissolved Copper Removal Cost (\$/g)	\$189	\$150	\$387	\$251	\$127	\$86
Total Copper Removal Cost (\$/g)	\$93	\$75	\$139	\$108	\$66	\$44
Dissolved Zinc Removal Cost (\$/g)	\$19	\$15	\$23	\$18	\$13	\$10
Total Zinc Removal Cost (\$/g)	\$6	\$5	\$7	\$6	\$4	\$3
Dissolved Lead Removal Cost (\$/g)	\$1,317	\$1,051	\$1,578	\$1,284	\$923	\$626
Total Lead Removal Cost (\$/g)	\$188	\$148	\$225	\$183	\$128	\$89

CHAPTER SIX: MAINTENANCE

Frequent and proper maintenance is the key factor in maintaining effectiveness of LID systems. During the 3.5-year monitoring period, routine monthly maintenance was performed including collection and removal of debris and trash from the inlet channel and cells, hand-picking invasive plants and cleaning the inlet and outlet orifices to prevent any blockage. Annual maintenance was performed in late fall/early winter (December) to harvest and prune plants, deep clean the forebays, and to inspect and calibrate (if needed) the monitoring equipment. During the long dry periods in summer, an irrigation schedule was set to deliver 1-inch irrigation per week, by distributing the irrigation equally over the bioretention cells. Before and after each predicted and captured storm event, monitoring equipment including the flow meters, samplers, rain gauge, weirs, and bubbler and sampler lines were inspected to ensure all equipment ran properly and to conduct the required troubleshooting for any potential malfunctions.



Figure 6-1. Monthly and annual maintenance to remove debris, weeds and dead plants

We found pollutant removal efficiencies to be significantly impacted by the maintenance, where enhanced pollutant removal efficiencies were achieved after the annual maintenance (Figure 3-19), particularly due to pruning and removal of dead plant tissues (Figure 6-1). The before and after maintenance pictures (Figure 6-2) highlights the significance of annual maintenance, and the additional maintenance that was performed after the Yuri winter storm in February 202, which killed most plants in the LID testbed.

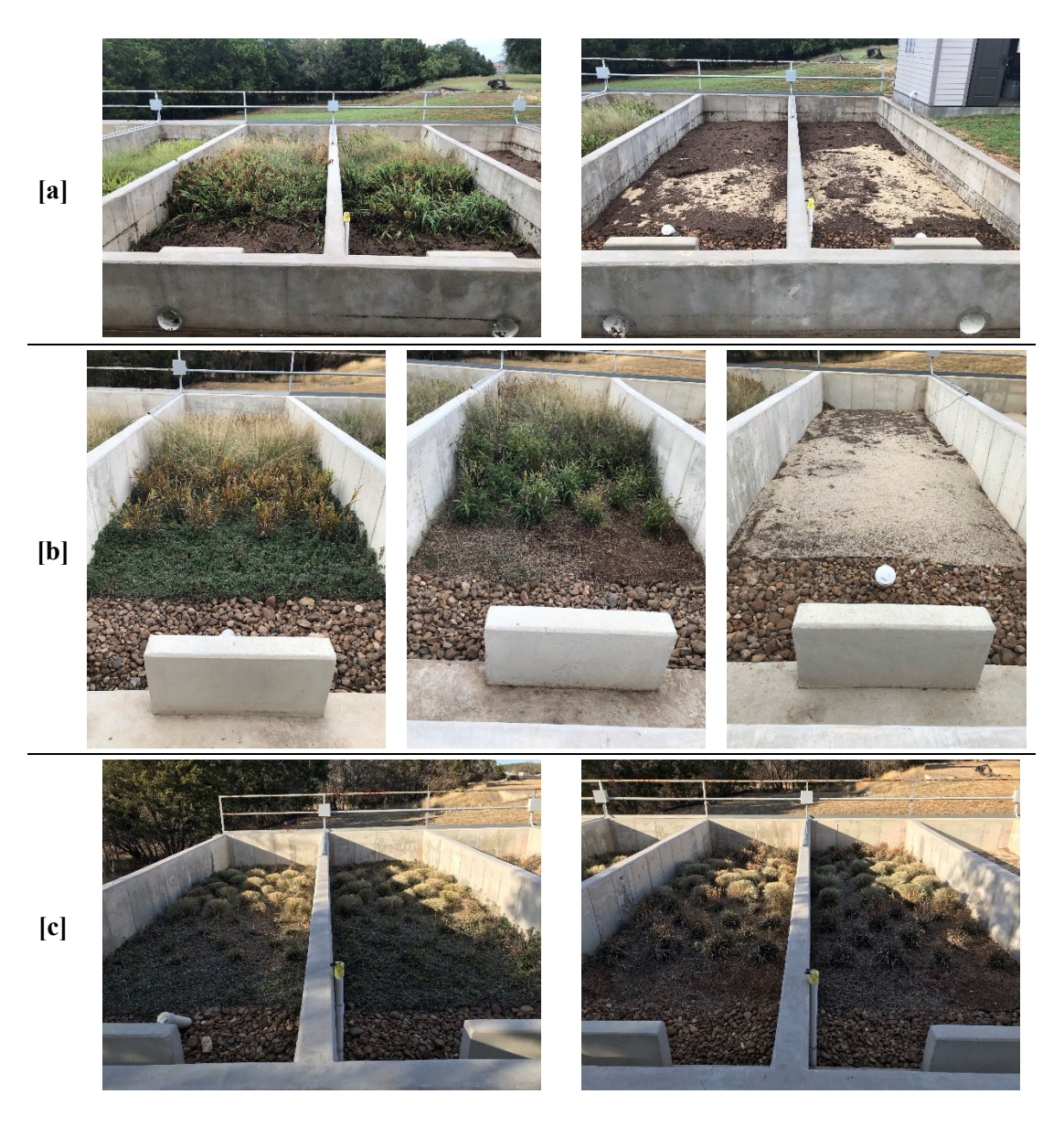


Figure 6-2. Before [a] November 2020, and after maintenance [b] December 2020, and [c] February 2021

Regarding the maintenance efficiency, we found limestone-mix more efficient than bioretention-mix. Richness of the bioretention-mix in organic matter and nutrients caused excessive growth of plants and weeds in cells 3 and 4 (Figure 3- 20). Excess weeds and invasive plant species not only reduce the treatment efficiencies (Figure 3- 19), but also negatively impact the health of the bioretention design plants, particularly the Frogfruits as ground cover. The abundance and health of Frogfruit plants in limestone-mix cells as opposed to the nearly bare ground in bioretention-mix cells is evident in Figure 6- 2 [b, c]. Limestone-mix can effectively and consistently maintain the health of plants, thus requiring less maintenance than bioretention-mix.

One of the main issues hindering maintenance and monitoring activities was caused by wildlife on site, particularly fire ants within the LID testbed cells. Proper sealing and protection of all monitoring device and wiring is required to prevent any potential damage to the equipment by rodents, raccoons and deer. Fire ant mounds hinder maintenance activities, damage plants, and are likely to change the water movement by creating preferential flow path through the sublayer tunnels. To avoid the potential impacts of chemical pest controls on water quality, we employed alternative fire ant control techniques including frequent (daily) disturbance and application of hot water on the mounds, which was somewhat effective but did not completely eradicate or displace the fire ants.

SUMMARY, CONCLUSION AND RECOMMENDATIONS

A multi-phase study was conducted aiming to evaluate hydrologic and treatment performance of bioretention and sand filter basins systems, while exploring the influencing factors such as the filtration media design, and storm characteristics. In the first phase of the study, we focused on the filtration media design by conducting a pilot-test in a controlled setting. The pilot-test consisted of series of bioretention column experiments to evaluate pollutant removal efficiencies of various filtration media using synthetic stormwater. We tested total of nine filtration media including conventional commonly use media (such as silica-based sand in sand filter basins, and bioretention sandy loam in bioretention systems), as well as custom media composed of several alternatives such as the limestone sand that is abundant, cost-effective and likely to improve pollutant treatment. The results established that the pollutant removal processes are strongly impacted by the media physical and chemical characteristics, such as gradation, and phosphorus and organic matter content. Thus, each tested filtration media showed diverse pollutant-dependent performances. We found significant improvement in pollutant removal efficiencies with use of limestone sand alone and in the bioretention soil mixture, particularly for the dissolved pollutants due to its high adsorption capacity. The results of the column experiments also proved plants to be effective in enhancing nutrient removal and reducing the leaching of bioretention soil mixtures, while no significant difference was observed in the performance of three different tested plants.

The second phase of the study incorporated a full-scale LID testbed filled with the top performing media from the pilot test. Three and a half years of monitoring data on the hydrologic and treatment performance of the LID testbed was used for comparative evaluation of three LID designs, including a sand filter basin and two bioretention basins filled with limestone sand,

bioretention-mix, and limestone-mix in duplicates- with and without impermeable liner. Monitoring data from phase one without IWS layer suggested no significant difference between the hydrologic and treatment performance of bioretention basins versus sand filter basins, except for the bioretention-mix leaching most pollutants as a result of its high organic matter content. Results suggested significant improvement in pollutant removal efficiencies with use of limestone sand in the sand filter basin as well as the bioretention basin, which was consistent with our findings from the pilot study. No significant difference was observed between the lined and unlined cells for water quality performance; however, greater runoff volume and peak flow control was observed in the unlined cells. The second monitoring phase with IWS layer showed enhanced pollutant removal efficiencies particularly for particulate pollutants including TSS, bacteria and heavy metals. Bioretention-mix showed even greater leaching of nutrients, which is likely due to desorption and washoff of nitrogenous solids from the dead plant tissues. Besides the significant nutrient leaching in bioretention-mix, no significant difference was found between the EMC efficiencies of lined versus unlined cells, as well as bioretention versus sand filter basins. As for the hydrologic performance, addition of IWS reduced outflow volume and peak flow, and increased recharge.

The relationship between the pollutants and storm characteristics was explored to identify potential correlations and co-contaminants. A strong positive correlation between the antecedent dry periods and influent EMC (total nitrogen, and heavy metals) confirmed the impact of pollutant buildup through dry deposition, whereas negative correlation with runoff volume and peak flow highlighted the dilution effect on pollutant loading. Correlations were found between conductivity and pollutant concentrations in the outflow, while the influent pollutants were found to be more particulate-bound and strongly correlated with TSS. It is important to note that a linear regression

between influent and effluent does not accurately depict their relationship due to the complex interactions between the pollutants and stormwater chemistry matrix. Therefore, use of non-linear and more complex modeling methods is recommended in order to better unveil the influent-effluent pollutant relationship, and to identify co-contaminants. Moreover, calibrated stormwater quality models can be used to further investigate the sole impact of each influencing factor (e.g., storm characteristics) on pollutant loads.

An EPA-SWMM model was developed using the field monitoring data to further investigate the hydraulics of the LID testbed, and to better quantify the mass balance considering the climatic components (e.g., evaporation) of the system over continuous simulation. The model showed overall satisfactory to very good performance under event-based and continuous simulations. The model was used to reevaluate the mass balance in the LID testbed cells, considering the climatic components and the actual inflow into each cell. The results suggested 10-20% greater runoff control in unlined cell corresponding to the direct infiltration, while no significant difference was evident between different filtration media. The model then was also used to examine the long-term performance of the LID testbed with and without IWS layer. The results of the 15-year continuous simulation suggested 20-45% recharge increase for unlined cells in presence of IWS layer. Further research is required to assess the impact of aging and maintenance on the performance of the LID testbed by simulating the changes in the media characteristics such as clogging, compaction and plant growth.

Maintenance was identified as a crucial component of LID controls' effectiveness. Substantially higher effluent pollutant loads during plant's die-off season, and significantly lower effluent pollutant after annual full maintenance was observed. Therefore, timely and proper maintenance is required to maintain effectiveness of LID controls and to deliver consistent pollutant removal at

all times. Quarterly to biannual full maintenance, including harvesting and pruning of plants, is recommended for bioretention systems. In terms of maintenance efficiency, limestone-mix was found to be low-maintenance in comparison to the bioretention-mix, which required continual maintenance to keep weeds at bay and design plants flourishing. Cost-benefit analysis also recommended limestone-mix as more cost-effective compared to the bioretention-mix, which has greater maintenance cost coupled with lower pollutant removal and recurrent leaching to the outflow.

Furthermore, this project supported an educational program by providing K-12 students/school tours in collaboration with UTSA engineering summer school, and undergraduate research partnership with STIR-UP student cohort and internships. Over the 4-year period, we hosted total of 339 middle/high school students for the UTSA engineering summer camps and 6 undergraduate students for the STIR-UP student cohort program. We also prepared videos of the LID testbed and filtration lab experiment for the 2020 virtual engineering summer camp. Total of nine undergraduate students and three graduate students have been involved in the LID testbed project, who presented their research in UTSA annual undergraduate research showcase as well as national and local conferences. Additionally, LID educational modules were prepared and taught to the civil engineering undergraduate students participating the water resources engineering course.

Recommendations

Based on the results obtained in this investigation, the research team recommends the following:

• The need of impermeable liner in BMPs are likely unnecessary since it didn't add any observed water quality benefits to stormwater effluents. We recommend this requirement to be discussed by technical staff at TCEQ and other partners to evaluate the possibility to remove liner

requirements from TCEQ Manual, especially for low concentration watersheds (e.g. residential areas).

- The operation of cells with Internal Water Storage enhanced the quality of effluents for many parameters in comparison to bottom underdrain operations. These results are consistent with other literature. We recommend the application of IWS on bioretentions and sand filter basins, whenever appropriate conditions exist.
- The results show that limestone-based media outperformed conventional bioretention media. Similar treatment performance of limestone-mix and limestone sand highlights the impact of filtration media on pollutant removal efficiencies, regardless of the LID design type. Thus, use of limestone sand as an extra filtration layer to enhance performance of bioretention cells and capture the leachates is recommended. We recommend the inclusion of limestone-based media into LID/BMP Manuals, although future research for identifying optimal parameters of media are still needed.

Future Research

Future research could investigate innovative methods to further improve LID effectiveness through modification of design features, such as alternative soil amendments and inverse drainage systems. Moreover, although low hydraulic conductivity of the bioretention-mix provided somewhat better quantity control, it did not help with the pollutant removal processes and resulted in even more export of the pollutants with addition of the IWS layer. The limestone-mix, on the other hand, performed well with and without IWS. Thus, combination of IWS layer and filtration media with relatively medium hydraulic conductivity seems to be more effective. Furthermore, the impact of preferential flow path on the performance of LID cells needs further investigation, to identify and hinder by altering the hydraulic structure. Additionally, repeated application of

surface-amendments such as fungi, mycorrhizae, and bone char can improve and extend the effectiveness of LID controls while maintaining treatment efficiency and plant health (Palacios and Winfrey 2021; Tirpak et al. 2021). Media amendments is an active and promising research topic in the area of innovated and sustainable stormwater management.

APPENDIX A

The flow weighted mean concentration (FWMC) is a measure of total pollutant load per total discharge. To calculate the FWMC, the following formula was applied for each soil media–pollutant pair.

$$FWMC = \frac{\sum_{1}^{n} (C_i t_i q_i)}{\sum_{1}^{n} (t_i q_i)}$$

where C_i is the concentration of a specific pollutant in the i^{th} sample, t_i is the time for the i^{th} sample, q_i is the flowrate for the i^{th} sample, and n is the number of samples.

Table A1. Effluent flow weighted mean concentration (FWMC) values for each media

W 4 0 14	Flow Weighted Mean Concentration (FWMC)														
Water Quality Parameter	Sand	Man. Sand	Biofilter 532	R.G.+ Biofilter	Lime- Mix	Blend#1	Blend#2	Biofilter 433MS	Biofilter 433						
TSS	2.22	2.19	12.06	8.87	2.15	14.2	7.47	21.6	13.3						
Orthophosphate	0.09	0.01		0.86	0.03	0.14	0.02	1.03	0.64						
Total Phosphorus	0.53	0.32	1.38	5.05	0.33	0.65	0.28	3.41	2.21						
Nitrate	2.24	0.86			0.41	0.55	0.69	0.89	0.30						
Total Nitrogen	1.01	1.86	0.87	3.32	1.47	1.95	1.67	1.35	1.45						
Dissolved Lead	0.36	0.08	0	1.14	0	0	0	2.50	0.14						
Total Lead	1.12	0.13	0.41	4.17		0	0	2.01	1.44						
Dissolved Copper	5.93	0.62	41.5	19.6	6.94	9.82	7.41	15.6	9.28						
Total Copper	9.47	1.19	51.5	43.9	4.46	12.6	7.46	19.4	24.8						
Dissolved Zinc	4.37	0.49	8.76	12.1	20.3	10.3	1.25	9.88	6.89						
Total Zinc	15.8	5.74	15.0	14.5		21.7	29.8	26.9	12.3						

⁻⁻ Sufficient data was not available.

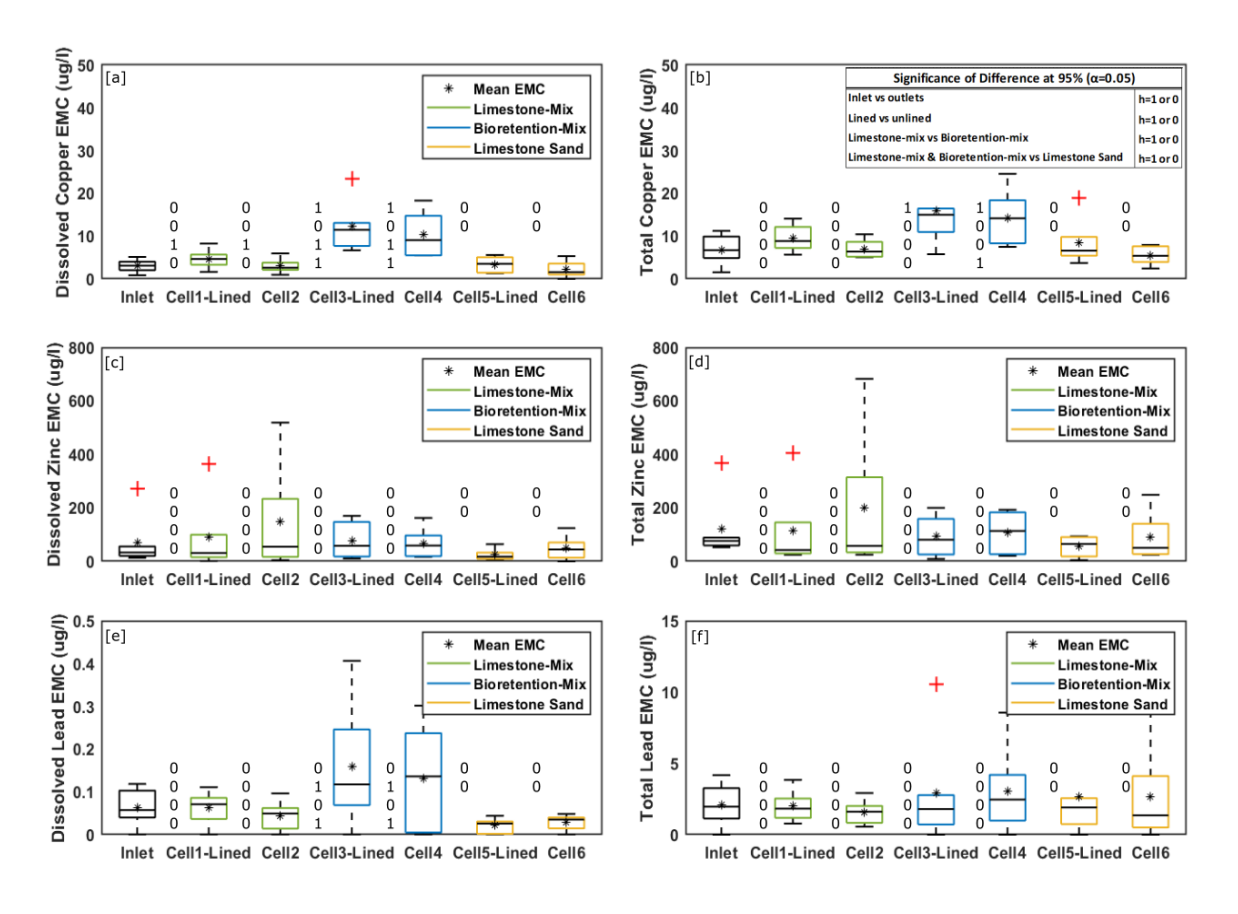


Figure A1. Heavy metals EMC Boxplots, Inlet vs. outlets - Phase I. h-value of 1 indicates significant difference between the median EMCs (p<0.05)

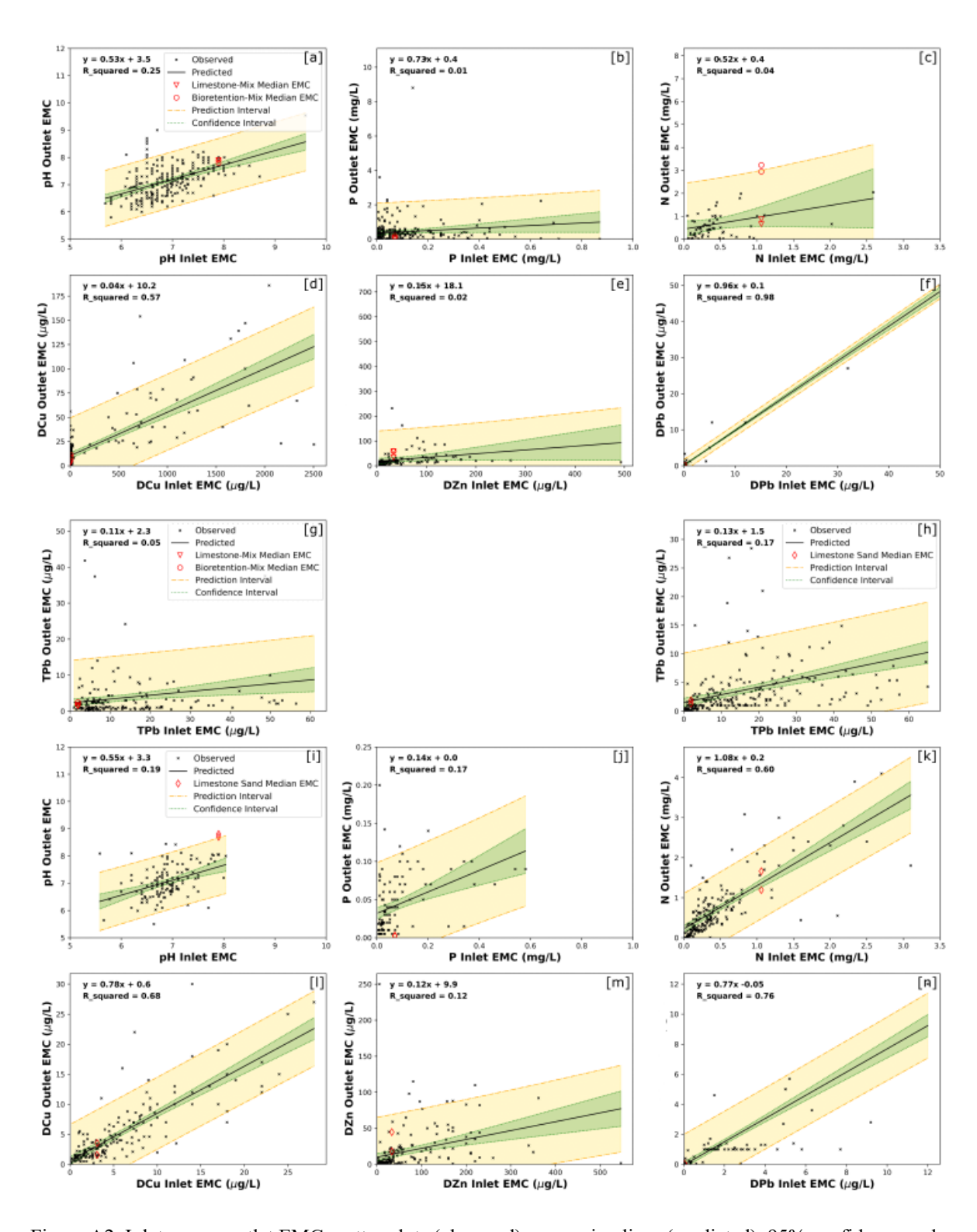


Figure A2. Inlet versus outlet EMC scatter plots (observed), regression lines (predicted), 95% confidence and prediction intervals for [a-g] Bioretentions, and [h-n] Sand filter basins

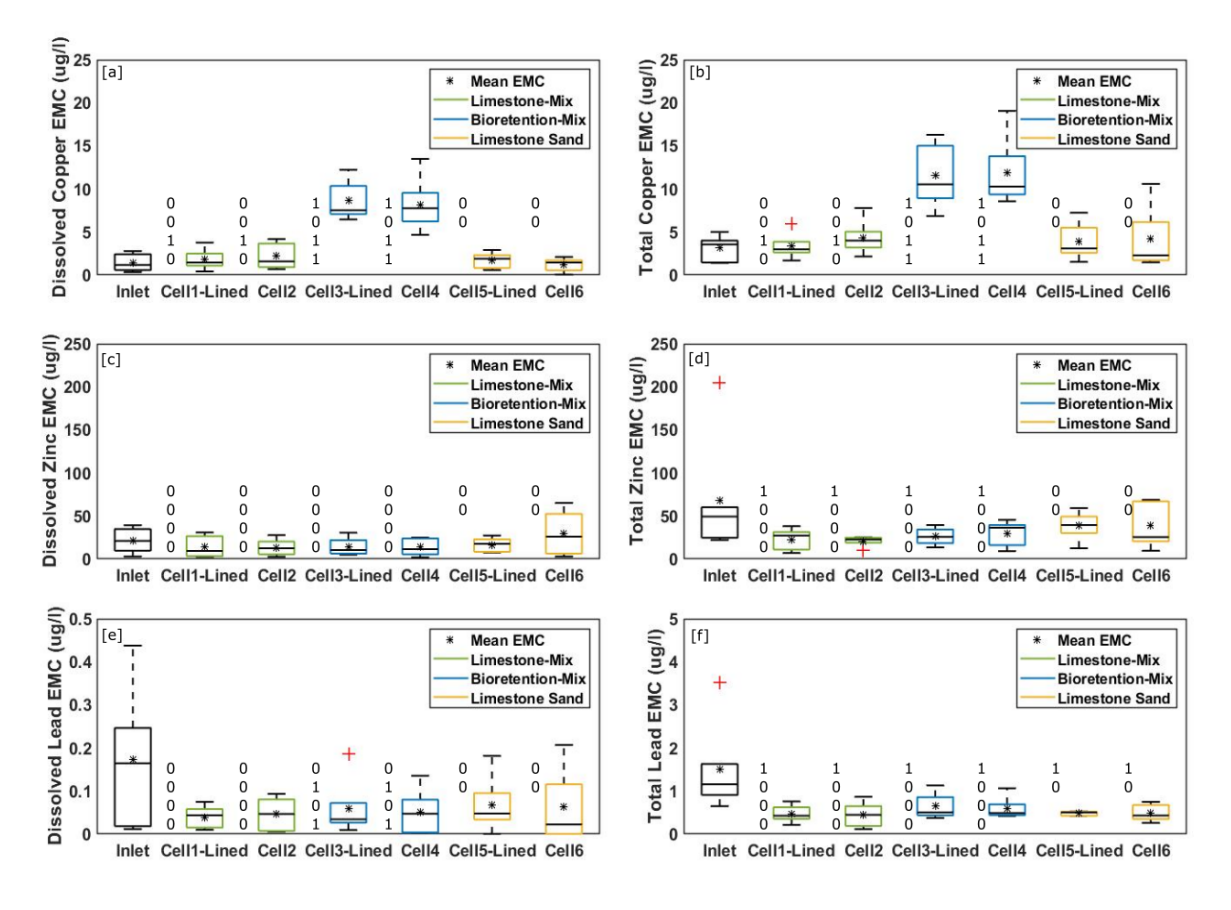


Figure A3. Heavy metals EMC Boxplots, Inlet vs. outlets - Phase II. h-value of 1 indicates significant difference between the median EMCs (p<0.05)

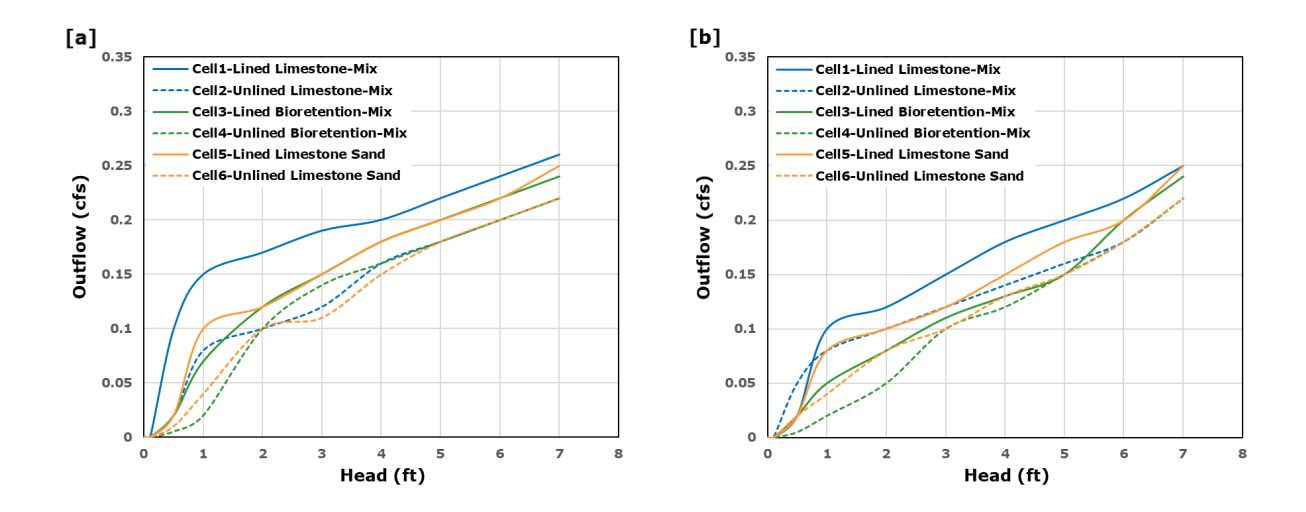


Figure A 4. Rating curves assigned to the LID testbed cells' outlets [a] Phase I with no IWS, [b] Phase II with IWS

Table A 2. Details of captured storm events at the LID testbed, phase I and II

Storm Events	Inflow (cf)			Cell3 outflow				Total Outflow		Cell1 Peakflow						Rainfall (in)	Duration (min)	Maximum	ADP (days)
- 1 - 1		(cf)	(cf)	(cf)	(cf)	(cf)	(cf)		(cfs)	(cf)	(cf)	(cf)	(cf)	(cf)	(cf)			(in/hr)	,
6/17/2019	503	92	70	131	59	120		472	0.20	0.03	0.03	0.03	0.02	0.04		1.05	65	3.6	45
6/24/2019	1556	360	238	405	218	389	223	1833	0.63	0.10	0.08	0.03	0.03	0.11	0.07	1.44	155	2.04	7
6/30/2019	2291	516	358	402	344	516	346	2482	0.96	0.14	0.10	0.02	0.02	0.14	0.13	1.55	280	4.68	6
9/19/2019	1320	293	225	273	207	233	176	1408	0.92	0.23	0.12	0.12	0.11	0.12	0.09	1.33	60	5.52	81
10/24/2019 *	18529	2124	1611	1955	1452	1872	1534	10548	3.42	0.25	0.19	0.21	0.17	0.22	0.20	2.32	360	2.52	35
2/12/2020	114	6		14		20		40	0.02	0.003		0.005		0.005		0.72	465	0.84	3
4/4/2020	1202	126	113	129	76	115	83	641	0.43	0.04	0.03	0.03	0.01	0.04	0.03	1.35	290	1.32	14
5/16/2020	1428	182	64	135	4	128	44	556	0.60	0.12	0.04	0.05	0.00	0.05	0.03	1.29	195	2.16	42
5/24/2020	3593	247	181	376	204	246	184	1439	1.73	0.12	0.09	0.11	0.06	0.10	0.06	1.71	290	3.36	8
5/28/2020 **	1403	46	28	75	0.4	59	16	224	0.89	0.03	0.03	0.04	0.0003	0.05	0.01	0.79	35	2.64	4
9/3/2020	728	33	13	42		35	12	135	0.28	0.01	0.03	0.01		0.02	0.03	1.17	140	2.28	94
9/9/2020	9484	1204	811	1047	996	1013	805	5877	2.88	0.30	0.18	0.20	0.21	0.19	0.19	2.24	90	3.72	6
9/10/2020 **	4044	241	177	323	264	290	257	1552	1.05	0.07	0.07	0.09	0.09	0.09	0.08	1.31	600	2.04	1
11/28/2020	613	82	26	107				215	0.29	0.04	0.02	0.04				1.11	330	0.96	79
4/28/2021	3351	869	806	492	469	897	824	4357	1.00	0.23	0.12	0.11	0.11	0.14	0.20	3.08	910	5.16	76
4/30/2021	18644	1620	1621	1393	1287	1688	1615	9224	3.45	0.17	0.18	0.13	0.14	0.18	0.18	2.45	350	2.04	2
5/1/2021 *	20574	1051	941	756	755	884	732	5121	5.38	0.16	0.13	0.10	0.11	0.14	0.12	1.6	105	2.28	1
5/28/2021	3723	242	311	329	187	229	121	1419	1.60	0.11	0.10	0.11	0.07	0.10	0.08	1.06	55	5.4	4
7/5/2021	5726	496	562	461	395	459	381	2755	2.47	0.15	0.13	0.11	0.11	0.15	0.16	1.74	205	3.84	32
7/6/2021 *	51332	2032	1862	1671	1531	1981	1946	11023	7.16	0.17	0.15	0.14	0.14	0.17	0.17	5.36	220	4.08	1
9/6/2021	8663	907	763	843	745	812	707	4778	2.2	0.16	0.12	0.13	0.13	0.16	0.15	2.77	240	3.6	35
10/13/2021 *	29651	2033	1865	1708	1325	1873	1648	10452	6.84	0.18	0.16	0.15	0.11	0.17	0.16	3.87	370	4.68	2

^{*} Inlet channel overflowed through overflow weir ** Inlet gate valve was open

Table A 3. Median EMC for six qualified storm events, phase I

Median EMC Phase I	рН	Conductivity (μS/cm)	TSS (mg/L)	VSS (mg/L)	P (mg/L)	TP (mg/L)	N (mg/L)	TN (mg/L)	Total Bacteria (CFU/100)	E-Coli (CFU/100)	D-Cu (μg/L)	T-Cu (μg/L)	D-Zn (μg/L)	T-Zn (μg/L)	D-Pb (μg/L)	T-Pb (μg/L)
Inlet	7.8	74.1	81.9	22.4	0.07	0.15	1.09	4.24	97555	10826	3.1	6.7	32.9	76.6	0.08	1.96
Cell 1 - Lined Limestone-Mix	7.9	142.3	93.7	9.4	0.008	0.10	0.90	5.48	94835	1670	4.6	8.8	31.1	42.2	0.07	1.83
Cell 2 - Unlined Limestone-Mix	7.9	144.1	38.5	4.8	0.004	0.06	0.63	4.44	53008	6299	2.6	6.4	54.8	57.8	0.05	1.61
Cell 3 - Lined Bioretention-Mix	7.9	431.0	56.8	9.6	0.16	0.33	2.93	6.29	184437	3660	11.5	15.0	58.0	80.8	0.12	1.80
Cell 4 - Unlined Bioretention-Mix	7.8	367.0	80.0	10.9	0.08	0.23	2.99	6.99	80409	16372	9.0	14.1	58.8	113.8	0.14	2.46
Cell 5 - Lined Limestone Sand	8.8	103.2	127.1	5.2	0.002	0.05	1.61	6.46	97170	2484	3.5	6.6	17.5	64.9	0.03	1.91
Cell 6 - Unlined Limestone Sand	8.7	70.5	61.5	3.9	0.003	0.04	1.19	4.54	129737	2673	1.6	5.4	44.6	50.3	0.04	1.35

Table A 4. Median EMC for five qualified storm events, phase II

Median EMC Phase II	рН	Conductivity (μS/cm)	TSS (mg/L)	VSS (mg/L)	P (mg/L)	TP (mg/L)	N (mg/L)	TN (mg/L)	Total Bacteria (CFU/100)	E-Coli (CFU/100)	D-Cu (μg/L)	T-Cu (μg/L)	D-Zn (μg/L)	T-Zn (μg/L)	D-Pb (μg/L)	T-Pb (μg/L)
Inlet	7.9	59.4	50.0	16.3	0.06	0.16	0.71	1.74	374350	10547	1.2	3.6	21.1	49.3	0.16	1.16
Cell 1 - Lined Limestone-Mix	8.0	166.5	19.1	5.1	0.02	0.09	0.68	1.61	103638	1370	1.5	3.0	9.3	27.3	0.04	0.42
Cell 2 - Unlined Limestone-Mix	7.9	175.9	13.9	6.5	0.02	0.11	0.27	1.41	105008	1719	1.6	4.0	12.3	22.5	0.05	0.45
Cell 3 - Lined Bioretention-Mix	7.8	371.7	29.2	11.9	0.19	0.34	6.73	18.84	88706	1345	7.5	10.5	10.4	25.6	0.03	0.50
Cell 4 - Unlined Bioretention-Mix	7.7	320.0	30.5	6.8	0.14	0.24	3.92	15.93	157825	689	7.7	10.3	11.5	36.3	0.05	0.49
Cell 5 - Lined Limestone Sand	8.6	92.9	25.9	4.5	0.02	0.12	1.22	1.94	37823	908	1.9	3.1	17.8	39.5	0.05	0.50
Cell 6 - Unlined Limestone Sand	8.7	85.1	36.6	5.5	0.03	0.10	0.91	1.44	56263	1151	1.4	2.3	25.8	25.5	0.02	0.43

Table A 5. Total (sum) pollutant loading for six qualified storm events, phase I

Total Pollutant Loading Phase I	TSS (Kg)	VSS (Kg)	P (Kg)	TP (Kg)	N (Kg)	TN (Kg)	Total Bacteria (log(CFU))	E-Coli (log(CFU))	D-Cu (g)	T-Cu (g)	D-Zn (g)	T-Zn (g)	D-Pb (g)	T-Pb (g)
Inlet	116.8	26.6	0.23	0.46	1.09	4.74	54.2	51.1	2.58	8.60	27.0	71.0	0.09	3.13
Cell 1 - Lined Limestone-Mix	10.3	0.8	0.01	0.04	0.08	0.72	38.5	32.6	0.46	1.04	7.0	8.9	0.01	0.26
Cell 2 - Unlined Limestone-Mix	3.3	0.4	0.01	0.02	0.06	0.48	28.5	26.2	0.24	0.53	7.0	9.0	0.01	0.13
Cell 3 - Lined Bioretention-Mix	10.6	1.2	0.09	0.13	0.68	0.83	49.6	45.6	1.15	1.57	6.3	7.8	0.02	0.29
Cell 4 - Unlined Bioretention-Mix	5.8	0.7	0.04	0.07	0.38	0.65	38.1	35.4	0.78	1.03	4.2	7.1	0.01	0.19
Cell 5 - Lined Limestone Sand	13.3	0.4	0.00	0.02	0.14	0.54	47.0	42.8	0.23	1.32	1.7	4.1	0.003	0.26
Cell 6 - Unlined Limestone Sand	5.1	0.3	0.01	0.01	0.09	0.33	38.8	34.3	0.14	0.51	3.2	4.7	0.003	0.16

Table A 6. Total (sum) pollutant loading for five qualified storm events, phase II

Total Pollutant Loading Phase II	TSS (Kg)	VSS (Kg)	P (Kg)	TP (Kg)	N (Kg)	TN (Kg)	Total Bacteria (log(CFU))	E-Coli (log(CFU))	D-Cu (g)	T-Cu (g)	D-Zn (g)	T-Zn (g)	D-Pb (g)	T-Pb (g)
Inlet	91.9	32.9	0.50	1.19	1.12	3.19	70.8	62.0	87.6	175.6	838.4	2525.5	11.8	82.0
Cell 1 - Lined Limestone-Mix	2.5	0.8	0.02	0.06	0.10	0.23	52.7	42.4	7.8	15.8	39.4	83.2	0.17	2.60
Cell 2 - Unlined Limestone-Mix	2.0	0.9	0.02	0.05	0.07	0.19	52.7	42.4	8.4	20.1	51.3	93.5	0.28	2.51
Cell 3 - Lined Bioretention-Mix	4.2	1.5	0.08	0.14	2.46	1.49	51.9	42.2	41.8	51.2	48.6	111.8	0.33	3.57
Cell 4 - Unlined Bioretention-Mix	2.9	0.9	0.05	0.10	1.96	0.83	51.5	40.2	29.6	44.6	33.4	96.7	0.21	2.75
Cell 5 - Lined Limestone Sand	3.8	0.5	0.01	0.06	0.23	0.22	49.7	41.0	6.3	23.1	69.4	182.3	0.46	2.47
Cell 6 - Unlined Limestone Sand	3.6	0.4	0.01	0.04	0.19	0.18	50.4	41.6	4.6	14.8	105.6	107.6	0.20	2.21

Table A 7. Particle size distribution of tested media.

% Passing through	Sieve Number														
Media	1	3/4	1/2	3/8	4	8	16	30	50	100	200	230	270	325	400
Gravel ASTM#57	100%	89%	43%	32%	14%	2%	1%	0%							
Chocking Stone ASTM#8			100%	100%	74%	6%	2%		1%	1%	1%	0%			
Regular Sand ASTM C33				100%	99%	87%	50%		10%	4%	3%	0%			
Limestone Sand (Man.Sand)				100%	100%	84%	53%	31%	12%	2%	0%				
Recycled Glass		100%	100%	100%	35%	6%	5%		3%	1%	0%				
Sandy Loam (Biofilter 532)				100%	96%	90%	84%		63%			2%		1%	1%
Limestone Mixture (Lime-Mix)				78%	61%	44%	28%		7%	2%	0%	0%	0%	0%	0%
Limestone Mixture (Blend1)				99%	80%	50%	22%		4%	1%	0%	0%	0%	0%	0%
Limestone Mixture (Blend2)				98%	93%	74%	34%		6%	2%	0%	0%	0%	0%	0%
Limestone Mixture (433MS)				98%	93%	73%	28%		6%	3%	1%	1%	1%	1%	0%
Sandy Loam (BioMix 433)				99%	95%	89%	76%		8%	2%	0%	0%	0%	0%	0%

REFERENCES

- ASTM C33/C33M-18 Standard Specification for Concrete Aggregates, West Conshohocken, PA, 2018, https://doi.org/10.1520/C0033 C0033M-18
- ASTM C136/C136M-14 Standard Test Method for Sieve Analysis of Fine and Coarse Aggregates, ASTM International, West Conshohocken, PA, 2014, https://doi.org/10.1520/C0136 C0136M-14
- ASTM F1815-11 Standard Test Methods for Saturated Hydraulic Conductivity, Water Retention, Porosity, and Bulk Density of Athletic Field Rootzones, ASTM International, West Conshohocken, PA, 2011, https://doi.org/10.1520/F1815-11
- ASTM C20-00(2015), Standard Test Methods for Apparent Porosity, Water Absorption, Apparent Specific Gravity, and Bulk Density of Burned Refractory Brick and Shapes by Boiling Water, ASTM International, West Conshohocken, PA, 2015 https://doi.org/10.1520/C0020-00R15
- Afrooz, A. R. M. N., and A. B. Boehm. 2017. "Effects of submerged zone, media aging, and antecedent dry period on the performance of biochar-amended biofilters in removing fecal indicators and nutrients from natural stormwater." *Ecol. Eng.*, 102: 320–330. https://doi.org/10.1016/j.ecoleng.2017.02.053.
- Ahiablame, L. M., B. A. Engel, and I. Chaubey. 2012. "Effectiveness of Low Impact Development Practices: Literature Review and Suggestions for Future Research." *Water. Air. Soil Pollut.*, 223 (7): 4253–4273. https://doi.org/10.1007/s11270-012-1189-2.
- APHA, AWWA, WEF. 2012. Standard Methods for the Examination of Water and Wastewater. (E. W. Rice, R. B. Baird, A. D. Eaton, and L. S. Clesceri, eds.). Washington, DC: American Public Health Association, American Water Works Association, Water Environment Federation.
- Aziz, H. A., Mohd. N. Adlan, and K. S. Ariffin. 2008. "Heavy metals (Cd, Pb, Zn, Ni, Cu and Cr(III)) removal from water in Malaysia: Post treatment by high quality limestone." *Bioresour. Technol.*, 99 (6): 1578–1583. https://doi.org/10.1016/j.biortech.2007.04.007.
- Aziz, H. A., N. Othman, M. S. Yusuff, D. R. H. Basri, F. A. H. Ashaari, M. N. Adlan, F. Othman, M. Johari, and M. Perwira. 2001. "Removal of copper from water using limestone filtration technique: determination of mechanism of removal." *Environ. Int.*, Environmental Geochemistry in the Tropics and Subtropics, 26 (5): 395–399. https://doi.org/10.1016/S0160-4120(01)00018-6.
- Barrett, M. E. 2003. "Performance, cost, and maintenance requirements of Austin sand filters." *J. Water Resour. Plan. Manag.*, 129 (3): 234–242. https://doi.org/10.1061/(ASCE)0733-9496(2003)129:3(234).
- Barrett, M. E. 2010. *Evaluation of Sand Filter Performance*. 113. Center for Research in Water Resources Bureau of Engineering Research The University of Texas at Austin.
- Barrett, M. E., M. Limouzin, and D. F. Lawler. 2013. "Effects of Media and Plant Selection on Biofiltration Performance." *J. Environ. Eng.*, 139 (4): 462–470. https://doi.org/10.1061/(ASCE)EE.1943-7870.0000551.
- Baum, P., B. Kuch, and U. Dittmer. 2021. "Adsorption of Metals to Particles in Urban Stormwater Runoff—Does Size Really Matter?" *Water*, 13 (3): 309. Multidisciplinary Digital Publishing Institute. https://doi.org/10.3390/w13030309.

- Bedient, P. B., J. L. Lambert, and N. K. Springer. 1980. "Stormwater Pollutant Load-Runoff Relationships." *J. Water Pollut. Control Fed.*, 52 (9): 2396–2404. Water Environment Federation.
- Belson, C. S. 1999. Karst Waters Institute's second annual top ten list of endangered karst ecosystems. KWI Conduit 8.
- Blecken, G.-T., Y. Zinger, A. Deletić, T. D. Fletcher, and M. Viklander. 2009. "Impact of a submerged zone and a carbon source on heavy metal removal in stormwater biofilters." *Ecol. Eng.*, 35 (5): 769–778. https://doi.org/10.1016/j.ecoleng.2008.12.009.
- Clary, J., J. Jones, M. Leisenring, P. Hobson, and E. Strecker. 2020. "International Stormwater BMP Database: 2020 Summary Statistics." 118.
- Costello, D. M., E. W. Hartung, J. T. Stoll, and A. J. Jefferson. 2020. "Bioretention cell age and construction style influence stormwater pollutant dynamics." *Sci. Total Environ.*, 712: 135597. https://doi.org/10.1016/j.scitotenv.2019.135597.
- CWC. 1995. Evaluation of Crushed Recycled Glass as a Filtration Medium in Slow Sand Filtration. Recycling Technology Assistance Partnership (ReTAP) A program of the Clean Washington Center (CWC), a division of the Pacific Northwest Economic Region, 42. Seattle, Washington: Gray & Osborne, Inc.
- Davis, A. P., R. G. Traver, and W. F. Hunt. 2010. "Improving urban stormwater quality: Applying fundamental principles." *J. Contemp. Water Res. Educ.*, 146 (1): 3–10. https://doi.org/10.1111/j.1936-704X.2010.00387.x.
- DelVecchio, T., A. Welker, and B. M. Wadzuk. 2017. "Field and Laboratory Studies of Nutrient Removal in Different Soil Types for Vegetated Stormwater Control Measures." *World Environ. Water Resour. Congr. 2017*, Proceedings, 345–356. Sacramento, California.
- Donaghue, A. G., N. Morgan, L. Toran, and E. R. McKenzie. 2022. "The impact of bioretention column internal water storage underdrain height on denitrification under continuous and transient flow." *Water Res.*, 214: 118205. https://doi.org/10.1016/j.watres.2022.118205.
- Dorman, T., M. Ferry, J. Wright, B. Wardynski, J. Smith, B. Tucker, J. Riverson, A. Teague, and K. Bishop. 2013. *San Antonio river basin low impact development technical guidance manual*. San Antonio, Texas: San Antonio River Authority.
- Eckart, K., Z. McPhee, and T. Bolisetti. 2018. "Multiobjective optimization of low impact development stormwater controls." *J. Hydrol.*, 562: 564–576. https://doi.org/10.1016/j.jhydrol.2018.04.068.
- Edwards, E. C., C. Nelson, T. Harter, C. Bowles, X. Li, B. Lock, G. E. Fogg, and B. S. Washburn. 2022. "Potential effects on groundwater quality associated with infiltrating stormwater through dry wells for aquifer recharge." *J. Contam. Hydrol.*, 246: 103964. https://doi.org/10.1016/j.jconhyd.2022.103964.
- Elliot, R. W. 2001. "Evaluation of the use of crushed recycled glass as a filter medium." *Water Eng. Manag.*, (148): 17–20.
- EPA. 1983. 40 CFR Part 122 -- EPA Administered Permit Programs: the National Pollutant Discharge Elimination System.
- Esfandiar, N., and E. R. McKenzie. 2022. "Bioretention soil capacity for removing nutrients, metals, and polycyclic aromatic hydrocarbons; roles of co-contaminants, pH, salinity and dissolved organic carbon." *J. Environ. Manage.*, 324: 116314. https://doi.org/10.1016/j.jenvman.2022.116314.
- Ford, D., and P. Williams. 2007. *Karst Hydrogeology and Geomorphology*. John Wiley & Sons, Ltd.

- Gironas, J., L. A. Roesner, and J. Davis. 2009. *Storm Water Management Model Applications Manual*. EPA/600/R-09/077. Washington, DC: EPA.
- Göbel, P., C. Dierkes, and W. G. Coldewey. 2007. "Storm water runoff concentration matrix for urban areas." *J. Contam. Hydrol.*, Issues in urban hydrology: The emerging field of urban contaminant hydrology, 91 (1): 26–42. https://doi.org/10.1016/j.jconhyd.2006.08.008.
- Guo, J. C., and B. Urbonas. 2009. "Conversion of Natural Watershed to Kinematic Wave Cascading Plane." *J. Hydrol. Eng.*, 14 (8): 839–846. American Society of Civil Engineers. https://doi.org/10.1061/(ASCE)HE.1943-5584.0000045.
- Han, Y. H., S. L. Lau, M. Kayhanian, and M. K. Stenstrom. 2006a. "Correlation analysis among highway stormwater pollutants and characteristics." *Water Sci. Technol.*, 53 (2): 235–243. IWA Publishing. https://doi.org/10.2166/wst.2006.057.
- Han, Y., S.-L. Lau, M. Kayhanian, and M. K. Stenstrom. 2006b. "Characteristics of Highway Stormwater Runoff." *Water Environ. Res.*, 78 (12): 2377–2388. https://doi.org/10.2175/106143006X95447.
- Hathaway, J. M., and W. F. Hunt. 2011. "Evaluation of First Flush for Indicator Bacteria and Total Suspended Solids in Urban Stormwater Runoff." *Water. Air. Soil Pollut.*, 217 (1): 135–147. https://doi.org/10.1007/s11270-010-0574-y.
- Hejazi, M., and M. Markus. 2009. "Impacts of urbanization and climate variability on floods in Northeastern Illinois." *J. Hydrol. Eng.*, 14 (6): 606–616. https://doi.org/10.1061/(ASCE)HE.1943-5584.0000020.
- Herzog, T., A. Mehring, B. Hatt, R. Ambrose, L. Levin, and B. Winfrey. 2021. "Pruning stormwater biofilter vegetation influences water quality improvement differently in Carex appressa and Ficinia nodosa." *Urban For. Urban Green.*, 59: 127004. https://doi.org/10.1016/j.ufug.2021.127004.
- Horan, N. J., and M. Lowe. 2007. "Full-scale trials of recycled glass as tertiary filter medium for wastewater treatment." *Water Res.*, 41 (1): 253–259. https://doi.org/10.1016/j.watres.2006.08.028.
- Hsieh, C., and A. P. Davis. 2005a. "Evaluation and Optimization of Bioretention Media for Treatment of Urban Storm Water Runoff." *J. Environ. Eng.*, 131 (11): 1521–1531. https://doi.org/10.1061/(ASCE)0733-9372(2005)131:11(1521).
- Hsieh, C.-H., and A. P. Davis. 2005b. "Multiple-event study of bioretention for treatment of urban storm water runoff." *Water Sci. Technol.*, 51 (3–4): 177–181. https://doi.org/10.2166/wst.2005.0589.
- Jones, P. S., and A. P. Davis. 2013. "Spatial Accumulation and Strength of Affiliation of Heavy Metals in Bioretention Media." *J. Environ. Eng.*, 139 (4): 479–487. https://doi.org/10.1061/(ASCE)EE.1943-7870.0000624.
- Kandel, S., J. Vogel, C. Penn, and G. Brown. 2017. "Phosphorus Retention by Fly Ash Amended Filter Media in Aged Bioretention Cells." *Water*, 9 (10): 746. Multidisciplinary Digital Publishing Institute. https://doi.org/10.3390/w9100746.
- LeFevre, G. H., K. H. Paus, P. Natarajan, J. S. Gulliver, P. J. Novak, and R. M. Hozalski. 2015. "Review of Dissolved Pollutants in Urban Storm Water and Their Removal and Fate in Bioretention Cells." *J. Environ. Eng.*, 141 (1): 04014050. American Society of Civil Engineers. https://doi.org/10.1061/(ASCE)EE.1943-7870.0000876.
- Li, H., and A. P. Davis. 2008. "Heavy Metal Capture and Accumulation in Bioretention Media." *Environ. Sci. Technol.*, 42 (14): 5247–5253. https://doi.org/10.1021/es702681j.

- Li, M.-H., C. Y. Sung, and M. H. Kim. 2010. Bioretention for Stormwater Quality Improvement in Texas: Pilot Experiments. 56. Technical. College Station, Texas: TEXAS TRANSPORTATION INSTITUTE, The Texas A&M University System.
- Li, S., Y. Deng, X. Du, K. Feng, Y. Wu, Q. He, Z. Wang, Y. Liu, D. Wang, X. Peng, Z. Zhang, A. Escalas, and Y. Qu. 2021. "Sampling cores and sequencing depths affected the measurement of microbial diversity in soil quadrats." *Sci. Total Environ.*, 767: 144966. https://doi.org/10.1016/j.scitotenv.2021.144966.
- Li, Y., S.-L. Lau, M. Kayhanian, and M. K. Stenstrom. 2005. "Particle Size Distribution in Highway Runoff." *J. Environ. Eng.*, 131 (9): 1267–1276. American Society of Civil Engineers. https://doi.org/10.1061/(ASCE)0733-9372(2005)131:9(1267).
- Limouzin, M., D. F. Lawler, and M. E. Barrett. 2011. *Performance Comparison of Stormwater Biofiltration Designs*. CRWR Online Report 10-05. University of Texas at Austin: Center for Research in Water Resources.
- Mateus, D. M. R., M. M. N. Vaz, and H. J. O. Pinho. 2012. "Fragmented limestone wastes as a constructed wetland substrate for phosphorus removal." *Ecol. Eng.*, 41: 65–69. https://doi.org/10.1016/j.ecoleng.2012.01.014.
- McNett, J. K., W. F. Hunt, and A. P. Davis. 2011. "Influent Pollutant Concentrations as Predictors of Effluent Pollutant Concentrations for Mid-Atlantic Bioretention." *J. Environ. Eng.*, 137 (9): 790–799. American Society of Civil Engineers. https://doi.org/10.1061/(ASCE)EE.1943-7870.0000373.
- Minnesota Public Works Association. 2007. Public Works Perspective Regarding Cost vs. Benefit for Various Stormwater Best Management Practices (BMPs) Utilized to Manage Stormwater.
- Musgrove, M., S. P. Opsahl, B. J. Mahler, C. Herrington, T. L. Sample, and J. R. Banta. 2016. "Source, variability, and transformation of nitrate in a regional karst aquifer: Edwards aquifer, central Texas." *Sci. Total Environ.*, 568: 457–469. https://doi.org/10.1016/j.scitotenv.2016.05.201.
- Oates, J. A. 2007. "Introduction." *Lime Limest. Chem. Technol. Prod. Uses*, 1–5. John Wiley & Sons, Ltd.
- Oates, J. A. 2008. *Lime and limestone: chemistry and technology, production and uses.* John Wiley & Sons.
- Oates, J. A. H. 1998. Lime and limestone: chemistry and technology, production and uses. Weinheim: Wiley-VCH.
- Palacios, Y. M., and B. K. Winfrey. 2021. "Three mechanisms of mycorrhizae that may improve stormwater biofilter performance." *Ecol. Eng.*, 159: 106085. https://doi.org/10.1016/j.ecoleng.2020.106085.
- Paus, K. H., J. Morgan, J. S. Gulliver, T. Leiknes, and R. M. Hozalski. 2014. "Assessment of the Hydraulic and Toxic Metal Removal Capacities of Bioretention Cells After 2 to 8 Years of Service." *Water. Air. Soil Pollut.*, 225 (1): 1–12. Dordrecht, Netherlands: Springer Nature B.V. https://doi.org/10.1007/s11270-013-1803-y.
- Peck, D. L., J. W. Troester, and J. E. Moore. 1988. *KARST HYDROGEOLOGY IN THE UNITED STATES OF AMERICA*. 21st Congress of the International Association of Hydrogeologists- Karst Hydrogeology and Karst Environment Protection, 23. China: USGS.

- Prince George's County. 1999. Low Impact Development Design Strategies An Integrated Design Approach. Largo, Maryland: Prince George's County, Maryland Department of Environmental Resource Programs and Planning Division.
- Reck, A., M. Thalmann, E. Paton, and B. Kluge. 2021. "Seepage metal concentrations beneath long-term operated bioretention systems." *Blue-Green Syst.*, 3 (1): 128–144. https://doi.org/10.2166/bgs.2021.014.
- Roos, M., and A. Peace. 2015. "Edwards Aquifer Region of South-Central Texas: Unique Challenges and Solutions for LID Implementation." 411–418. Reston, VA: American Society of Civil Engineers.
- Rossman, L. A. 2015. Storm Water Management Model (SWMM) User's Manual Version 5.1. EPA/600/R-14/413 (NTIS EPA/600/R-14/413b), 353. Washington, DC: U.S. EPA Office of Research and Development.
- Rossman, L., and W. Huber. 2015. *Storm Water Management Model Reference Manual Volume I, Hydrology*. EPA/600/R-15/162A. Washington, DC: U.S. EPA Office of Research and Development.
- Rutledge, S. O., and G. A. Gagnon. 2002. "Comparing crushed recycled glass to silica sand for dual media filtration." *J. Environ. Eng. Sci.*, 1 (5): 349–358. https://doi.org/10.1139/s02-023.
- San Antonio River Authority. 2015. San Antonio River Basin low impact development technical guidance manual 2nd Edition. San Antonio River Basin Low Impact Development Technical Design Guidance Manual. San Antonio, Texas: San Antonio River Authority.
- Scaccia, N., I. Vaz-Moreira, and C. M. Manaia. 2020. "Persistence of wastewater antibiotic resistant bacteria and their genes in human fecal material." *FEMS Microbiol. Ecol.*, 96 (fiaa058). https://doi.org/10.1093/femsec/fiaa058.
- Shahrokh Hamedani, A., A. Bazilio, C. Cerda, A. Manjarres, A. Hall, H. Shipley, and M. Giacomoni. 2019. "Assessing the Performance of Bioretention and Sand Filter Media Using Columns and Synthetic Stormwater." World Environ. Water Resour. Congr. 2019 Water Wastewater Stormwater Urban Water Resour. Munic. Water Infrastruct., 14. Pittsburgh, Pennsylvania: ASCE.
- Shahrokh Hamedani, A., A. Bazilio, H. Soleimanifar, H. Shipley, and M. Giacomoni. 2021. "Improving the Treatment Performance of Low Impact Development Practices—Comparison of Sand and Bioretention Soil Mixtures Using Column Experiments." *Water*, 13 (9): 1210. Multidisciplinary Digital Publishing Institute. https://doi.org/10.3390/w13091210.
- Shang, J., P. Li, L. Li, and Y. Chen. 2018. "The relationship between population growth and capital allocation in urbanization." *Technol. Forecast. Soc. Change*. https://doi.org/10.1016/j.techfore.2018.04.013.
- Shrestha, P., M. T. Salzl, I. J. Jimenez, N. Pradhan, M. Hay, H. R. Wallace, J. N. Abrahamson, and G. E. Small. 2019. "Efficacy of Spent Lime as a Soil Amendment for Nutrient Retention in Bioretention Green Stormwater Infrastructure." *Water*, 11 (8): 1575. Multidisciplinary Digital Publishing Institute. https://doi.org/10.3390/w11081575.
- Skorobogatov, A., J. He, A. Chu, C. Valeo, and B. van Duin. 2020. "The impact of media, plants and their interactions on bioretention performance: A review." *Sci. Total Environ.*, 715: 136918. https://doi.org/10.1016/j.scitotenv.2020.136918.

- Søberg, L. C., M. Viklander, and G.-T. Blecken. 2021. "Nitrogen removal in stormwater bioretention facilities: Effects of drying, temperature and a submerged zone." *Ecol. Eng.*, 169: 106302. https://doi.org/10.1016/j.ecoleng.2021.106302.
- Sun, X., and A. P. Davis. 2007. "Heavy metal fates in laboratory bioretention systems." *Chemosphere*, 66 (9): 1601–1609. https://doi.org/10.1016/j.chemosphere.2006.08.013.
- TCEQ. 2005. Complying with the Edwards Aquifer rules. 415. Austin, Texas: Texas Commission on Environmental Quality (TCEQ), Michael E. Barrett.
- Tian, J., J. Jin, P. C. Chiu, D. K. Cha, M. Guo, and P. T. Imhoff. 2019. "A pilot-scale, bi-layer bioretention system with biochar and zero-valent iron for enhanced nitrate removal from stormwater." *Water Res.*, 148: 378–387. https://doi.org/10.1016/j.watres.2018.10.030.
- Tirpak, R. A., A. N. Afrooz, R. J. Winston, R. Valenca, K. Schiff, and S. K. Mohanty. 2021. "Conventional and amended bioretention soil media for targeted pollutant treatment: A critical review to guide the state of the practice." *Water Res.*, 189: 116648. https://doi.org/10.1016/j.watres.2020.116648.
- Tong, S. T. Y., A. J. Liu, and J. A. Goodrich. 2009. "Assessing the water quality impacts of future land-use changes in an urbanising watershed." *Civ. Eng. Environ. Syst.*, 26 (1): 3–18. https://doi.org/10.1080/10286600802003393.
- Ulrich, B. A., M. Loehnert, and C. P. Higgins. 2017. "Improved contaminant removal in vegetated stormwater biofilters amended with biochar." *Environ. Sci. Water Res. Technol.*, 3 (4): 726–734. https://doi.org/10.1039/C7EW00070G.
- United Nations. 2014. World Urbanization Prospects: The 2014 Revision, Highlights (ST/ESA/SER.A/352). Department of Economic and Social Affairs, Population Division.
- US Census Bureau. 2017. "City and Town Population Totals: 2010-2017." Accessed December 9, 2018. https://www.census.gov/data/tables/2017/demo/popest/total-cities-and-towns.html.
- US EPA. 2007. Reducing stormwater costs through low impact development (LID) strategies and practices. 37. Washington, DC: United States Environmental Protection Agency, Nonpoint Source Control Branch (4503T).
- USGPR. 2017. *Climate Science Special Report: Fourth National Climate Assessment*. Wuebbles, D.J., D.W. Fahey, K.A. Hibbard, D.J. Dokken, B.C. Stewart, and T.K. Maycock (eds.).
- USGS Groundwater. 2012. "USGS Groundwater Issues :: Karst :: Aquifers :: Edwards Balcones Fault Zone Aquifer." Accessed February 24, 2019. https://water.usgs.gov/ogw/karst/aquifers/edwards/index.
- Wan, Z., T. Li, and Z. Shi. 2017. "A layered bioretention system for inhibiting nitrate and organic matters leaching." *Ecol. Eng.*, 107: 233–238. https://doi.org/10.1016/j.ecoleng.2017.07.040.
- Wang, R., X. Zhang, and M.-H. Li. 2019. "Predicting bioretention pollutant removal efficiency with design features: A data-driven approach." *J. Environ. Manage.*, 242: 403–414. https://doi.org/10.1016/j.jenvman.2019.04.064.
- Weiss, J. D., M. Hondzo, and M. Semmens. 2006. "Storm Water Detention Ponds: Modeling Heavy Metal Removal by Plant Species and Sediments." *J. Environ. Eng.*, 132 (9): 1034–1042. https://doi.org/10.1061/(ASCE)0733-9372(2006)132:9(1034).
- Yang, F., D. Fu, S. Liu, C. Zevenbergen, and R. P. Singh. 2020. "Hydrologic and Pollutant Removal Performance of Media Layers in Bioretention." *Water*, 12 (3): 921. Multidisciplinary Digital Publishing Institute. https://doi.org/10.3390/w12030921.

Zarezadeh, V., T. Lung, T. Dorman, H. J. Shipley, and M. Giacomoni. 2018. "Assessing the performance of sand filter basins in treating urban stormwater runoff." *Environ. Monit. Assess.*, 190 (12): 1–15.